



IMPI'S  
52<sup>ND</sup> ANNUAL MICROWAVE  
POWER SYMPOSIUM  
(IMPI 52)

# 2018 PROCEEDINGS

June 26-28, 2018

**The Hilton Hotel  
Long Beach, California, USA**

ISSN 1070-0129

Presented by the  
INTERNATIONAL MICROWAVE POWER INSTITUTE  
PO Box 1140, Mechanicsville, VA 23111  
Phone: +1 (804) 559 6667 • Email: [info@impi.org](mailto:info@impi.org)  
[WWW.IMPI.ORG](http://WWW.IMPI.ORG)

© International Microwave Power Institute, 2018



# WELCOME TO LONG BEACH FOR THE 52<sup>ND</sup> IMPI SYMPOSIUM

---

Each year, IMPI brings together researchers from across the globe to share the latest findings in microwave and RF heating theories and applications, and this year we have an outstanding array of researchers in attendance. If you are not yet a member of IMPI, we strongly encourage you to consider joining onsite. IMPI membership connects you to microwave and RF academia, researchers, developers and practitioners across the globe. Talk to an IMPI member today to learn more about the value of joining our outstanding organization!

Thank you for joining us. We hope you learn from the technical presentations, interact with your colleagues, and enjoy the atmosphere of the Symposium. And do take the opportunity to visit the many interesting sites in and around Long Beach.

Special thanks to Shanghai Ocean University for sponsoring the printed Proceedings:



IMPI wishes to express its gratitude to the following individuals:

## **TECHNICAL PROGRAM COMMITTEE**

### **Chairmen**

Graham Brodie, University of Melbourne, Australia  
Ric Gonzalez, Conagra Brands, Inc., USA

### **Members**

Kostiantyn Achkasov, SAIREM, France  
Raymond Boxman, Tel Aviv University, Israel  
Sumeet Dhawan, Nestle, USA  
John F. Gerling, Gerling Consulting Inc., USA  
Shenghui Guo, Kunming University of Science and Technology, P.R. China  
Satoshi Horikoshi, Sophia University, Japan  
Klaus Werner, RF Energy Alliance, The Netherlands  
Roger Williams, AMPLEON, USA  
Vadim V. Yakovlev, Worcester Polytechnic Institute, USA

## **FOOD SCIENCE AND TECHNOLOGY COMMITTEE**

### **Chairman**

Ulrich Erle, Nestle R&D, USA

### **Members**

Jean-Paul Bernard, SAIREM, France  
Yang Jiao, Shanghai Ocean University, China  
Marie Jirsa, Tyson Foods, USA  
Jennipher Marshall-Jenkinson, MTA, United Kingdom  
Pranjali Muley, Louisiana State University, USA  
Jeyamkondan Subbiah, University of Nebraska- Lincoln, USA  
Juming Tang, Washington State University, USA  
Mark Watts, Campbell Soup Company, USA

*Purchasing Information: Copies of the Proceedings of the 52nd Annual Microwave Power Symposium, as well as back issues from prior years, are available for purchase. Contact Molly Poisant, Executive Director of IMPI, at +1 804 559 6667 or [molly.poisant@impi.org](mailto:molly.poisant@impi.org) for details.*

# TABLE OF CONTENTS

---

## SPOTLIGHT SESSION

<b>The Early History of Microwave Processing – An Overview</b> Robert F. Schiffmann .....	11
<b>Opportunities for Microwave Technology in Small Scale Hydrogen Production</b> John F. Gerling .....	12
<b>Microwave Assisted Crystallization; Recent Advanced Applied to Freezing of Foods (FREEZEWAVE Project)</b> Alain Le-Bail .....	15
<b>Neutron Generators Employing Solid State Microwave Sources</b> David L. Williams .....	18
<b>A Changing Landscape in Industrial Microwave Thanks to Solid State Microwave Sources</b> John Mastela .....	21

## KEYNOTE

<b>Microwave Food Processing – Reinventing Packaged Food</b> Lora Spizzirri .....	22
--	----

## MICROWAVABLE PACKAGING

<b>Use of Separation Technology to Retain Essential Carbohydrate Cooking Properties after Thermal Processing in Microwave Packaging</b> David S. Lambert .....	25
<b>Effect of Metal Shielding Food Carrier on Heating Pattern Inside Food Packages Processed with a Microwave Assisted Pasteurization System (MAPS)</b> Yoon-Ki Hong .....	28
<b>Potato Cooking in a Microwavable Self-Venting Pouch</b> Roberto Nigro .....	31

## MODELING, CAD, & OPTIMIZATION

<b>Multiphysics Simulation of Temperature Profiles in a Triple-Layer Model of a Microwave Heat Exchanger</b> A.A. Mohekar .....	33
<b>Mode Fitting and Evenness Studies in Loaded Microwave Cavities</b> Gregory J. Durnan .....	36

MICROWAVE EQUIPMENT, PRODUCT VALIDATION & NEW  
(NON-COMMUNICATION) TECHNOLOGIES

**Investigation on Orthogonal Antenna Configurations for Large Scale Microwave Ovens**  
Sergey Soldatov ..... 39

**2.45 GHz into 4.9 GHz Power Conversion**  
Nguyen Tran ..... 42

**Study of Radio Frequency Pasteurization and Drying of Poria cocos Solid-state Fermented Product**  
Su-Der Chen ..... 45

**A Small-Size Microwave Applicator for Liquid Heating over a Wide Frequency Range**  
Tomohiko Mitani ..... 48

NOVEL MICROWAVE APPLICATIONS

**Microwave-assisted Mechanical Equipment in Mining Industry**  
P. Nekoovaght ..... 51

**In-liquid Plasma using Microwave Power for Waste Water Treatment**  
S. Sawada ..... 54

**Development and Evolution of Novel Hg-free Electrodeless Lamp using Microwave-synthesized Quantum-dot Luminescence**  
K. Hagiwara ..... 57

SOLID STATE & MATERIAL HANDLING UP

**Solid-state RF Energy: The Industry After the First Consumer Launch**  
Klaus Werner ..... 60

**High Power Combining and Control Techniques for 2450MHz Solid-state Power Amplifiers**  
Rick Rigby ..... 61

**Microwave Assisted Manufacturing of Package-less Coffee-tablet: Magnetron Vs Solid State Sources**  
M. Garuti ..... 64

**Solid State Plasma Light source operated by a differential RF applicator**  
S. Holtrup ..... 67

**Solid-State RF Energy – Advancements in Industrial Applications and Market Opportunities**  
RF Energy Alliance ..... 70

**CiMPAS – A Novel Approach for Fast Inline Microwave Pasteurization and Sterilization**  
Klaus-Martin Baumgaertner ..... 71

# FOOD SAFETY & MICROWAVE OVENS: USAGE, DESIGN, AND STANDARDS

<b>Ensuring Safe Consumption of Frozen Foods: A Call for Transformative Innovation</b> S. Gummalla .....	73
<b>Consumer Countertop Microwave Ovens Market Study</b> Marie Jirsa .....	75
<b>Transparent Observation Window for Microwave Oven</b> B.Q. Zeng .....	76
<b>The Influence of Microwave Frequency on Heating Uniformity</b> Z.M. Tang .....	79

## KEYNOTE

<b>Millimeter Wave Interactions with High Temperature Materials and Their Application to Power Beaming</b> Brad W. Hoff .....	82
--	----

## MICROWAVE ASSISTED CHEMISTRY

<b>Solid-State RF-Energy Powered Atmospheric Pressure Ion Sources for Mass Spectrometry</b> Ralf D. Dumler .....	84
<b>Development of Resonant Cavity System, and its Application to Low Permittivity Solvents</b> Hiromichi Odajima .....	85
<b>Use of Microwaves in Molecular Modeling to Study Protein Structures</b> Vijaya Raghavan .....	88
<b>Development of Small Size Microwave Reactor using LTCC Cavity and Solid-state Device</b> M. Nishioka .....	91
<b>Exploiting Microwave Activated Combustion Synthesis for Metallurgy</b> E. Colombini .....	94
<b>Dry Microwave Chemistry Enabled Fabrication of Pristine Holey Graphene Nanoplatelets with Rich Zigzag Edges</b> Huixin He .....	97
<b>Microwave-assisted Preparation of Polyphosphoric Acid in a Continuous Flow Reactor</b> Chun Zhang .....	100

## FOOD & AGRICULTURE

<b>Using Evanescent Field Applicators for Shallow Microwave Heating</b> Graham Brodie .....	103
<b>The Influence of Microwave Soil Treatment on the Toxicity of Arsenic in Wheat (Triticum aestivum L.)</b> Humayun Kabir .....	106
<b>Investigation of Radio Frequency Heating as A Dry-blanching Method for Carrot Cubes</b> Chuting Gong .....	109
<b>Industrial Microwave Assisted Pressurized Induction Heating (MAPIH) Thermal Processing System – An Application of Microwavable Brown Rice Preparation</b> Hong-I Chang .....	112
<b>Improving Plant’s High Temperature Tolerance and Pest Resistance by Microwave Effective Stimulation</b> K. Kadomatsu .....	115
<b>Radiofrequency Inactivation of Enterococcus faecium NRRL B-2354 in Cumin Seeds</b> Long Chen .....	118

## INDUSTRIAL PROCESSING

<b>Development of a Computer Simulation Model for a 915 MHz Single-mode Microwave Heating System Applied in Thawing Process</b> Donglei Luan .....	119
<b>Microwave Heating of a Thin Composite Part: a Parametric Study</b> H. Tertrais .....	122
<b>Effect of Microwave Absorber and Power Level on Microwave-assisted Pyrolysis of Pine Sawdust</b> Candice Ellison .....	125
<b>Research Progress of Microwave Rapid Hardening for Ultra-large Artificial Marble Blocks</b> Haibing Ding .....	128
<b>Rapid Microwave Assisted Delignification of Biomass Using Deep Eutectic Solvents</b> Pranjali D. Muley .....	131

## PROCESSING OF FOOD

<b>Microwave-Freeze-Drying of Fruit Foams for the Production of Healthy Snacks</b> Mine Ozcelik .....	134
<b>Sterilization of Raw Milk with Radio-Frequency Heating Technology: Quality, Safety and Shelf Life Evaluation</b> F. Leone .....	136
<b>Are Enzymes Used in Foods Affected by Microwaves? – Exploring With a Semiconductor Microwave Generator</b> Satoshi Horikoshi .....	138

**A Novel Method of Radio Frequency (RF) Tempering Irregular-shape Frozen Food**

Yang Jiao ..... 141

**Continuous In-Flow Microwave Preservation of Particulate Foods at High Temperatures**

B. Raaholt ..... 144

**Analysis of Food Heating in a Multi-Source Solid State Microwave Oven**

Christopher Hopper ..... 146

POSTERS**Virtual Tools for the Simulation of RF Assisted Thawing of Food Products**

Tesfaye F. Bedane ..... 149

**Microwave Drying of Fabrics**

Baoqing Zeng ..... 152

**MW Processing of Bakery Products to Prevent Checking & Breakage; State of the Art (BRICE Project)**

Patricia Le-Bail ..... 155

**Evaluating Control of Ascochyta lentis in Lentil Seeds by Means of Microwave Processing**

Saeedeh Taheri ..... 158

**Coupled Simulation of Electromagnetic and Thermal Fields for Multi-Source Microwave Oven**

Baoqing Zeng ..... 161

**Design of a L-Band High Power Hermetic Window for Industrial Microwave Heating**

Liang Tang ..... 164

**Implementation of 100kW L-band Window-type Water Load**

Zhiqiang Zhang ..... 167

# NOTES

---

# NOTES

---

# The Early History of Microwave Processing – An Overview

**Robert F. Schiffmann**

R. F. Schiffmann Associates, Inc., New York

**Keywords:** microwave processing, early processing systems, reasons for failure, chicken, donut and sausage processing, potato chip drying.

## INTRODUCTION

Soon after Percy Spencer's discovery of the heating ability of microwave energy and how to apply it, interest grew in the potential of applying microwaves for the processing of materials. Beginning in the 1960s, there were many attempts to commercialize such ideas, resulting in a number of successful microwave processes. However, despite their commercial success, all ultimately failed, i.e. they were supplanted by other technologies, or removed from the marketplace. The reason for these failings is instructive and will be the subject of this paper.

## DISCUSSION

The early history of the adoption of microwave energy for industrial processing will begin with the invention of the microwave oven, followed soon thereafter with conveying materials through a microwave field, and the invention of simple choke systems, and on to other microwave devices. A number of significant and successful industrial microwaves systems will be described, as well as the reasons for the demise, including, potato chip drying, chicken cooking, donut processing, sausage patty manufacture. Such things as technical issues, changes in the marketplace (1), and the innovation being ahead of its time are important reasons.

## REFERENCES

- [1] J.P. O'Meara, Why did they fail? A backward look at microwave applications in the food industry, A Backward Look at Microwave Applications in the Food Industry, *J. Microwave Power*, vol. 8, no 2, pp.167 - 172, 1973.

# Opportunities for Microwave Technology in Small Scale Hydrogen Production

**John F. Gerling**

Gerling Consulting, Inc., Modesto, CA, USA

**Keywords:** Microwave heating, hydrogen production, electrolysis, fuel cells

## INTRODUCTION

As the demand for hydrogen fuel cells is rapidly becoming a multi-billion (US) dollar market opportunity [1], their usage in broadly distributed applications such as stationary energy storage and transportation presents a need for distributed hydrogen production. In 2008 over 96% of all molecular (gaseous) hydrogen was centrally produced by large scale fossil fuel reforming [2], primarily by steam methane reforming (SMR) which is more efficient and cost-effective than smaller scale distributed processes. The costs associated with distribution and storage of centrally produced hydrogen incentivize the development of smaller scale distributed production methods. Additionally, as all fossil fuel reforming processes generate CO<sub>2</sub> as a by-product, much of the current research and development activities focus on alternate zero-emission technologies that avoid the added costs associated with CO<sub>2</sub> capture, conversion and/or sequestration. The utilization of sustainable and renewable energy sources (e.g. solar, wind, hydro-electric) further motivates development of these alternate technologies.

## WATER ELECTROLYSIS

Hydrogen production by water electrolysis (aka “water splitting”) has advantages and disadvantages compared to fossil fuel reforming methods. Water electrolysis uses electricity to split water molecules into molecular hydrogen and oxygen, which is potentially a zero-emission source of hydrogen when utilizing energy sources such as solar, wind, nuclear and hydro-electric. However, due to the inherently smaller economies of scale, the cost of hydrogen produced by water electrolysis is currently higher than by SMR. Cost reduction of electrolysis methods is a major focus of ongoing research [3].

The proton exchange membrane (PEM, aka polymer electrolyte membrane) electrolysis method is gaining momentum and market acceptance as a scalable technology that operates at low temperatures (< 100 °C) and requires only electricity as the source of energy [4]. A disadvantage of PEM electrolysis is reduced conversion efficiency, whereas other methods operating at higher temperatures achieve higher electrical efficiency and potentially reduced hydrogen production costs [5]. Two such methods are of interest: high

temperature electrolysis (HTE) that utilizes solid oxide electrolyte cells (SOEC) operating at around 800 °C [6], and hybrid thermochemical-electrolysis such as the Copper-Chlorine cycle operating at around 500 °C [7]. In both methods the thermal heat source required to achieve the operating temperature is traditionally provided by nuclear (e.g. Figure 1) or concentrated solar energy which limits scalability.

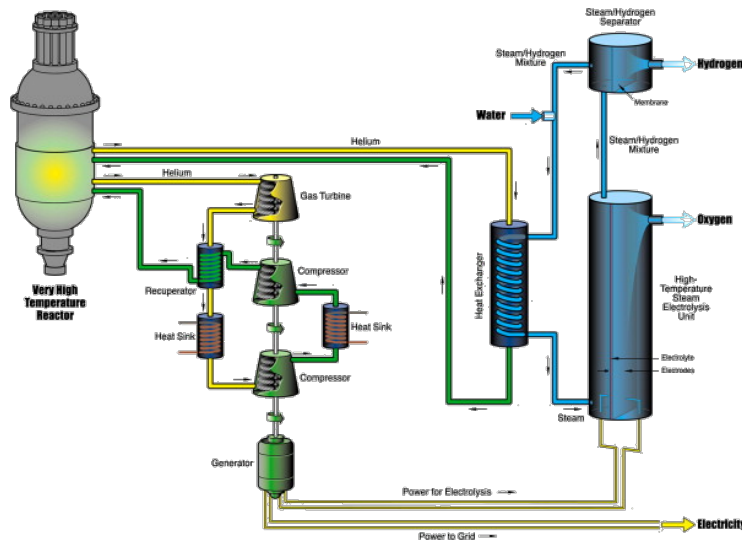


Figure 1, High Temperature Electrolysis (HTE) utilizing nuclear energy as the source of thermal heat.

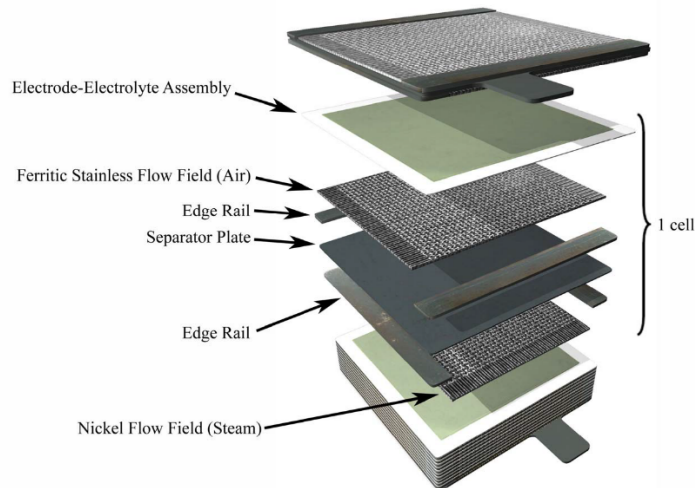


Figure 2, Solid oxide electrolyte cell (SOEC) for steam HTE [8].

**APPLICATION OF MICROWAVE TECHNOLOGY**

Microwave technology may be applicable to higher temperature hydrogen production methods that require an external source of energy to heat the cell or reactor. Because microwave technology is highly scalable, the advantages of these methods that

otherwise are viable only at larger scales can be realized across a broader range of scales. In the case of HTE, conventional SOEC designs (Figure 2) can be modified for microwave compatibility and efficient energy coupling.

The total energy required in a laboratory HTE system at Argonne National Laboratory is 47 kWh/kg, of which 77% is electrical for electrolysis and 23% is thermal for heating [9]. On a smaller scale utilizing 1 kW of microwave power, a similar system could produce up to 2.2 kg/day of hydrogen. As the typical driving range of fuel cell electric vehicles (FCEV) is 60 miles/kg [10], this production rate easily meets the demand of a typical consumer driving 12,000 miles/year. Considering a 65% electrical conversion efficiency of the microwave source, the cost of hydrogen based on local utility rates can be within USD 5.20-6.80/kg. This cost can be reduced when utilizing lower cost renewable sources of electricity (e.g. solar), which on a per-mile basis becomes roughly comparable to current prices for gasoline fuel.

## CONCLUSION

Microwave technology in the production of hydrogen has been shown to enable economic feasibility for small-scale application at the consumer level. Although the technical challenges may be significant, these results warrant further study to identify the most practical methods and techniques to develop.

## REFERENCES

- 
- [1] T.G. Benjamin, J. Gangi, S. Curtin, *The Business Case for Fuel Cells: Delivering Sustainable Value*, 7<sup>th</sup> Edition, *Argonne National Laboratory*, ANL-17/08, June 2017.
  - [2] R.J. Press, K.S. Santhanam, M.J. Miri, A.V. Bailey, G.A. Takacs, *Introduction to hydrogen Technology*. John Wiley & Sons. ISBN 978-0-471-77985-8, 2008.
  - [3] "Hydrogen and Fuel Cells," 2016 Annual Report of the Hydrogen and Fuel Cell Technical Advisory Committee, *Department of Energy*, submitted June 2017.
  - [4] R.E. Clarke, S. Giddey, F.T. Ciacchi, S.P.S. Badwal, B. Paul, J. Andrews, Direct coupling of an electrolyser to a solar PV system for generating hydrogen, *International Journal of Hydrogen Energy*, 2009, 34 (6): 2531–42.
  - [5] Y. Zheng, et al, A review of high temperature co-electrolysis of H<sub>2</sub>O and CO<sub>2</sub> to produce sustainable fuels using solid oxide electrolysis cells (SOECs): advanced materials and technology, *Chemical Society Reviews*, 2017, 46, 1427-1463
  - [6] S.P.S. Badwal, S. Giddey, C. Munnings, Hydrogen production via solid electrolytic routes, *WIREs; Energy and Environment*, Sept 2012, 2 (5): 473–487.
  - [7] M.A. Rosen, G.F. Naterer, R. Sadhankar, S. Suppiah, Nuclear-Based Hydrogen Production with a Thermochemical Copper-Chlorine Cycle and Supercritical Water Reactor, *Canadian Hydrogen Association Workshop*, Quebec, October 19 – 20, 2006.
  - [8] J.S. Herring, C.M. Stoots, J.E. O'Brien, High Temperature Electrolysis for Hydrogen Production, *Materials Innovations in an Emerging Hydrogen Economy*, Cocoa Beach, FL, Feb 2008.
  - [9] R. Doctor, D. Matonis, R. Lyczkowski, High-Temperature Electrolysis, *DOE Solar-Hydrogen Workshop*, Adelphi, MD, Nov 2004.
  - [10] S. Satyapal, Hydrogen and Fuel Cell Progress Overview, *US DOE Fuel Cell Technologies Office*, H2@Scale Workshop, Houston, TX, May 2017.

# Microwave Assisted Crystallization; Recent Advanced Applied to Freezing of Foods (FREEZEWAVE Project)

**Alain LE-BAIL**<sup>a,b</sup>, Piyush Kumar JHA<sup>a,b</sup>, Mathieu SADOT<sup>a,b</sup>, Olivier ROUAUD<sup>a,b</sup>, Vanessa JURY<sup>a,b</sup>, Michel HAVET<sup>a,b</sup>, Sylvie CHEVALLIER<sup>a,b</sup>, Sébastien CURET<sup>a,b</sup>, Epameinodas XANTHAKIS<sup>c</sup>, Sven ISAKSSON<sup>c</sup>, Lovisa ELIASSON<sup>c</sup>, Julien HUEN<sup>d</sup>, Marie SHRESTHA<sup>d</sup> & Jean Paul BERNARD<sup>e</sup>

a ONIRIS, BP 82225, 44322 Nantes, France

b CNRS UMR 6144 GEPEA CNRS, 44307 Nantes,

c RISE-Agrifood and Bioscience, Gothenburg, Sweden

d TTZ-BILB, Bremerhaven, Germany

e SAIREM, France

**Keywords:** Freezing, crystallization, microwave, radiofrequency, food.

## INTRODUCTION

Phase change in biological tissues yields mechanical (volume change during water to ice transition) and biochemical damages (due to freeze concentration). The resulting freeze damage remains a challenge for the food industry. Phase change in an aqueous solution containing solutes induces electric charge displacement. Also, the interaction between water molecules is governed by hydrogen bonds, which are related to a balance in electrical charges. Based on this, it can be understood that freezing could be affected by electrical and magnetic disturbances. This presentation proposes a review based on existing literature as well as some very recent results on Micro Wave (2450 MHz) Assisted Freezing (MW-AF). Results of the ongoing Collaborative European FREEZEWAVE Project are presented in the case of apple freezing.

## THE FREEZEWAVE PROJECT

FREEZEWAVE is a SUSFOOD ERA-NET project (2015 – 2018) about Micro Wave Assisted Freezing (MW-AF). Partners are ONIRIS, RISE, TTZ and the company SAIREM, which provides prototype equipment. A previous study [1] showed a 62% decrease of the average ice crystal size for samples frozen under microwave irradiation compared to the control (Xanthakis et al., 2014, IFSET - study on pork meat). A similar improvement was reported by [2] with RF waves applied to meat freezing. MW-AF with low energy microwave permits to obtain a higher number of nucleation sites and in the end a higher frozen food quality with less freeze damage. FREEZEWAVE aims at optimizing the freezing rate and the quality of frozen foods in the case of MW-AF; sauce, meat, fish, fruits, vegetables are considered. At the end of the project, the design of a continuous industrial scale equipment is foreseen.

## METHODOLOGY

Low power MW were applied using a domestic cavity connected to a solid state emitter. Apple was considered as a model food, and selected quality attributes were studied: image analysis (Cryo-SEM and X-ray tomography), texture etc. Different strategies have been used to apply MW power, either continuously or as pulsed emission at regular time spacings.

Sample preparation (cylinders of apple with a diameter of 8 mm and height of 10 mm)

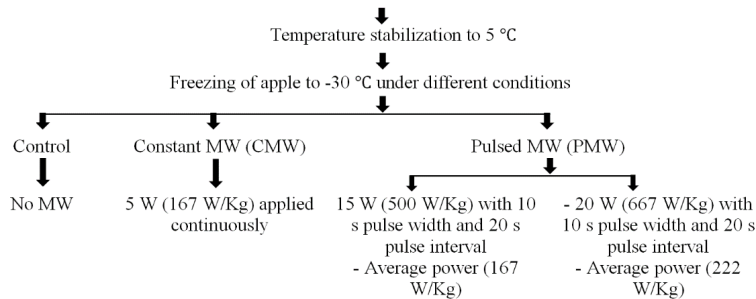


Figure 1. Flowchart representing the freezing strategies that were studied.

## RESULTS

In Figure 2, the microstructure of control and MW-AF apples obtained using x-ray tomography techniques are presented. The lighter regions in the figure correspond to the cellular matrix, while darker region corresponds to the ghost of ice microcrystal that sublimed during freeze drying. The X-ray images clearly show the difference in voids left by ice crystals, and in addition, differences in material microstructure are seen for different freezing conditions. It reveals that freezing in absence of MW produces larger voids area and greater destruction to the cellular matrix compared to the MW-AF conditions. Further, the image analysis was performed to evaluate the effect of microwaves in improving the microstructure of the apple during freezing. Figure 3 shows the frequency curves of the pore size distribution in the apple samples frozen under various conditions. The pore size distribution depicts that the MW-AF conditions produced a better microstructure than the control condition.

## DISCUSSION

With respect to the effect of MW on the microstructure, our observations are in accordance with [3], [2] and [1], who found a better microstructure with numerous ice crystals for freezing conditions assisted by electromagnetic radiation. The production of small size ice crystals in food products can be related to better quality preservation upon thawing. Similarly, with respect to the effect of MW power on microstructure, our results are in line with [1] who observed a decrease in the size of ice crystals with an increase in applied MW power level. As reported in the literature for MW-AF by [1], [4] and [5], MW can exert a torque which can displace the water molecules from their equilibrium relationships in the ice and limit its growth, thus, favouring the genesis of numerous ice crystals in the food.

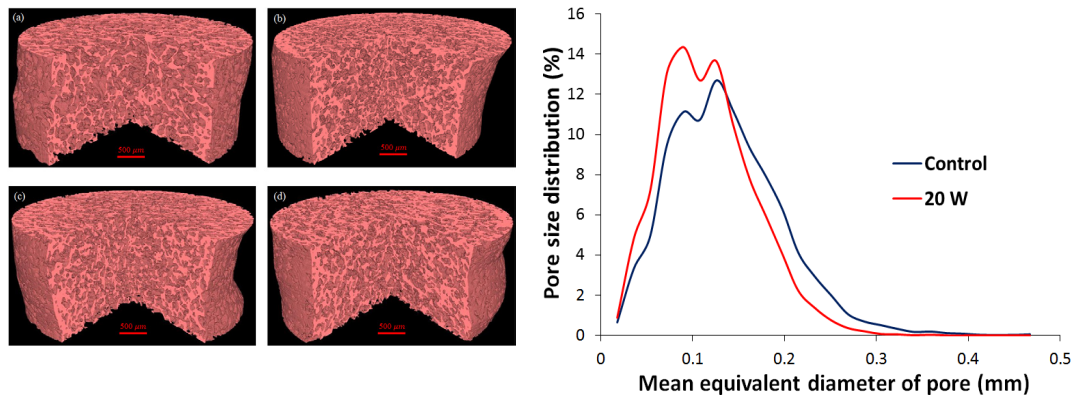


Figure 2. Microstructure of apple after freezing under different conditions: (a) control, (b) 5 W constant power, (c) 15 W pulse condition, and (d) 20 W pulse condition.

Figure 3. Frequency curve for apple sample frozen under control condition and the best MW-AF condition.

## CONCLUSION

MW-AF process produced smaller size ice crystals in the food product compared to conventional freezing and in turn would promote better quality retention. It would also allow us to switch to less energy-intensive freezing, because the freezer could be operated at a higher temperature. 20 W pulsed MW emission conditions yielded the best microstructure followed by 15 W pulsed conditions and 5 W continuous microwaves conditions. The final results from FREEZEWAVE will be presented during an End of Project conference in Nantes – France on 5<sup>th</sup> Nov 2018. The detailed project and program of this even is available on [www.freezewave.eu](http://www.freezewave.eu).

## REFERENCES

- [1] Xanthakis, E., Le-Bail, A., Ramaswamy, H., 2014. Development of an innovative microwave assisted food freezing process. *Innovative Food Science & Emerging Technologies*, 26, 176–181.
- [2] Anese, M., Manzocco, L., Panozzo, A., Beraldo, P., Foschia, M., Nicoli, M.C., 2012. Effect of radiofrequency assisted freezing on meat microstructure and quality. *Food Research International*, 46(1), 50–54.
- [3] Hafezparast-Moadab, N., Hamdami, N., Dalvi-Isfahan, M. Farahnaky, A., 2018. Effects of radiofrequency-assisted freezing on microstructure and quality of rainbow trout (*Oncorhynchus mykiss*) fillet. *Innovative Food Science & Emerging Technologies*. In Press, Accepted Manuscript
- [4] Hanyu, Y., Ichikawa, M., Matsumoto, G., 1992. An improved cryofixation method: cryoquenching of small tissue blocks during microwave irradiation. *Journal of Microscopy*, 165(2), 255–271.
- [5] Jackson, T.H., Ungan, A., Critser, J.K., Gao, D., 1997. Novel microwave technology for cryopreservation of biomaterials by suppression of apparent ice formation. *Cryobiology*, 34(4), 363–72.

# Neutron Generators Employing Solid State Microwave Sources

David L. Williams<sup>1</sup>, Charles K. Gary<sup>1</sup>, Melvin A. Piestrup<sup>1</sup>

<sup>1</sup>Adelphi Technology Inc., Redwood City, California, USA

**Keywords:** Neutron generator, 2.45 GHz power amplifier

## INTRODUCTION

Neutron generators have a range of uses including imaging, materials analysis, medical isotope generation and cancer therapy. The first neutron generator was developed by Bothe and Becker in 1930 [1], prior to the discovery of the neutron by Chadwick in 1931 [2]. In 1942 the reactor pile was developed and provided the possibility of very large neutron fluxes [3]. By 1949 neutron generators using isotopes of hydrogen had been developed [4]. Such devices produce fewer neutrons than a nuclear reactor, but as the technology has evolved, and neutron yields have increased, these devices have begun to emerge as a suitable neutron source for industrial and medical applications. Recent developments in the 2.45 GHz RF power amplifier technology has enabled neutron generator performance improvements as well as reductions in size weight and cost of these machines.

## NEUTRON GENERATOR TECHNOLOGY

Adelphi Technology Inc. has been manufacturing neutron generators for over 10 years, making generators that produce either 14.1 MeV neutrons (employing the deuterium-tritium, DT reaction), 2.45 MeV neutrons (employing the deuterium-deuterium, DD reaction) or thermal neutrons which have an energy of 0.025eV, produced by moderating neutrons produced via the DD reaction. Adelphi's early generators had an output of  $3 \times 10^7$  neutrons/second (DD). The largest output to date is  $1 \times 10^{11}$  n/s (DD). This is more than a thousand-fold increase in neutron yield over 10 years, and is both the result of numerous engineering improvements, as well as an increase in customer interest.

Adelphi's neutron generators consist of an Electron Cyclotron Resonance, ECR, ion source, a target and an acceleration section. Either deuterium gas, or a mixture of deuterium and tritium is fed into the ion source. RF energy excites a plasma within the ion source. A high voltage (typically upwards of 100kV) is then used to pull ions out of the ion source and implant them into a target. After a few minutes of operation, sufficient ions are loaded into the target that subsequent ions collide with ions that are loaded into the target material. The binding energy of these light ions is such that nuclear fusion occurs. The reactions of interest are  $D + T \rightarrow \alpha + n$  (14.1 MeV), and  $D + D \rightarrow \alpha + n$  (2.45 MeV). A mid-range DD neutron generator is shown in Figure 1.



Figure 1. A DD neutron generator. From left to right: magnetron box, waveguide+matching stub, ECR ion source, acceleration chamber. White material surrounding generator: neutron shielding.

**SOLID STATE MICROWAVE SOURCE**

Recently Adelphi has explored replacing magnetrons with solid state microwave sources since these do not require a high voltage power supply, and potentially allow reductions in size, weight, power and cost of a system. Figure 2a gives the performance of the neutron generator when the ion source is driven by a solid state microwave source and a magnetron. Figure 2b shows the frequency response. The ability to tune the frequency of these microwave sources, and their resilience to back-reflections from the plasma, has led to the performance improvements shown in Figure 2a.

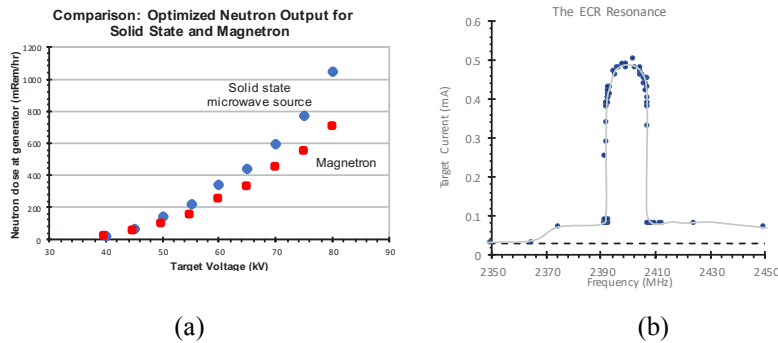


Figure 2. Performance of a neutron generator (a) comparison of the neutron dose from a solid state RF source and a magnetron (b) frequency response of the neutron generator

**APPLICATIONS**

Neutrons tend to pass through materials with a large atomic mass and are moderated by materials with a low atomic mass. This results in an imaging technology with completely different contrast characteristics than X-rays. Used in combination with x-rays, scanning systems can offer greater ability to detect illicit materials. The images shown in Figure 3 show that water and plastic exhibit high contrast, which is the opposite of x-ray systems.



# A Changing Landscape in Industrial Microwave Thanks to Solid State Microwave Sources

**John Mastela**

Global Director Industrial Microwave Business Unit  
Richardson Electronics, Ltd.

**Keywords:** Solid State Microwave Generators, Solid State Microwave Sources, High Power Microwave Generator, Industrial Microwave Generators, Industrial Heating

## INTRODUCTION

Ever since Percy Spencer first melted a chocolate bar in his shirt pocket in 1945, the main source for industrial microwave power has not changed. Our familiar friend, the magnetron, has been the stalwart power source for our industry for well over half a century. It has served us well, enabling scientific discovery which has spawned inventions and innovation which we benefit from daily. However, technology has advanced. We no longer seek out a phone booth to make a call because the smartphones we carry today are far more convenient and millions of times more powerful than all of NASA's combined computing power was in 1969. It is now time for the transistor, which has enabled today's solid state microwave power sources, to usher in the next generation, re-ignite the scientific community's imagination and spirit of invention with a new set of 21<sup>st</sup> century tools. Those tools are the enabling features of today's solid-state microwave sources. No longer will we be required to design systems to accommodate the limitations and idiosyncrasies of magnetrons. The new generation of solid state microwave sources will give us the ability to overcome system design constraints, and to embark upon a new generation of discovery and innovation in physics, chemistry, material sciences, food processing, and where ever our curious nature leads us.

## DISCUSSION

The benefits of Solid State Microwave Sources will be reviewed. Key points will include precise control over frequency, phase, and power, and the benefits of new capabilities such as frequency sweeping, band mapping, and pulse width modulation. Also discussed will be the vastly improved reliability and safety, and the ability to configure systems with output power capability matched to the exact needs of the application. Additionally, the profound impact that a high level of software control and monitoring has over all aspects of the microwave signal, system and process will be discussed.

# Microwave Food Processing – Reinventing Packaged Food

Lora Spizzirri

915 Labs LLC, Centennial, Colo., USA

**Keywords:** Microwave sterilization, microwave pasteurization, packaged food, food safety

## INTRODUCTION

MATS/MAPS technology has the potential to disrupt the food industry by helping to solve some of its most challenging problems. These include food insecurity, food waste, supply chain inefficiency and lack of convenient, packaged, healthy, fresh-tasting food. Companies, such as Amazon, view this technology as an important enabler to providing direct-to-consumer, healthy meals.

Microwave Assisted Thermal Sterilization (MATS) and Microwave Assisted Pasteurization (MAPS) is a game-changing food processing technology developed by the Microwave Research Consortium, led by Washington State University. Consortium members included the Natick Research Labs, food companies and packaging companies.

MATS/MAPS is a thermal process using microwave energy to rapidly reach sterilization or pasteurization temperatures in pre-packaged product. As a result, the flavors, textures and colors lost in traditional thermal processes are maintained, allowing for the production of high quality, clean label foods or beverages. The MAPS technology can also be used for pasteurization to extend the shelf life of chilled products.

The current state of MATS/MAPS technology is perfectly timed to relieve the market tension that exists today between consumers' need for convenient, ready-to-eat foods and their desire to eat foods that are healthy and fresh tasting.

## HISTORY/BACKGROUND

The use of microwaves to sterilize or pasteurize pre-packaged food has been the subject of research for the last 40 years. Much of this research focused on the 2450 MHz wavelength typically utilized for home microwave ovens. The application of 2450 MHz to sterilizing pre-packaged food resulted in some limitations. "Major challenges reported in early research on microwave sterilization technologies included non-uniform and often unpredictable EM fields in multi-mode microwave cavities, as well as a lack of high-barrier microwave transparent packaging materials and reliable means to monitor product temperature, in particular in moving packages (Decareau 1994). In addition, 2450 MHz microwaves could only process foods of shallow thicknesses (Ohlsson 1992), due to limited penetration in foods ...

“Recognizing the limitations of 2450 MHz microwaves, the Washington State University team selected 915 MHz microwaves in system design. In 2001, a microwave consortium was formed consisting of 7 food processing, packaging, and equipment companies and the U.S. Army Natick Soldier Center. The goal was to develop a microwave in-package sterilization technology for production of high quality shelf stable read-to-eat meals for the U.S. Army and the retail market. The (results of this research and development yielded): (1) a microwave cavity design scalable for industrial implementation that provided predictable and stable heating patterns; (2) an effective method to determine heating patterns and identify cold spots in food packages; (3) methods to accurately measure temperature at cold spots of food in continuous microwave heating systems for process development; (4) procedures to file for FDA and USDA-FSIS acceptance.”<sup>1</sup>

Several food safety validations have been successfully completed making MATS the first and only in-package microwave sterilization technique accepted by the U.S. FDA.

### **MATS/MAPS ADVANTAGES**

The processing and distribution of today’s packaged foods is no longer meeting consumer and market needs. Consumers are demanding higher quality, more nutritious foods made with recognizable ingredients, but they don’t have the time or skills to prepare them from scratch. Processed food manufacturers are witnessing declining sales of their legacy brands and are having difficulty reformulating to deliver a cleaner ingredient line. While traditional grocers are seeing declining sales in center-of-store and growth in the perimeter, fresh, chilled foods are lower margin due to higher operating costs. On a global basis, large populations are without access to nutritious foods while one-third of food produced is wasted.

MATS/MAPS technology can solve some of these universal problems facing the food industry by delivering a wide variety of cleaner label, great-tasting foods in convenient packaging. MATS/MAPS is a thermal process which has been perfected in sterilized foods. However, with MATS, foods are subjected to far less thermal history than traditional retort, thereby retaining flavor, color, texture and nutrients. The system can be utilized to sterilize and obtain an ambient shelf life of one year. It can also be used for pasteurization and shelf-life extension of chilled foods.

### **COMMERCIAL IMPLEMENTATION**

In 2014, 915 Labs LLC was founded to harness the power of MATS/MAPS and scale the technology to large commercial applications. 915 Labs holds the exclusive worldwide license for MATS/MAPS technology, enabling the company to commercialize the technology globally in partnership with system manufacturers that produce machines. Since its inception, the company has launched both pilot and commercial scale systems, including the MATS-B and MATS-30, and has grown its portfolio to nearly 70 patents worldwide

The MATS-B pilot-scale system can process up to 60, 8.5oz packages per hour and can be utilized for sterilization or pasteurization. It is ideal to conduct process/product development, consumer testing and small regional test markets. The

MATS-30 is a continuous process with a throughput of up to 30, 8.5oz packages per minute and can also be used for sterilization or pasteurization. Both units utilize a universal carrier to convey packages through the system that is configurable for a variety of packaging formats and sizes.

The MATS process has four phases:

1. Preheat – Packaged, sealed foods are conveyed through a vessel with water spray and water immersion to raise the packages to a homogeneous temperature (typically 65 to 85C).
2. Microwave – After passing through a pressure lock, packages submerged in pressurized water are heated with microwaves to sterilization set point temperature.
3. Hold – Packages are conveyed through a vessel submerged in pressurized water to hold for several minutes to allow the coldest spot to reach sterilization set point temperature.
4. Cool – Packages are conveyed through a cooling vessel submerged in pressurized water to cool to atmospheric temperature before passing through another pressure lock for atmospheric cooling.

The MAPS process is similar; however, overpressure is not required because processing temperatures are lower. Residence time in each vessel is also adjusted depending on the process conditions required of the product.

915 Labs has also developed a Packaging Solutions program. The program offers customers a variety of stock tray/lidding and pouch options developed specifically for MATS processing. Packaging is delivered in partnership with certified packaging suppliers subjected to rigorous requirements. Custom packaging can also be developed for the MATS system.

In addition to MATS systems and packaging, 915 Labs, in conjunction with its world-wide partners, offers a variety of services to guide customers from product development to commercial production. These include product development and testing, product optimization and production scale-up.

## REFERENCES

- [1] Juming Tang, “Unlocking Potentials of Microwaves for Food Safety and Quality”, *Journal of Food Science*, Vol. 80, Nr. 8, 2015.

# Use of Separation Technology to Retain Essential Carbohydrate Cooking Properties after Thermal Processing in Microwave Packaging

David S. Lambert<sup>1</sup> and Daniel S. Lambert<sup>2</sup>

<sup>1</sup>Research & Development Systems Ltd., Newcastle upon Tyne, United Kingdom

<sup>2</sup>Advanced Food Technologies Ltd., London, United Kingdom

**Keywords:** food & food packaging wastage, thermal-processing, separation technology, differential dielectric heating.

## INTRODUCTION

The Food and Agriculture Organization of the United Nations estimates that, each year, one-third of all food produced for human consumption in the world (around 1.3 billion tons) is lost or wasted. In the developed world, a significant proportion of food waste has been caused over the past 30 years by the move away from canned foods towards fresh chilled foods with short shelf-life (< 7 days). The retention of the essential physical properties of pasta, noodles, rice and other carbohydrates during thermal-processing is one of the most significant problems for food manufacturers to overcome if they are to arrest the relative decline in canned foods and thereby contribute to the war against food and food packaging waste. The finished product quality of the carbohydrate component of prepared foods, including visual appearance (color, brightness, surface texture), cooking behaviour [1] and eating quality (mouth feel, chewiness, elasticity, firmness and slipperiness) [2] are of critical importance to the ever more sophisticated end consumer. Food manufacturers often assemble the carbohydrate, protein, vegetables and sauce in single compartment containers. Whilst this is acceptable for short-life chilled products it is not so for extended life products. If the carbohydrate is in contact with excess water during thermal processing significant damage to the protein chains and starch molecules of the carbohydrates can occur resulting in unacceptable organoleptic end quality for the consumer. It is possible to avoid most of this damage by restricting the free water available to the carbohydrate during thermal processing, and then re-introducing the missing water to the carbohydrate during microwave cooking immediately prior to consumption by using purpose made packs and different rates of dielectric heating caused by individual component position and lossiness.

## EXPERIMENTAL APPARATUS AND PROCEDURE

A twin compartment container was developed within which the carbohydrates and other solids (such as proteins and vegetables) are kept separated from the liquid component

(typically sauces, marinades or dressings) during thermal processing and storage. This container automatically combines the solid and liquid food materials during microwave cooking such that the carbohydrates become fully hydrated just before serving, as would be the case with freshly prepared carbohydrate with protein, vegetable garnish and sauce.

The microwaveable food package that was developed was a stand-up, gusseted retort pouch divided vertically into a small compartment and a large compartment with two interconnecting channels within the gusseted base at the bottom of the two compartments. The channels were designed to automatically open when a differential pressure threshold between the two compartments was reached, and then close again when the pressure equalizes after the sauce transfers. The pressure is created by leaving the smaller sauce compartment sealed so steam generated during microwave heating forces the sauce through the bottom channels into the larger compartment which was vented before cooking.

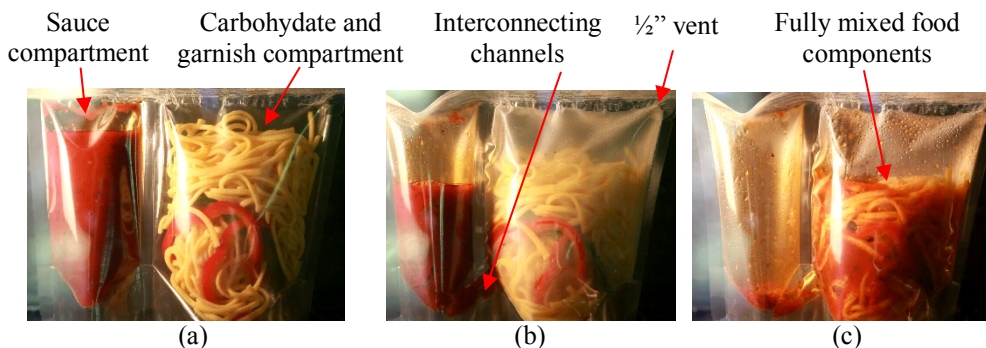


Figure 1. Still frames from video of the final twin compartment pouch during microwave cooking; (a) at start of heating, (b) at start of sauce transfer (2 min 30 sec), and (c) at end of cooking (4 min)

Various types of channels were designed and tested, including thin welded seals, seals with weak points, peelable seals and pressure-sensitive, shape-restricted open seals.

Test pouches were made from standard 4-ply retort laminate which was bonded by the application of heat and pressure between shaped anvils. These pouches were then filled with 250g of cooked pasta and vegetables in the large compartment and 170g of pasta sauce in the small compartment before the tops of the two compartments were heat sealed.

Prior to microwave cooking the top of the large compartment of each trial pack was cut open 1/2 inch to allow venting to atmosphere. A pressure monitoring tube was bonded into the top seal of the small compartment and connected to an external pressure gauge mounted on top of the microwave oven to monitor the differential pressure during heating and sauce transfer. The small opening in the microwave was shielded and earthed.

Each pouch design was heated for up to 5 minutes on full power (800W) in the microwave oven, and the times and differential pressures needed for the starch solution to start and then finish transferring into the large compartment were compared. An infra-red non-contact thermometer was used to measure temperatures within both compartments.

Initial tests were conducted on filled pouches that had not been retorted. The designs that performed best were sterilised in a water immersion retort at 122°C (252°F) to an Fo5 lethality before cooling and re-testing in the microwave oven as above.

## RESULTS

Significant difficulties were encountered in finding a reliable design because of the flexible nature of the retort pouch laminate at the elevated temperatures (110°C / 230°F) encountered during microwave heating. This flexibility resulted in constantly variable three-dimensional pouch shapes during heating, pressurization and then sauce transfer.

The need for 100% reliability of sauce transfer placed high demands on the functional packaging design. Channel opening by means of various frangible seals had to be dropped because of their unreliable performance during testing.

Discussions with established retort pouch manufacturers precluded the use of peelable seals due to the difficulties that would be encountered during pouch manufacture.

The unsealed channel design, forced closed by the contours of the filled compartments, provided a sufficiently effective barrier to unwanted liquid transfer during filling, sealing, retort processing and final handling to provide the expected product quality benefits combined with quick and reliable sauce transfer during microwave cooking.

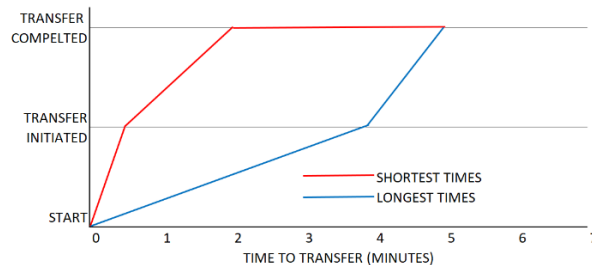


Figure 2. The envelope of longest & shortest transfer times by valve designs & product type

## DISCUSSION

The final design derived from this project has been patented in 21 countries and the commercialization of the technology has now started. Testing has been undertaken with several international food manufacturers and retailers, with results confirming the anticipated benefits of the separation technology. Further research work using these twin pouches is welcomed to more fully quantify the benefits for a wider range of food components when kept away from excess water during thermal processing and storage.

## CONCLUSION

Separation technology can be an effective tool for food manufacturers to increase product shelf life for microwaveable products without causing unacceptable loss of organoleptic quality. In this way food and food packaging waste can be very substantially reduced.

## REFERENCES

- [1] Feillet, P., Autran, J.-C., & Icard-Vernière, C. (2000). Mini Review pasta brownness: An assessment. *Journal of Cereal Science*, 32(3), 215–233. doi:10.1006/jcers.2000.0326.
- [2] Oh, N. H., Seib, P.A., Deyoe, C. W., & Ward, A. B. *Cereal Chem.* 60(6):433-438 (1983) Measuring the Textural Characteristics of Cooked Noodles.

# Effect of Metal Shielding Food Carrier on Heating Pattern Inside Food Packages Processed with a Microwave Assisted Pasteurization System (MAPS)

Yoon-Ki Hong<sup>1</sup>, Deepali Jain<sup>1</sup>, Fang Liu<sup>1</sup>, Zhongwei Tang<sup>1</sup>, Zhi Qu<sup>1</sup>, Stewart Bohnet<sup>1</sup> and Juming Tang<sup>1,\*</sup>

<sup>1</sup>Washington State University, Pullman, WA, United States

\*Corresponding author

**Keywords:** Microwave pasteurization, metallic shielding, packaged food, heating pattern, computer simulation

## INTRODUCTION

The microwave assisted pasteurization system (MAPS) developed at Washington State University (WSU) for pre-packaged food products combines 915 MHz single-mode cavity design with emerging water at high temperature to provide predictable heating pattern without edge heating [1]. The unique system design also allows the use of metal carriers with partial metal shielding to alter electric field distribution in food packages when moving through microwave cavities [2]. In this presentation, we describe the development of a computer simulation model based on QuickWave Software to provide useful insight into how different metal shielding patterns change electric field distribution in food packages in a pilot-scale MAPS, and present experimental results to validate the simulation results.

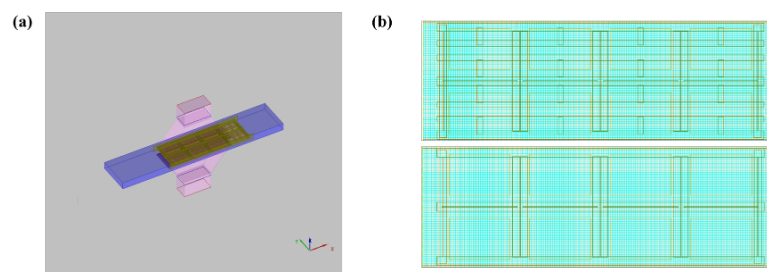


Figure 1. Schematics of (a) microwave cavity design and (b) food tray carrier (upper: with metallic shielding; lower: without metallic shielding).

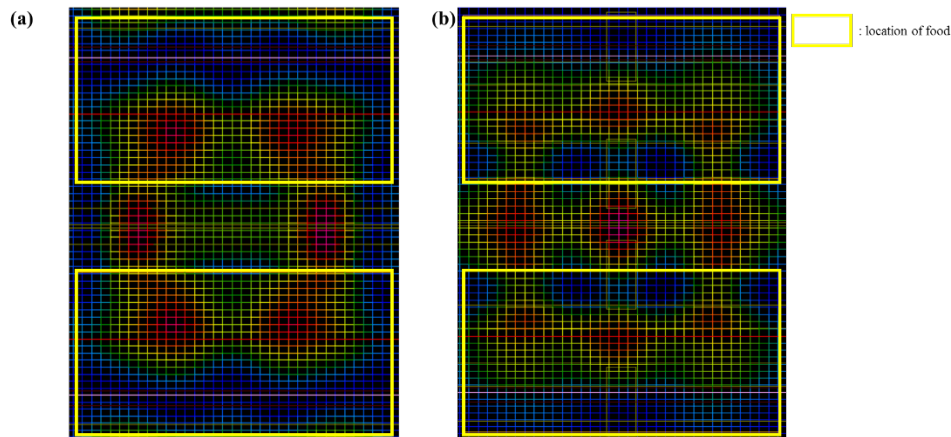


Figure 2. Simulated electric field pattern in middle layer of food trays: (a) food tray carrier without metal shielding, (b) food tray carrier with metal shielding (Tang Cage).

## METHODOLOGY

QuickWave Software (ver 7.5C, Warsaw, Poland) was used to simulate the electric field and microwave heating using food tray carriers in the pilot scale MAPS (Figure 1). In the simulation, food samples were located in the center of the microwave cavity. Dielectric and thermal properties of the food were measured and obtained [3]. To validate the heating patterns in 10-oz trays, the trays filled with a model food based on mashed potato and M1 chemical marker were processed in the four cavity MAPS with 30 kW power generators. The MAPS consists of four sections: preheating, microwave heating, holding, and cooling. Packaged model food sequentially moved through the four sections during processing. The heating patterns were determined using computer vision method [3].

## RESULTS

Electric field in the microwave heating cavity was predicted using a computer simulation model. As showed in Figure 2, electric field distribution is affected by food tray carrier and packaged food. With metal shielding on the top and bottom of the carrier, the electric field is more concentrated in the middle of the food trays. Without metal shielding on the carrier, the electric field distributed toward the food tray edges closed to central line of the carrier in moving direction. Figure 3 shows the experimental and simulated heating patterns in 10-oz trays. The red and blue regions in Figure 3 indicate the hot and cold areas, respectively.

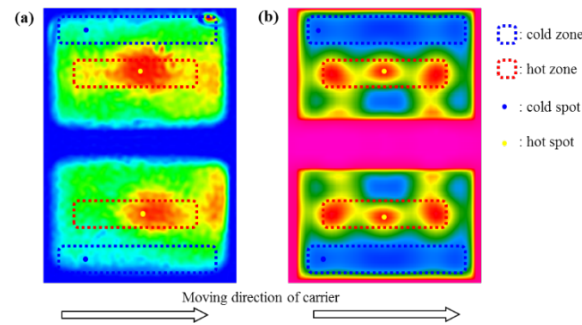


Figure 3. Heating patterns in 10-oz single-compartment trays processed in MAPS by (a) experimented M1 model food and (b) computer simulation.

## DISCUSSION

Based on the simulated results, the metallic shield changed the electric field distribution which could affect the resulting heating pattern in the food trays. Experimental heating patterns matched well with the electric distribution during computer simulation in the cavity; this validated that the developed simulation model worked well for heating pattern prediction. Simulation results show that metallic shields could affect cold and hot spot locations and provide more uniform heating pattern. Thus, carrier design with metallic shielding could improve heating uniformity in microwave processing systems.

## CONCLUSION

The effect of metallic shielding on microwave heating was investigated using computer simulation and experiments. A metallic shielding effectively changes cold and hot zones in food trays. Thus, it can provide more uniform heating in prepackaged foods in MAPS.

## REFERENCES

- [1] J. Tang, Unlocking potentials of microwaves for food safety and quality. JFS Special Issue: 75 Years of Advancing Food Science, and Preparing for the next 75. *J. Food Sci.*, Vol. 80 issue 8, pp.E1776-1793, 2015.
- [2] J. Tang, , F. Liu, Microwave Sterilization or Pasteurization Transport Carriers and System (*US Patent, filed on July 18, 2016, Application Number 15212655, WSU OC 1687*).
- [3] D. Jain, J. Wang, F. Liu, J. Tang, S. Bohnet, Application of non-enzymatic browning of fructose for heating pattern determination in microwave assisted thermal pasteurization system. *J. Food Eng.*, vol. 210, pp.27-34. 2017.

# Potato Cooking in a Microwavable Self-venting Pouch

Veneranda De Cristofano<sup>1</sup>, Giulia Saccone<sup>1</sup> and Roberto Nigro<sup>1</sup>

<sup>1</sup>Department of Chemical, Materials and Production Engineering, University of Naples Federico II, Naples, Italy

## INTRODUCTION

Ready-to-eat products are a growing market reality. In order to meet the specific requirements of utilization and conservation and ensuring quality and storability, it has become necessary to evaluate the development of dedicated packaging. In most cases, commercially available microwave cooking packages are equipped with special micro-valves that regulate the pressure inside the packaging and, consequently, affect the cooking temperature. The aim of this work is to study the cooking of potatoes (cultivar Tondello) in a domestic flatbed microwave oven equipped with a wave stirrer (@2450 MHz) using self-venting polyethylene flowpacks (MWP).

## METHODS AND MATERIALS

The cooking tests were carried at different power levels, 160, 350, 560, 700 and 800W, with a total weight of potatoes of about 300g for each power level tested.

The measurement of the cooking temperature of the product, inside the potatoes, was obtained through a flexible fiber optic probe, totally immune to electromagnetic interference and coupled to a Luxtron FOT Lab Kit.

Microwaved baked potatoes, traditional boiled potatoes, and microwave steamed samples were compared through the analysis of the following parameters: temperature and pressure profiles, moisture content, colour, texture, damaged starch and dielectric properties (dielectric constant  $\epsilon'$ , loss factor  $\epsilon''$  and tangent of loss angle,  $\tan(\delta)$ ). All these properties were evaluated during cooking tests.

The microstructure of cooked samples was examined using a SEM-EDAX microscope.

## RESULTS AND DISCUSSION

The temperatures levels achieved during MW cooking were in the range between 102 and 120 °C. Up to 200 seconds of cooking time, the internal temperature was approximately 20-30 °C higher than the surface temperature with peak reaching 120 °C. After this time, the two temperatures became equal, with a value in the range 102-107 °C remaining constant until the end of cooking.

During the cooking phase in the MWP, the moisture loss was observed to depend on the power level and sample weight, as well as by the cooking time, reaching values of about 35%, that was much greater than that obtained in boiling cooking and in potatoes steamed in microwave (10%).

Cutting force measurement of potatoes can be used as a good indicator of optimum cooking time. Values between 3 N and 4 N were measured.

At the end of microwave cooking, an amount of damaged starch was measured to between 15 and 20%. At varying temperature (increasing from 25 to 120°C), dielectric properties  $\epsilon'$  and  $\epsilon''$  showed a similar trend during microwave cooking ranging, respectively, from 60 to 10 and from 16 to 3. Finally, values of  $\tan(\delta)$  remained almost constant in all range of temperature tested (about 0.27).

# Multiphysics Simulation of Temperature Profiles in a Triple-Layer Model of a Microwave Heat Exchanger

A.A. Mohekar, J.M. Gaone, B.S. Tilley, and V.V. Yakovlev

Worcester Polytechnic Institute, Worcester, MA, USA

**Keywords:** Microwave heating, multiphysics modeling, power response curve, thermal runaway

## INTRODUCTION

Conventional applications of microwave (MW) heating systems include food processing, microwave assisted chemistry, high temperature treatment of materials, etc. [1], [2]. Relatively new devices are MW heat exchangers (MHE), which are used in solar energy collectors [3], power beaming applications [4], and MW thermal thrusters [5]. Working principle of the MHE is governed by coupling between electromagnetic, heat transfer, and fluid flow phenomena, and thus require particularly extensive experimental developments. This raises demand on multiphysics models that are capable of adequately simulating all essential effects occurring in MHEs.

Heat generation in a ceramic material undergoing MW heating is dependent on the electrical conductivity, which often increases exponentially with temperature [6]. Such nonlinear coupling results may lead to thermal runaway. A mathematical model for a single lossy layer [7] describes thermal runaway with the help of a power response curve (also called *S*-curve because of its shape). It determines steady state temperature of the lossy layer as a multivalued function of the incident power. Recently, a model of a triple layer laminate mimicking a MHE [8] has shown that for particular values of the layer width and complex permittivity, the *S*-curve acquires another (third) stable branch and becomes the *SS*-curve. This work has demonstrated a possibility of operating within controllable temperatures so that MW energy can be harnessed in form of heat energy. A 2D numerical model capturing the appearance of the *SS*-curve has been described in [9]. It showed that efficiency of a MHE increases when thermal runaway is achieved. Yet, the behavior of temperature fields under different operating conditions remains insufficiently understood.

In this paper, we extend the approach of [8], [9] by introducing a hydrodynamically fully developed Poiseuille flow in fluid carrying channels. We present the steady-state temperature profiles in the three-layer laminate that correspond to different lengths of the channels. Since steady-state temperature profiles depend on operating conditions, geometry and material parameters, we show how temperature profile in a triple-layer laminate varies with the length of the channel.

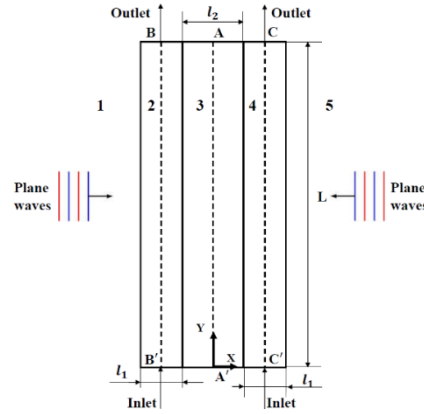


Figure 1. Triple-layered geometry subjected to symmetric MW irradiation; media 1 and 5 are free space, media 2 and 4 are lossless fluid, and medium 3 is lossy dielectric;  $L$  is the length of channels.

## NUMERICAL MODEL

We consider a triple-layered geometry shown in Figure 1. We construct a numerical model in *COMSOL Multiphysics* capable of solving a coupled system of Helmholtz's, heat, and Navier-Stokes equations:

$$\begin{aligned} \nabla^2 \vec{E}_j + k_0^2 \mu_{rj} \left( \epsilon'_{rj} - i \frac{\sigma_j(T_j)}{\omega \epsilon_0} \right) \vec{E}_j &= 0, \\ \rho_j C_{pj} \left( \frac{\partial T_j}{\partial t} + \vec{u}_j \cdot \nabla T_j \right) &= K_j \nabla^2 T_j + \sigma_j(T_j) |\vec{E}_j|^2, \\ \frac{\partial \vec{u}_j}{\partial t} + \vec{u}_j \cdot \nabla \vec{u}_j &= -\frac{\nabla P_j}{\rho_j} + \nu_j \nabla^2 \vec{u}_j, \quad \nabla \cdot \vec{u}_j = 0, \end{aligned}$$

where  $\vec{E}$  is electric field,  $k_0$  is wave number of free space,  $\mu_r$  and  $\epsilon_r$  are relative permeability and permittivity respectively,  $T$  is temperature,  $\sigma(T)$  is temperature dependent electrical conductivity,  $\omega$  is angular frequency,  $\epsilon_0$  is permittivity of free space,  $\rho$  is density,  $C_p$  is specific heat capacity,  $\vec{u}$  is velocity of fluid,  $K$  is thermal conductivity,  $P$  is pressure, and  $\nu$  is kinematic viscosity. Subscript  $j$  represents region of the solution.

Top and bottom boundaries of region 3 are assumed to be thermally insulated. Pressure and temperature at the inlet in regions 2 and 4 is 0.5 Pa at 300 K respectively, and the outlet in regions 2 and 4 was thermally insulated and maintained at zero pressure. No slip conditions are applied at external boundaries of channels 2 and 4. Boundaries between regions 1 and 2, 4 and 5 are exposed to ambient temperature of 300 K with heat transfer coefficient of 12.6 W/m<sup>2</sup>K undergoing Newton's law of cooling. In order to neglect fringe effect at the corners of the geometry, we set normal component of gradient of the electric field to be zero at the top and bottom boundaries of region 2, 3, and 4.

The developed COMSOL model was validated by comparing its 1D results for the case of no fluid flow with the output of the 1D mathematical model [8], [9]; corresponding power response curves were found to be in a satisfactory agreement. Dimensions were chosen accordingly to the criteria [8] so that the resonance occurs in the lossy layer, and material properties are taken from [9]; frequency of the incident wave is 2.45 GHz.

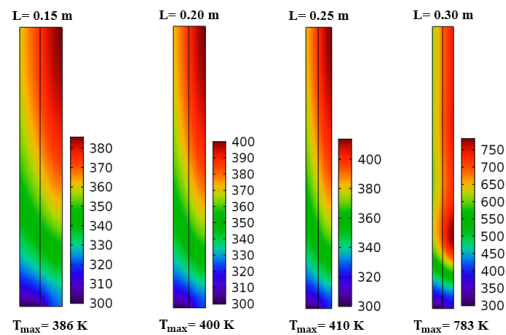


Figure 2. Three-layered scenario (Figure 1) with material parameters from [9]: steady-state temperature profiles for different lengths of the channel; incident power density  $4,200 \text{ W/m}^2$ .

## RESULTS AND DISCUSSION

The patterns in Figure 2 show that the maximum temperature  $T_{\max}$  increases with the length of the channel. As  $T_{\max}$  reaches a critical value, we observe a large increase in temperature due to thermal runaway. This suggests that high thermal efficiency can be obtained by appropriate length of the channel. As steady-state temperature profiles depend on operating conditions, geometry and material parameters, the presented model can help determine optimum design parameters of high-efficient triple-layered MHEs.

## ACKNOWLEDGEMENT

The authors are grateful for the support from the Air Force Office of Scientific Research; Award FA9550-15-0476.

## REFERENCES

- [1] A.C. Metaxas and R.J. Meredith, *Industrial Microwave Heating*, Peter Peregrinus, 1983.
- [2] M. Willert-Porada, Ed., *Advances in Microwave and Radio Frequency Processing*, Springer, 2006.
- [3] A. Jamar, Z.A.A. Majid, W.H. Azmi, M. Norhafana, and A.A. Razak, A review of water heating system for solar energy applications, *Int. Commun. in Heat and Mass Transfer*, vol. 76, pp. 178-187, 2016.
- [4] B. Jawdat, B. Hoff, M. Hilario, A. Baros, P. Pelletier, T. Sabo, and F. Dynys, Composite ceramics for power beaming, *2017 IEEE Wireless Power Transfer Conference*, 978-1-5090-4595-3/17.
- [5] K.L. Parkin, L.D. DiDomenico, and F.E. Culick, The microwave thermal thruster concept, In: *2nd Intern. Symp. on Beamed Energy Propulsion*, pp. 418-429, 2004, 0-7354-0175-6/04.
- [6] W.B. Westphal and A. Silas, *Dielectric Constant and Loss Data*, Laboratory for Insulation Research, MIT, Cambridge, MA, Tech. Rep. AFML-TR-72-39, April 1972.
- [7] G.A. Kriegsmann, Thermal runaway in microwave heated ceramics: A one-dimensional model, *J. Applied Physics*, vol. 71, no 4, pp. 1960-1966, 1992.
- [8] J.M. Gaone, B.S. Tilley, and V.V. Yakovlev, Permittivity-based control of thermal runaway in a triple-layer laminate, *IEEE MTT-S Intern. Microwave Symp. Dig. (Honolulu, HI, June 2017)*, 978-1-5090-6360-4.
- [9] A.A. Mohekar, J.M. Gaone, B.S. Tilley, and V.V. Yakovlev, A 2D coupled electromagnetic, thermal and fluid flow model: application to layered microwave heat exchangers, *IEEE MTT-S Intern. Microwave Symp. Dig. (Philadelphia, PA, June 2018)* (to be published).

# Mode Fitting and Evenness Studies in Loaded Microwave Cavities

Gregory J. Durnan<sup>1</sup>

<sup>1</sup>NXP Semiconductors, Chandler, Arizona, USA

**Keywords:** Multiphysics modeling of microwave heating systems, energy efficiency, power amplifiers, even microwave energy distribution.

## INTRODUCTION

Field uniformity, and therefore heating uniformity in the work load, is one of the grand challenges of microwave and radio frequency heating. The analytical basis for calculation of the fields within a cavity is well known and can be referenced in standard texts (e.g., [1]). For brevity, dielectric heating is of primary interest in cooking within a consumer (or commercial) microwave oven, and as such we are interested in the magnitude of the dissipated power due to an electric field impinging on the food being cooked (lossy dielectric material). From Poynting's theorem it is possible to state this directly as [2].

$$P_d = \frac{1}{2} \omega \epsilon_0 \epsilon'' |E|^2 \quad (1)$$

where  $\omega$  is the angular frequency in radians/seconds,  $\epsilon_0$  is the permittivity of free space and  $\epsilon''$  is the imaginary component of permittivity, and  $|E|$  is the magnitude of the impinging electric field.

The field distribution in a resonant cavity depends on the number of modes that can be excited within the cavity. In practice though only one mode may be excited at a single point in time, such that over the cooking cycle it is necessary to assign individual time slots for the mode being excited. Several strategies have been employed to excite multiple modes or disturb the dominant mode structure over the cooking period (using time slices or multiplexing over time of modes of interest), including turntables, mode stirrers and multiple waveguide feeds. Most of these strategies are frustrated by the lack of frequency and phase control associated with magnetron sources. The advent of solid state sources, based on power amplifiers, allows novel cavity fed systems to be explored. One such feed system is a phased array of antenna elements. This paper deals with work on loaded cavities when directly excited by phased array antennas rather than waveguide driven magnetrons. The use of a multiple element phased array allows us to phase one antenna against another and access a number of modes that a single element cannot.

## METHODOLOGY

Our approach was to design a cooking cavity, with a phased antenna array feed to maximize the number of accessible modes in the cavity (Fig. 1). It should be noted that

while we may maximize the number of modes, not all can be excited by our phased array, due to such practicalities as the placement and number of feed antennas. Optimizing a cooking cavity dimensions for the maximum number of intrinsic modes [3] yielded a mode count of 24 individual modes (TE and TM) for a cavity of depth = 43cm, width = 44 cm and height = 26 cm. These included both  $TE/TM_{mnp}$  modes some of which were degenerate modes. All equations of electric fields for both TE and TM modes were calculated in MATLAB [1] (summed in Fig. 2). Typically, with a 2-element phased array patch antenna on the side wall (in the typical magnetron position) we access 12-14 modes (dependent on cooking load) in the 2.4-2.5GHz range for the cavity dimensions given previously. These  $mnp$  integer indices correspond to the  $xyz$  plane periodicity of either sine or cosine waves that defines the mode's standing wave pattern.

**RESULTS**

Through the complex addition of all modes in an ideal cavity (eigen modes for a given cavity size), we show the likely heating pattern for an empty cavity (Fig. 2). It can also be shown that the use of optimization, in this case the use of simulated annealing with a fitness function that attempts to make the average electric field sum of all intrinsic modes of the cavity at defined points across the cooking space as flat as possible by minimizing

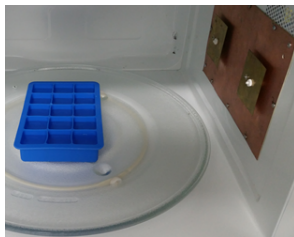


Fig. 1 (above): Showing a 2 element phased array on the right side wall of a consumer of dimensions described in Methodology. Each element is phased against the other using a solid-state source.

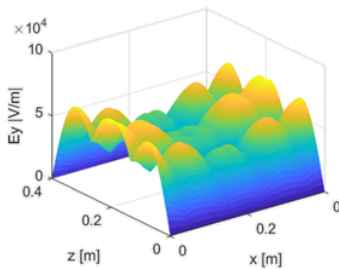


Fig. 2: Showing a dip in the center of the E field summation. Results are the sum of 24 intrinsic modes as calculated in MATLAB for an ideal cavity independent of applicator.

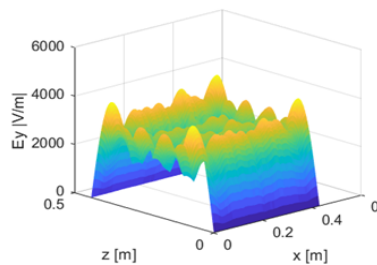


Fig. 3: The use of simulated annealing in MATLAB of the same ideal cavity and 24 intrinsic modes to optimize which modes to excite to yield a superior result in terms of evenness.

the E-field variation, produces a superior field distribution compared with a regular microwave oven.

**DISCUSSION**

The simulated annealing result, using just a few evenly weighted E field points across the cooking space as part of the minimized fitness function, gave a considerably improved field distribution, as shown in Fig. 3. It is envisaged that not only by selecting the correct modes but by giving some modes greater cook time than others can yield an even better result.

In a real cooking environment a method of measuring points of high dielectric heating (due to high electric fields) in a load, albeit as a scalar heating pattern using a thermal camera (Flir Lepton module – 120x160 pixels), will allow an adaptive phased array system (with the advantage of size and cost for a solid state system) to cycle through phase and frequency mapping so that modes are identified, that when summed, form the desired final heating pattern, as shown in Fig. 4 (for an even heating pattern). This approach of correlating the camera heating data with RF parameters (time, frequency, phase, power and return loss data) allows us to produce a real-world result for each cooking item. It also allows us to adjust the fitness function for irregularly sized food items (e.g. an object that is not uniform in shape, such as a chicken drumstick, may require more power to the bulk of its mass rather than its extremities to cook evenly without burning those areas of lower mass).

## CONCLUSION

This paper deals with the analytical basis of providing an even (or profiled) cooking result. Its most application is solid state cooking devices due to the ease of phase and

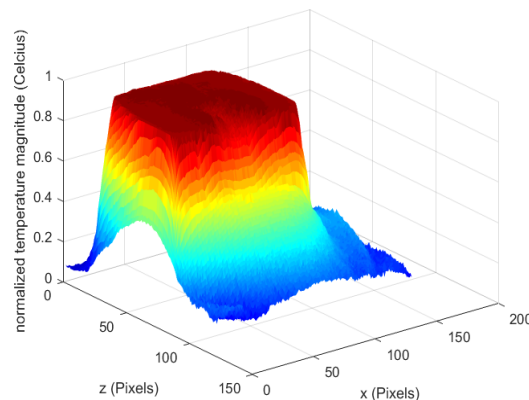


Fig. 4: A real world heating profile of 9% NaCl solution as extracted using a IR camera and manipulated using the same methods as per the analytical method discussed. *The goal /fitness function was the minimization of the average of 15 temperature points.* The resultant equation was found as be:

$$imc = (10*ima+imb)./11$$

frequency agility to generate the RF parameters for the phased array applicator that lead to heating in a known position in the food. In addition, the practical case of the food cooking environment is approached by replacing ideal analytical mode patterns with heat pattern feedback control, obtained on the fly from IR camera data. The system has the capability of obtaining heat patterns from several camera positions to provide a more complete picture of cooking uniformity.

## REFERENCES

- [1] B.M. Notaros, *MATLAB-Based Electromagnetics*, Pearson Education, 2014.
- [2] T.V.C.T. Chan and H.C. Reader, *Understanding Microwave Heating Cavities*, Artech House, 2000.
- [3] R.F.B. Turner, W.A.G. Goss, W.R. Tinga, and H.P. Baltes, On the counting of modes in rectangular cavities, *Journal of Microwave Power*, vol. 19 , no 3, 1984.

# Investigation on Orthogonal Antenna Configurations for Large Scale Microwave Ovens

Sergey Soldatov<sup>1</sup>, Guido Link<sup>1</sup>, Dominik Neumaier<sup>1</sup>, Vasileios Ramopoulos<sup>1</sup>,  
and John Jelonnek<sup>1,2</sup>

<sup>1</sup> IHM, <sup>2</sup>IHE, Karlsruhe Institute of Technology (KIT), Karlsruhe, Germany

**Keywords:** multi-mode applicator, slot antennas, heating uniformity

## INTRODUCTION

For an industrial scale microwave oven, the major issue is the homogeneous heating of the dielectric material [1-3]. It depends on the homogeneity of the absorbed power in the dielectric load, which, in its turn, depends on the electric field pattern. And the latter one results from the superposition of the excited eigenmodes of the microwave oven. Hence, the controlled excitation of eigenmodes is a key for homogeneous heating. For example, a mechanical mode stirrer influences the amplitudes of contributing modes, but such a control is *non-intelligent*, so it does not ensure that a homogeneous field distribution is achieved. For the oven, fed by several microwave sources, the control of the standing wave pattern is more efficient if it is driven by the variation of amplitude [4] and/or phase and/or frequency of every individual source. In addition to amplitude, phase and wavelength, the superposition of the modes depends also on the mode polarization. To a greater extent it is determined by the antenna radiative pattern. Moreover, the superposition of modes with orthogonal field orientation is supposed to result in more advanced wave pattern control.

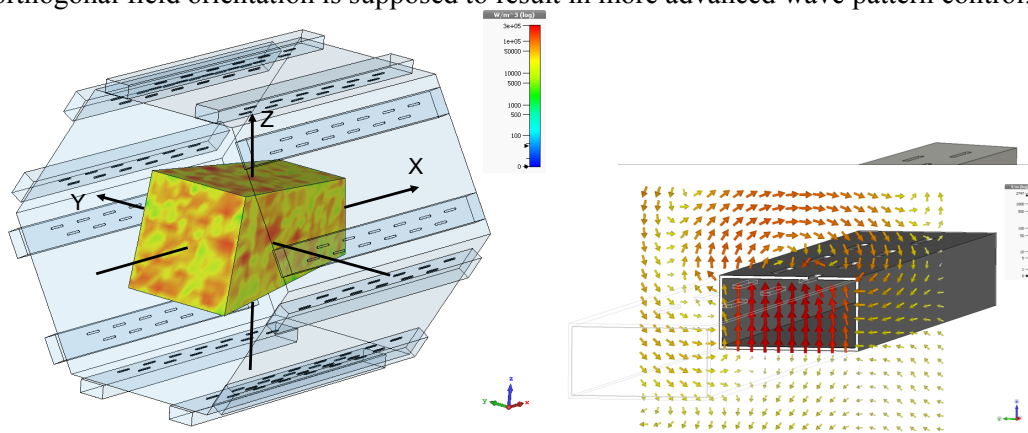


Figure 1. Model of HEPHAISTOS oven with the load inside (left). Slotted antenna with longitudinal (standard) orientation of slots and radiative electric field pattern (right).

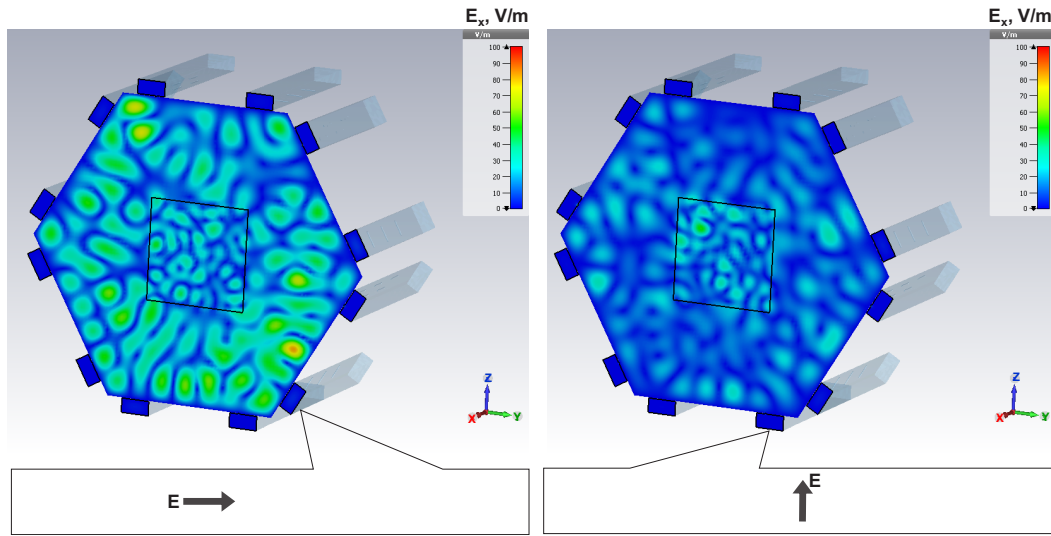


Figure 2. X-component of electric field (rms value) for a single antenna excitation at 2.45 GHz with slots oriented in transverse (left) and longitudinal (right) direction. Black arrows indicate the predominate polarization in the near-field zone of antennae.

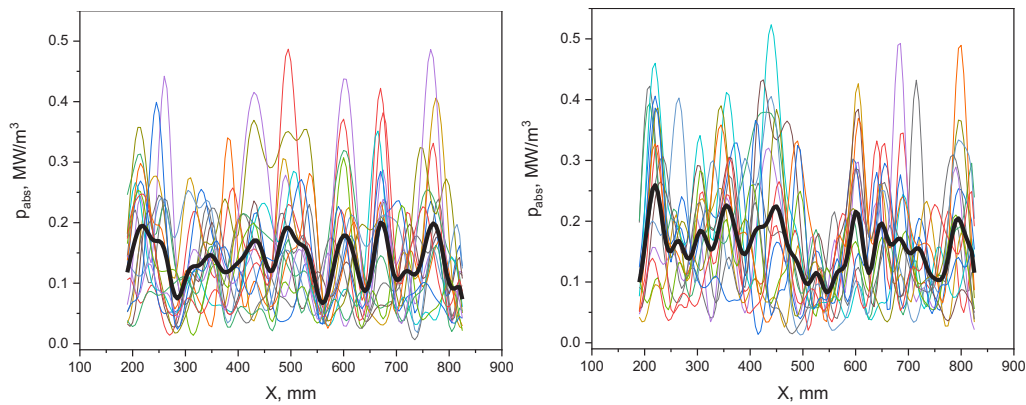


Figure 3. Distributions of absorbed power in the load for 17 phase sets of microwave sources at 2.45 GHz (thin colored lines) and their averaged superposition with equal amplitudes - with thick black line. Antennae configuration **12L** (left) and **6T+6L** (right).

In the present work we have considered the electrical large, multi-mode, hexagonal microwave oven HEPHAISTOS VHM 100/100 [5] equipped with 12 slot antennas and fed by 12 microwave sources (one source per antenna) of 0.8 kW each at ISM frequency band from 2.4 to 2.5 GHz. We have modelled the random phase variations in every source and have analyzed the resulted absorbed power distribution in the dielectric sample. We have considered two antennas configurations: i) 12 antennas with longitudinal (referred as **12L**) orientation of slots (Fig. 1) and ii) 6 antennas with transverse plus 6 antennas with longitudinal (referred as **6T+6L**) orientation of slots (Fig. 2).

## RESULTS

The electromagnetic problem is solved numerically using the commercial 3D simulation software CST Microwave Studio. The dielectric load has a form of rectangular prism with six non-parallel planes and placed in the center of oven (Fig. 1). Its permittivity is chosen as:  $\epsilon' = 2.8$  and  $\tan \delta = 0.01$  (typical for silicone resin and PVC plastic). Both types of antennas, with slots of longitudinal and transverse orientations, are designed in that way that all of them have a return loss of less than -15 dB within a frequency range from 2.4 GHz to 2.5 GHz. The radiation pattern is characterized by a strong E-field polarization perpendicular to the orientation of the slots (see Fig. 1). Correspondingly, the resulting wave pattern in the oven consists of modes, for which the E-field patterns are polarized in the same plane. The clear effect of slot orientation is seen in Fig. 2. There, the x-component of the electric field pattern for the excitation with different antenna configurations is presented. The modes excited with the antenna with transverse slots (oriented perpendicular to x direction) definitely have higher amplitude of x-component of electric field,  $E_x$ , as compared with the antenna with longitudinal slots. It proves the different excitation capability for antennas with different orientation of radiation slots.

The phase variations in twelve sources were simulated as random. This corresponds to non-coupled, independent sources whose phase relations are not predictable or spontaneous. Simulation results for 17 sets of random phases, both for **12L** and **6T+6L** configuration are shown in Fig. 3. The absorbed power density distribution along the x-axis of the dielectric load, for every phase set, is presented with thin colored lines and for their superposition with thick black line. It is evident that the phase of the source influences strongly the absorbed power pattern, each of which varies significantly (up to 100 %) as the load is not quite lossy and the standing wave pattern is pronounced. At the same time the absorbed power averaged over 17 phase sets definitely results in a much smoother absorbed power profile in the load. The combination of antennas with both longitudinal and transverse slots reduced the periodicity of the fluctuations along x-direction and, even with the random phase, the improvement in the absorbed power uniformity is pronounced. Thus, with active, *intelligent* control of phase, amplitude and frequency, a much higher enhancement in the heating uniformity is to be expected.

## REFERENCES

- [1] A. C. Metaxas and R. J. Meredith, Industrial microwave heating, Peter Peregrinus Ltd, 1988
- [2] G. Link, V. Ramopoulos, Simple Analytical Approach for Industrial Microwave Applicator Design, *Chem. Eng. and Proc.*, 2017, <https://doi.org/10.1016/j.cep.2017.12.015>
- [3] V.V. Yakovlev, Effect of frequency alteration regimes on the heating patterns in a solid-state-fed microwave cavity, *J. Microwave Power & Electromag. Energy*, 2018, vol. 52, No. 1, 31-34
- [4] Yiming Sun, Adaptive and Intelligent Temperature Control of Microwave Heating Systems with Multiple Sources, PhD Thesis, Karlsruhe Institute of Technology, KIT Scientific Publishing, 2016
- [5] Hephaistos Microwave Oven VHM 100/100. Technical Data. [Online]. Available [http://www.voetsch-ovens.com/sixcms/media.php/2323/W1\\_037neu.pdf](http://www.voetsch-ovens.com/sixcms/media.php/2323/W1_037neu.pdf)

# 2.45 GHz into 4.9 GHz Power Conversion

Nguyen Tran

Melbourne, Australia

**Keywords:** Converting 2.45 GHz power into 4.9 GHz power

## INTRODUCTION

The objective of this project is to convert 2.9 GHz power to 5.8 GHz power. It begins with the investigation of the conversion of the available 2.45 GHz power to 4.9 GHz power. The conversion to 5.8 GHz will then be followed by the conversion of 2.9 GHz power. Research in frequency doubling using ferrite was very extensive in the past [1-7]. High power in the past was limited by the properties of ferrite to a few hundred Watts and the conversion efficiency achieved was up to 40% [6]. This is about the same efficiency as a Klystron and will not be adequate for industrial applications. The advance in the development of ferrite and of simulation software has encouraged another look at frequency doubling.

A high power magnetron at 2.9 GHz like 2.45 GHz may be manufactured up to 20 kW. The frequency conversion of 2.9 GHz to 5.8 GHz may be a way to produce high power. A magnetron at 5.8 GHz has only a maximum power of 800 W. Projects intending to use high power 5.8 GHz can rely on frequency conversion for much higher power output.

## METHODOLOGY

The research begins with simulation using ferrite to double the frequency of 2.45 GHz. The principle of conversion has been well discussed in the paper by Weiss [6]. This is followed by experimental verification. Simulation software helps a lot in sorting out the resonance frequency, the length of the WR340 and WR157 waveguides. It also helps with the conversion of 2.45 GHz power to 4.9 GHz power and how to transfer the output power from the WR340 waveguide to a WR157 waveguide. Simulation also provides information on efficiency and maximum power output. It plays an important role in the

present project. Simulation software as is available now was not yet developed in the past.

## RESULTS

4.9 GHz produced from 1.2 kW of 2.45 GHz power is as shown in the microwave frequency counter and the frequency spectrum analyzer below.



Figure 1. The converted frequency is shown by a frequency counter and a spectrum analyzer.

## DISCUSSION

High power 4.9 GHz in excess of 800 W is achievable. This conclusion is based on the conversion of 1.2 kW of 2.45 GHz. The converted 4.9 GHz output power is high, corresponding to a conversion efficiency of well over 40%. In fact, the combined conversion efficiency is higher than 50%. This has given more encouragement for the 2.9 GHz high power magnetrons to produce 5.8 GHz at a power much greater than 800W. This will be possible when all obstacles associated with the project are settled.

## CONCLUSION

Our work on using 2.45 GHz high power, has shown that it is possible to generate a high power 4.9GHz. Further work is continued to produce practical high power generators at 5.8 GHz.

## REFERENCES

- [1] W.P. Ayres et al Microwave frequency doubling and mixing in ferrites, USA patent 2,922,876, patented Jan. 26, 1960.
- [2] N. Karayianis et al Frequency doubling microwave cavity, USA patent 3,041,524, patented June 26, 1962.
- [3] L. Kleinman et al Harmonic generator, USA patent 3,076,132 patented Jan. 29, 1963.
- [4] I. Kaufman et al Microwave harmonic generator utilizing self-resonant ferrite, USA patent 3,544,880, patented Dec. 1, 1970.
- [5] A.L. Lutsenko and G.A. Melkov Radio Eng. and Electron. Phys. USA 18 (1973) 1668.
- [6] E. Schied and O. Weis Microwave harmonic generation in ferrites at high power J. of Magnetism and Magnetic Materials 45 (1984) 377-381.
- [7] L. Dubrowsky et al High power X band ferrite frequency doubler, Microwave Symposium Digest, IEEE MTT-S International 30 April-2 May 1979.

# Study of Radio Frequency Pasteurization and Drying of *Poria cocos* Solid-state Fermented Product

Yu-Fen Yen, Yen-Hui Chen and Su-Der Chen\*

National Ilan University, I-Lan City, Taiwan 26041

**Keywords:** radio-frequency, solid-state fermented product, pasteurization, drying.

## INTRODUCTION

The soybean residue and rice bran were the media for *Poria cocos* solid-state fermentation to improve their antioxidant activities. Radio frequency (RF) can rapidly heat up water molecules or ions in food by rapid conversion of electric field; therefore, RF heating can overcome heat transfer resistance to accelerate pasteurization and drying processing of food product [1]. The drying time of 1.6 kg of in-shell walnuts reducing moisture content from 20% to 8% required 100 and 240 min by RF drying and only hot air drying, respectively [2]. After 90 s of RF treatment, the log reductions of *Salmonella* and *Escherichia coli* were 4.29, 4.55 and 4.39, 5.32 log CFU/g, respectively, in creamy and chunky peanut butter respectively, without affecting the quality [3]. Therefore, RF may applied in the downstream processing of *Poria cocos* solid-state fermentation.

## METHODOLOY

A 5 kW, 40.68 MHz pilot-scale RF with hot air drying system was used in this study (Figure 1(a)). The size of the parallel electrode plates were 35 cm x 35 cm. A pack of 500 g soybean residue and rice bran = 1:1, with 40% moisture content as *Poria cocos* solid-state fermented medium at 25°C for 30 days cultivation. After fermentation, one pack product was put on the bottom of RF electrode plate (Figure 1 (b)). The RF power was obtained by adjusting the gap between the electrodes from 14 to 22 cm. The surface temperature profiles and weight loss of 500 g *Poria cocos* solid-state fermented products during RF drying with hot air were measured.

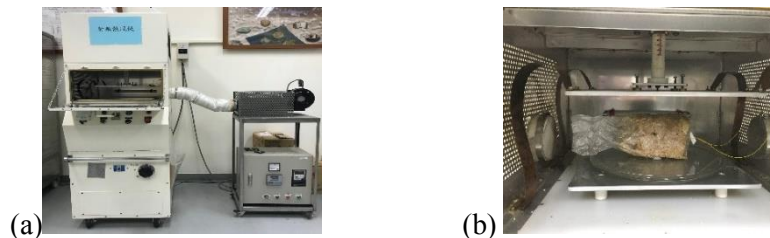


Figure 1. (a) Batch RF hot air heating equipment. (b) Product pack in the RF system.

**RESULTS**

RF output power was increased with decreasing electrode gap. (Figure 2) The surface temperature required only 60 sec to reach about 100°C at gaps of 14, 15 and 16 cm. (Figure 3) The 500 g fermented product took only 30 sec at the electrode gap of 15 cm to pasteurize, and there was no *Poria cocos* growth (Figure 4). Then it took only 200 sec to dry the fermented product from 40% moisture content to low than 15%. (Figure 5) However, the sterilization of fermented product in an autoclave required 60 min. The drying time of fermented products were 100 min in a 45°C cold air drier. (Table 1) The polysaccharide and triterpenoids contents in fermented products were no significantly difference between RF and traditional processing, but RF heating could avoid browning and achieve higher whiteness of product. (Table 2)

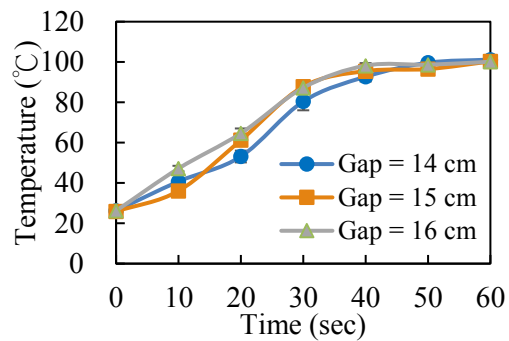
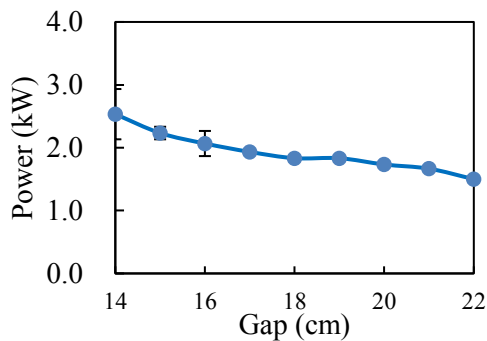


Figure 2. The RF power output at different electrode gaps for 500 g *Poria cocos* solid-state fermented product.

Figure 3. The temperature profile of *Poria cocos* solid-state fermented product at different electrode gap during RF heating.

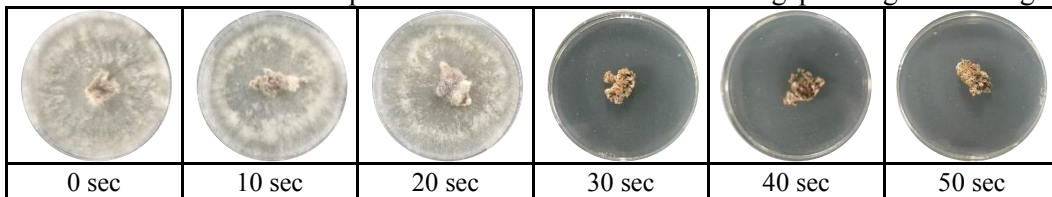


Figure 4. RF pasteurization at electrode gap of 15 cm for *Poria cocos* solid-state fermented product after *Poria cocos* 7 days cultivation.

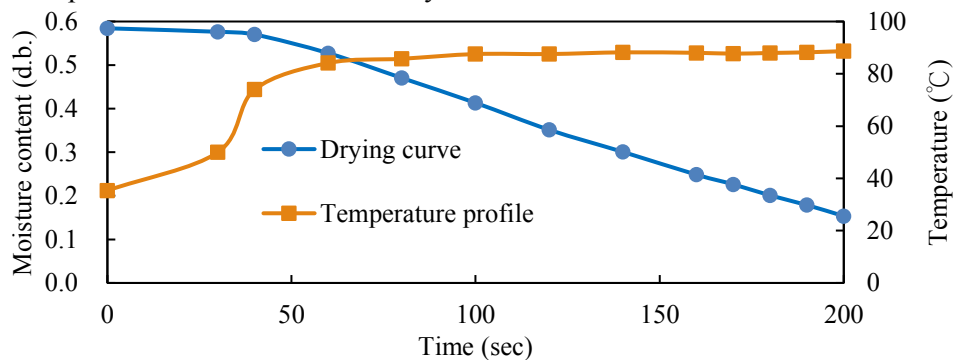


Figure 5. The average temperature profile and drying curve of *Poria cocos* solid-state fermented product during RF drying with gap of 15 cm.

Table 1. The drying rate, drying time and energy consumption of 500 g *Poria cocos* solid-state fermented product by RF drying and 45 °C cold air drying

Drying condition	Drying rate (g/min)	Drying time (min)	Energy consumption (kWh)
RF drying	45.837	3.33 (200 s)	0.34
Cold air drying	0.9089	180	7.38

Table 2. Effect of different pasteurization and drying methods on quality of *Poria cocos* solid-state fermented products

Treatment	Crude polysaccharide (%)	Crude triterpenoids (%)	L*	a*	b*	Whiteness (%)
RF pasteurization & RF drying	9.83 ± 0.24 <sup>a</sup>	4.43 ± 0.02 <sup>a</sup>	53.30±0.31 <sup>a</sup>	9.64±0.03 <sup>a</sup>	27.70±0.18 <sup>a</sup>	44.86±0.21 <sup>a</sup>
121 °C Autoclave & cold air drying	9.35 ± 0.30 <sup>a</sup>	4.32 ± 0.01 <sup>a</sup>	41.74±0.03 <sup>b</sup>	9.68±0.06 <sup>a</sup>	22.65±0.15 <sup>b</sup>	36.75±0.07 <sup>b</sup>

## DISCUSSION

RF heating 4 min of *Poria cocos* solid-state fermented products could replace the traditional sterilization 60 min in an autoclave and 100 min drying in a 45 °C cold air drier. RF could significantly decrease time and energy consumption of downstream process. Moreover, RF heating could avoid browning reaction and obtain white *Poria cocos* white mycelium appearance.

## CONCLUSION

RF pasteurization and drying of 500 g *Poria cocos* solid-state fermented product required only 4 min, and RF treatment had better quality than autoclave & cold air drying.

## REFERENCES

- [1] F. Marra, L. Zhang and J. G. Lyng, Radio frequency treatment of foods: Review of recent advances, *J. Food Eng.* vol. 91, no 4, pp.497-508, 2009.
- [2] B. Zhang, A. Zheng, L. Zhou, Z. Huang and S. Wang, Developing hot air-assisted radio frequency drying protocols for in-shell walnuts. *Emir. J. Food Agr.*, vol. 28, no 7, pp. 459-467, 2016.
- [3] J. W. Ha, S. Y. Kim, S. R. Ryu and D. H. Kang, Inactivation of *Salmonella enterica serovar* Typhimurium and *Escherichia coli* O157: H7 in peanut butter cracker sandwiches by radio-frequency heating. *Food Microbiol.*, vol. 34, no 1, pp. 145-150, 2013.

# A Small-Size Microwave Applicator for Liquid Heating over a Wide Frequency Range

Tomohiko Mitani<sup>1</sup>, Ryo Nakajima<sup>1</sup>, Naoki Shinohara<sup>1</sup>, Yoshihiro Nozaki<sup>2</sup>,  
Tsukasa Chikata<sup>2</sup> and Takashi Watanabe<sup>1</sup>

<sup>1</sup>Kyoto University, Uji, Japan

<sup>2</sup>Japan Chemical Engineering & Machinery Co. Ltd., Osaka, Japan

**Keywords:** Applicator, Wide frequency range, Small batch, Electromagnetic simulation.

## INTRODUCTION

A small-size microwave applicator for liquid heating is described in the present paper. Our group previously developed a coaxial applicator, which can be used within two ISM bands of 915 MHz and 2.45 GHz [1], [2]. Drawbacks of the previous applicator are slow heating rate (5-10 K/5 minutes) due to thermal dissipation from the applicator itself, and non-uniformity of temperature in the applicator due to unstirred structure. To solve these problems, the applicator volume is reduced from 360 ml to 20 ml, and the microwaves are radiated from the sidewall of the applicator to secure the space for placing a magnetic stirrer at the bottom. We verify viability of the improved small-size reactor through electromagnetic simulations and microwave reflection measurements.

## METHODOLOGY

Figure 1 shows simulation models of the developed small-size microwave applicator designed in the 3D electromagnetic simulator (ANSYS HFSS). The applicator has a cylinder structure whose diameter and height are 25 mm and 70 mm, respectively. A liquid sample is poured into the applicator. Microwave is input through the coaxial connector from the sidewall of the applicator. The inner conductor sticks out from the coaxial line in the applicator and is covered with alumina. A metal supporter is placed on the opposite sidewall side to support the inner conductor and alumina. At the bottom of the applicator, there is a space to place a magnetic stirrer. The applicator, the inner and outer conductors, and the supporter are made of stainless steel SUS 316L. The applicator volume is about 20 ml.

Figure 2 shows a photograph of reflection coefficient measurements of the applicator. A network analyzer (Agilent N5242A) was connected to the applicator to measure the S-parameter  $|S_{11}|$ , reflection coefficient. As shown in Figure 2, the top of the applicator is tightly shielded for leakage prevention of both microwaves and air pressure. In addition, the temperature monitor port is attached on the sidewall orthogonally to the

microwave input port. Also we conducted heating tests under 100 W microwaves at the frequencies of 1.7 GHz, 2 GHz and 2.45 GHz.

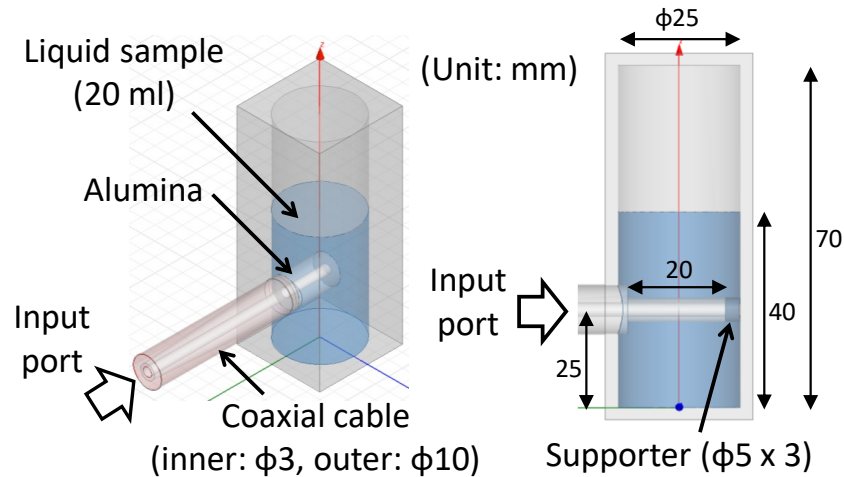


Figure 1. Overall view (left) and cross-section view (right) of the developed small-size applicator.

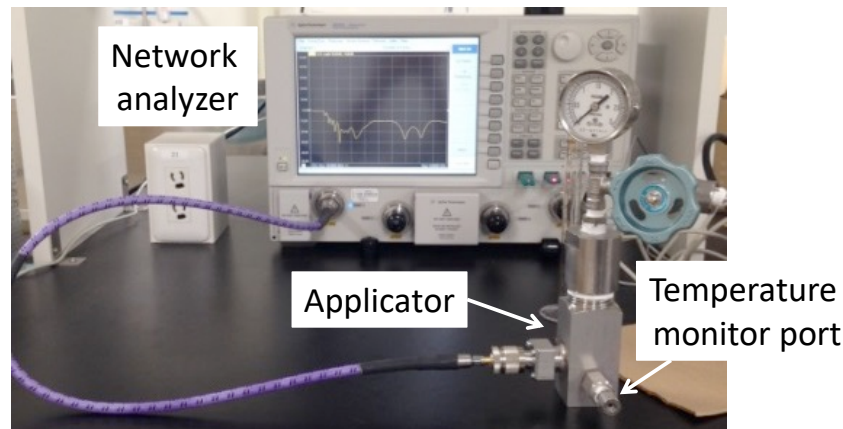


Figure 2. Reflection coefficient  $|S_{11}|$  measurements of the developed small-size applicator.

## RESULTS

Figure 3 shows simulation and measurement results of the reflection coefficient  $|S_{11}|$  of the developed applicator. The poured liquid sample was 2 M NaOH solution or ultrapure water at room temperature. The permittivity of the liquid sample was taken into account in the simulations. From heating tests, both ultrapure water and NaOH solution could be heated up to the boiling temperatures within 370 s at all the setting frequencies.

## DISCUSSION

As shown in Figure 3, measurement results agree well with simulations.  $|S_{11}|$  was smaller than -10 dB, *i.e.* the reflected power was less than 10%, from 1.45 GHz to 2.7 GHz

in the ultrapure water case, from 1.6 GHz to 2.7 GHz in the NaOH solution case. Even though  $|S_{11}|$  is larger than -10 dB, impedance tuning between the input port and the applicator will mitigate the microwave reflection level. The heating rates of the applicator were 63-69 K/5 minutes, more than 6 times faster than the previous applicator.

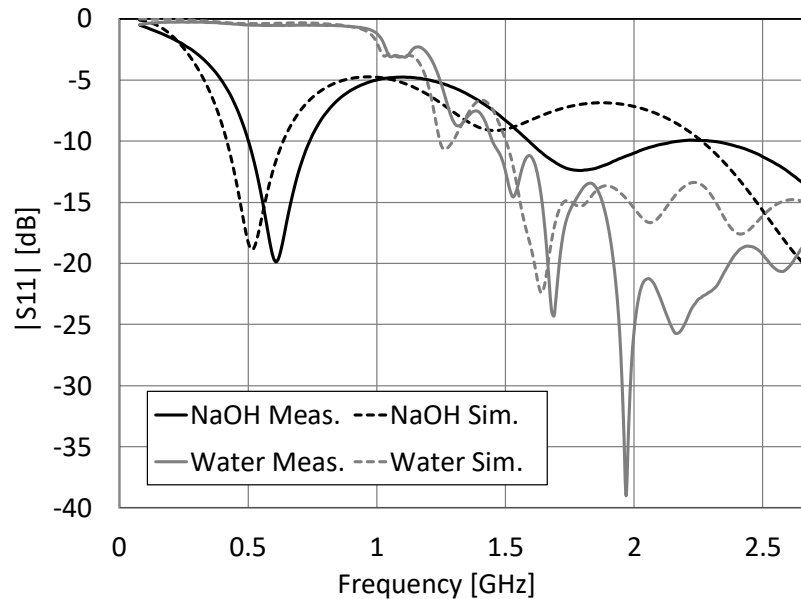


Figure 3. Simulation (Sim.) and measurement (Meas.) results of reflection coefficient  $|S_{11}|$ . Liquid sample is 2 M NaOH solution (NaOH) or ultrapure water (Water) at room temperature.

## CONCLUSION

A small-size microwave applicator of 20 ml was designed and developed. It is verified the microwave irradiation over a wide frequency range from 1.6 GHz to 2.7 GHz is realized by using the developed applicator without impedance tuning.

## ACKNOWLEDGEMENTS

This work was supported by CREST, JST. Measurements of the reflection ratios were conducted through a collaborative research program: the Analysis and Development System for Advanced Materials (ADAM) at the Research Institute for Sustainable Humanosphere, Kyoto University.

## REFERENCES

- [1] T. Mitani, N. Hasegawa, R. Nakajima, N. Shinohara, Y. Nozaki, T. Chikata and T. Watanabe, Development of a Coaxial Microwave Applicator for Liquid Heating over a Wide Frequency Range, *Proc. 50<sup>th</sup> IMPI Microwave Power Symp., Orlando, FL, June 2016*, pp. 79-81.
- [2] T. Mitani, N. Hasegawa, R. Nakajima, N. Shinohara, Y. Nozaki, T. Chikata and T. Watanabe, Development of a wideband microwave reactor with a coaxial cable structure, *Chem. Eng. J.*, vol. 299, pp.209-216, 2016.

# Microwave-assisted Mechanical Equipment in Mining Industry

**P. Nekoovaght**

Canmet MINING, Natural Resources Canada, Ottawa, ON, Canada  
Email: [pejman.nekoovaght@canada.ca](mailto:pejman.nekoovaght@canada.ca)

**Keywords:** Microwave-assisted rock breakage, microwaves in mining, rock comminution, microwave-assisted rock excavation.

## INTRODUCTION

One of the major challenges of mining industry is rock breakage, especially hard rocks. Rock breakage in any sense starts from extraction from its host (rock mass) all the way through the mineral processing circuit producing a few micron-sized particle powders. Transforming large sizes of rock extracted from its host to very fine powder is an energy intensive procedure.

Novel rock breakage techniques are becoming more viable and attractive to industry. Microwave power, as a technology that turns into thermal energy within a dielectric, is capable of inducing micro cracks through differential heating (therefore expansion) [1, 2, 3]. The application of microwave assistance is a technology gaining considerable attention in mineral processing and ore comminution applications. Recently, the use of microwave has been evaluated as a possible avenue for terrestrial and extra-terrestrial rock breakage (i.e. drilling) applications. Microwave-assisted full face tunneling machine is also another potential rock cutting technique that has been recently introduced. As part of an overall research on the use of microwave power in rock breakage, the influence of microwave energy on the mechanical properties of some common hard rock types has been investigated [4, 5, 6, 7, 8, 9, 10]. Experimental and simulation results underlined the potential impact of the use of microwave energy in underground or surface excavation as well as comminution applications. This will also contribute economically within a continuous mining method of operation. It also outlines the potential impact of a microwave power in comminution enhancing ore recovery.

The current research investigates the mechanism of stress development within natural rock materials when exposed to microwave irradiation. The understanding of such mechanism leads to the development of a mechanical rock breakage system combined with microwave technology.

## METHODOLOGY

One of the parameters that plays a very important role defining the amount of energy absorption is the volume and shape of the load within the electromagnetic field. A

variable power microwave apparatus able to irradiate up to 15 kW is used to treat various dimensions and volumes of rocks. An open horn antenna concept has been chosen to irradiate the surface of large blocks of rocks. For smaller sizes of rock particles, a multi-mode cavity is used with a mode stirrer inside to spread the energy intensity throughout the cavity. A few rock types are used, such as intrusive basalt, granite, norite and lime stone, to understand the influence of the microwave irradiation on their physical and mechanical properties. Analytical and numerical modelling studies are conducted extensively to understand the heat generation and damages caused respectively.

**RESULTS & DISCUSSION**

Theoretically, the penetration depth of microwave inside a dielectric is defined by the wavelength and electric intensity, which drops at 1/e of its surface intensity. The geology of rock materials have a natural and complex characteristics that are necessary to be taken into account. In mining applications, the destruction of the rock is key; therefore, the damage caused by the volumetric thermal expansion phenomenon is the objective to weaken the rock for further fragmentation.

The thermal characteristic of natural rocks indicates a low thermal conductivity in general. Depending on the shape and dimension as well as the electrical characteristics of rocks when exposed to microwave irradiation, the energy that transforms into heat may cause the temperature rise whether from the inside-out or from the outside-in the dielectric. The difference of temperature ( $\Delta T = T_2 - T_1$ ) will cause stress generation due to volumetric expansion; thus physical damage occurs.

In the case when the rock is a good absorbent and is larger than the wavelength of the microwaves irradiating, the concentration of heat starts from the surface toward inside the rock. Due to the nature of rock that is composed of more than two minerals, which has their own characteristics individually, the overall temperature difference leading to physical damage occurs at a different level than the theoretical penetration depth defined by the electric intensity (Figure 1). Such phenomenon lead the surface of the rock to spall as shear failure happens in the periphery of the affected area and tensile failure occurs in the center due to the volumetric expansion ratio difference (Figure 2).

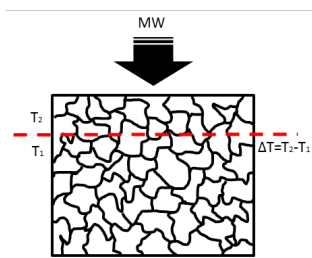


Figure 1. Imaginary depth where  $\Delta T$  would be at its highest.

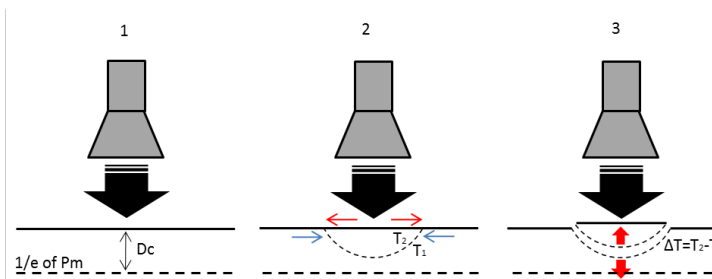


Figure 2. Mechanism of rock failure when exposed to microwave irradiation.

Such phenomenon of stress variation on the surface of the rock also occurs within a smaller size of rocks as well. The surface damages due to volumetric expansion can benefit to precondition the surface of the host rock to be broken by a mechanical machine at a higher efficiency and performance. Microwave irradiation may come in assistance with the mechanical machine for excavation purposes as described in [4, 5, 6, 10]. The in-depth volumetric expansion also may benefit the smaller size of rocks passing through the comminution circuit for mineral processing purposes.

## CONCLUSION

Natural rocks that are composed of a number of minerals behave differently within an electromagnetic field as all materials. Some transmits, some reflects and some absorbs partially the microwave energy and are called dielectrics. The loss factor of each rock is strongly defined by its mineral composition as well as grain sizes. To break further down of those rocks susceptible to microwaves there is great potential to improve the mechanical machines with microwave-assistance technology.

## REFERENCES

- [1] Maurer, W.C. *Novel Drilling Techniques*. London: Pergamon Press. 1968.
- [2] Chen, T.T.; Dutrizac, J.E.; Haque, K.E; Wyslouzil, W. and Kashyap, S. Relative transparency of minerals to microwave radiation. *Canadian Metallurgical Quarterly*, 23(3), 349-351. 1984.
- [3] Church, R.H., Webb, W.E. and Salsman, J.B. Dielectric properties of low-loss minerals. United-States Department of the Interior and The Bureau of Mines, Report of Investigation RI-9194. 1988.
- [4] P.Nekoovaght. *Physical and mechanical properties of rocks exposed to microwave irradiation: potential applications to tunnel boring*. McGill University, Montreal, 2015.
- [5] P.Nekoovaght and F.Hassani. The influence of microwave radiation on hard rocks as in microwave assisted rock breakage applications. *Rock engineering and rock mechanics: Structures in and on rock masses, The ISRM European rock mechanics Symposium (EUROCK 2014)*. Vigo, Spain., pp. 195-198. 2014.
- [6] P.Nekoovaght, N.Gharib and F.Hassani. Numerical simulation and experimental investigation of the influence of microwave radiation on hard rock surface. *Rock mechanics for global issues – natural disasters, environment and energy. ARMS8 – ISRM International symposium – 8<sup>th</sup> Asian rock mechanics symposium*. Sapporo, Japan, 7 p. 2014.
- [7] P.Nekoovaght, N.Gharib and F.Hassani. Microwave assisted rock breakage for space mining. *ASCE's Aerospace Division, 14th Earth and Space Conference*. St. Louis, Missouri (USA), 9 p. 2014.
- [8] P.Nekoovaght, N.Gharib and F.Hassani. Microwave assistance positive influence on rock breakage in space mining applications. *65<sup>th</sup> International Astronautical Congress*. Toronto, Canada, 7 p. 2014.
- [9] P.Nekoovaght, N.Gharib and F.Hassani. The behaviour of rocks when exposed to microwave radiation. *13th International Congress on Rock Mechanics (ISRM)*. Montreal, Canada, 11 p. 2015.
- [10] F.P. Hassani, P.Nekoovaght, and N.Gharib, The Influence of Microwave Irradiation on Rocks for Microwave-Assisted Underground Excavation Technique, *Journal of Rock Mechanics and Geotechnical Engineering*, 15 p. 2015.

# In-liquid Plasma using Microwave Power for Waste Water Treatment

S. Sawada, A. Tsuchida and S. Horikoshi

Sophia University, 7-1 Kioi-cho, Chiyoda-ku, Tokyo, 102-8554, Japan

**Keywords:** Microwave plasma; in-Liquid plasma, Wastewater treatment; Photocatalyst

## INTRODUCTION

Waste disposal contractors have treated solvents, organic chlorines and dyes which cannot be separated in factories by combustion. However, the pollution processing efficiency is low because of a lot of included water. Moreover, the combustion produces toxic degradation by-products. Electrical and physical phenomena in submerged plasma has been investigated [1]. The present investigation studied a novel in-liquid plasma excited by microwave power to degrade organic waste water. This method advantageously ignites a plasma even if the solution is not electrolytic. However, the microwave antenna melted from the plasma heat. Improvement by decompression was tested. The antenna was not melted and could continue to light up in-liquid plasma in this condition. The decomposition efficiency of the device was evaluated by the degradation of 1,4-dioxane, rhodamine B dye, hypochlorous acid, and herbicides (asulam or atrazine) as model waste waters. As a further challenge, it combined the in-liquid plasma with photocatalyst degradation process as a hybrid method.

## METHODOLOGY

A photograph and schematic diagram of the in-liquid plasma device is presented in **Figures 1**. The microwave generator was constructed using a Micro Denshi Co., Ltd. 2.45-GHz microwave generator (maximal power, 1500 W) coupled to an air-cooled isolator, a power monitor, a three-stub tuner and a short-circuit plunger. Microwaves continuously irradiated the liquid through a tungsten antenna (dia.: 10 mm; length: 200 mm). Metal cones were used in the waveguide to efficiently focus the microwaves onto the tungsten antenna tip, through which the microwaves irradiated the aqueous solution and generated the in-liquid plasma. The tungsten antenna was isolated from the reactor and the waveguide using a ceramic spacer, such that the microwave irradiated only the solution. The cylindrical-shaped reactor consisted of an 80-mm dia. quartz vessel, fabricated such that the pressure could be reduced from the top of the reactor using an aspirator. The irradiating microwaves were adjusted by a three-stub tuner such that there were no reflected waves. The emission spectrum of the in-liquid plasma was measured through an optical fiber

using a UV-Vis spectrophotometer (Ocean Optics MayaPro2000). The measured spectrum was analyzed using Ocean Optics PLASUS SpecLine software (Ver. 2.1). The model waste water (50 mL; 1,4-dioxine, rhodamine B dye, hypochlorous acid, asulam and atrazine) was placed in the quartz reactor.

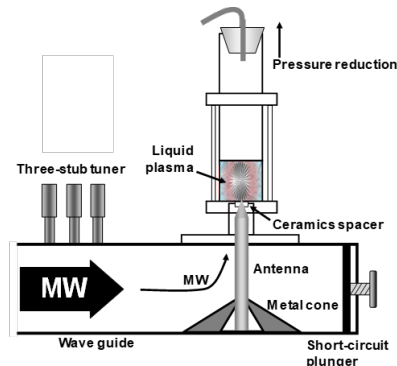


**Figure 1.** Schematic diagram of the in-liquid plasma device.

## RESULTS AND DISCUSSION

One of the problems in generating plasma continuously in the liquid using microwave radiation at high applied microwave power levels is the deterioration of the tungsten antenna tip because of the heat produced by the plasma that can reach temperatures well above the melting point of tungsten (3422 °C). In this regard, **Figure 2i** shows photographs of three tungsten antennas. The tip of a new unused tungsten antenna is displayed in **Figure 2i-a**, while **Figures 2i-b** and **2i-c** display the antennas after use in treating aqueous media contaminated with 1,4-dioxane employed as a test pollutant. After the device performed water treatment of the pollutant, the antenna was not melted in **Figure 2i-b** and the top of one was melted in **Figure 2i-c**. Using the apparatus shown in **Figure 1**, approximately 700 W of microwave power was required to generate plasma in pure water under atmospheric pressure (101.3 kPa). However, after generating the in-liquid plasma for 20 s the antenna was observed to have been severely deteriorated as shown in **Figure 2i-c**. On the other hand, reducing the pressure to 22 kPa in the reactor with an aspirator generated in-liquid plasma that necessitated only a microwave power output of 150 W, which when increased to 200 W yielded thereafter stable in-liquid plasma. Most importantly, under the latter conditions no deterioration of the antenna occurred even if the in-liquid plasma was generated and used continuously for about 1 hr (**Figure 2i-b**). This phenomenon seems to be due to the fact that the boiling point of the aqueous solution is lowered together with the number of bubbles, in addition to the pressure reduction in the fine bubbles as a result of the reduced pressure. Moreover, it is also possible that oxidation was suppressed in the aqueous solutions because the amount of dissolved oxygen increased due to the reduced pressure. When the microwave power was less than 150 W, no plasma was generated in the liquid. Microwave leakage outside the reaction vessel under our experimental conditions were investigated using a leak detector; none was detected.

Further, the microwave energy not consumed by the plasma was absorbed by the aqueous solution in the reaction vessel.

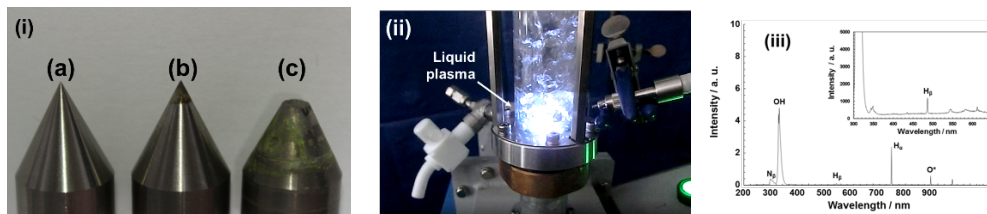


**Figure 2.** (i) Photographs showing (a) a new antenna tip, (b) the antenna tip after a 1-hr continuous generation of the in-liquid plasma inside the reactor under depressurized conditions (pressure: 22 kPa), and (c) antenna tip after a 20-s continuous generation of the in-liquid plasma under atmospheric pressure (101.3 kPa). (ii) Photograph of the generated in-liquid plasma with 150 W microwave power in reduced pressure (pressure: 22 kPa). (iii) Spectrum of the light emitted from the in-liquid plasma generated in pure ion-exchanged water.

A reasonable mechanism for the generation of in-liquid plasma considers that the water near the tip of the tungsten antenna has evaporated through microwave heating, causing the plasma to be generated within the vapor bubble. It further considers the boiling point of water to be lowered by depressurizing the inner part of the reactor, thereby facilitating the water near the antenna to form bubbles and facilitating the generation of plasma even under microwave irradiation at low power levels. Evidently, a decrease of the microwave power reduces the stress at the tip of the antenna, so that it didn't deteriorate.

The in-liquid plasma generated in ion-exchanged water at a microwave power of 200 W emitted a pale blue light (**Figure 2ii**). An analysis with a UV-visible spectrophotometer (**Figure 2iii**) revealed relatively intense emission lines attributed to formation of  $\cdot\text{OH}$  radicals (316 nm),  $\text{H}_\alpha$  hydrogen (656 nm) and to  $\text{O}^*$  oxygen (778 nm); peaks belonging to  $\text{N}_\beta$  nitrogen (289 nm), CO (298 nm) and  $\text{H}_\beta$  hydrogen (484 nm) were also detected, albeit less intense. Note that the plasma was generated in the inner part of the microbubbles formed near the antenna (Fumagalli et al., 2012; Kregar et al., 2009; Nomura et al., 2008).

Water with dissolved 1,4-dioxane was degraded using in-liquid plasma (LP) with the equipment in **Figure 1**. The LP method was compared with other more conventional waste water treatment methods such as UV photodegradation, NaClO chemical treatment, UV/NaClO chemical/photodegradation and the UV/TiO<sub>2</sub> photocatalytic degradation method (NaClO (0.5 mg · L<sup>-1</sup>), TiO<sub>2</sub>-particles (P-25; 10 mg) and solution volume: 50 mL).

The order of degradation was shown to be LP (34%) > UV/NaClO (12%) ≈ NaClO (12%) > UV/TiO<sub>2</sub> (10%) > UV (0%). Though the experimental conditions were not totally identical, nonetheless the in-liquid plasma method was significantly more effective than the conventional water treatment methods.

## REFERENCES

- [1] S. Horikoshi and N. Serpone, *RSC Adv.*, Vol.7, pp. 47196–47218, 2017.
- [2] A. Tsuchida and S. Horikoshi, et. al., *Rad. Phys. Chem.*, accepted 2018.

# Development and Evolution of Novel Hg-free Electrodeless Lamp using Microwave-synthesized Quantum-dot Luminescence

K. Hagiwara and S. Horikoshi

Sophia University, 7-1 Kioi-cho, Chiyoda-ku, Tokyo, 102-8554, Japan

**Keywords:** Mercury-free lamp; Quantum-dot, Microwave chemical synthesis

## INTRODUCTION

The Minamata Convention, an international treaty regulating the manufacture, import and export of products using mercury, was concluded in 2013, and enacted in 2017, from which time the sale of mercury lamps became limited. In response to this, the switching of the LED from the fluorescent lamp advanced; however, since the LED is a point (dot) light source, it is known to be inconvenient for use in gymnasiums, machine factories, and plant factories, etc. Also, since the LED is a point light source, it creates a very intense light and there is a problem with hand shadows over work pieces. Therefore, there are many demands that LEDs should produce similar light quality to a classical surface light source. Since 2000, we have been developing microwave discharged electrodeless lamps (MDELs) using microwaves as energy sources [1]. This lamp has a very long life like an LED. In this research, we examined substitution of mercury with another gas, using our developed lamp as a platform. When determining the optimum filling gas for various conditions, it was also necessary to develop a fluorescent agent with higher luminous efficiency. For this purpose, we synthesized quantum dots to be used by the microwave system as a possible fluorescent agent.

## METHODOLOGY

The quartz valve of the ampule type was installed in the vacuum system, the pressure inside the valve was reduced, and the sealing gas was introduced. This series of operations was done with a prototype gas inclusion and lighting test equipment (**Figure 1a**). A single or mixed gas of nitrogen (N<sub>2</sub>), argon (Ar), helium (He), xenon (Xe), or sulfur hexafluoride (SF<sub>6</sub>) was sealed in a synthetic quartz lamp bulb prototyped for gas selection. The conditions of the filling gas were adjusted for pressure (10000 to 10<sup>-2</sup> Pa) and mixing volume ratio (1:1, 1:3, 3:1). In the experiments, a radio frequency (RF) generator was used as the energy source, not microwave. Note that a RF system can be

achieved with a simple device configuration. With reference to the results of the electric field simulation (**Figure 1b**), a lamp and a high frequency electrode were installed. Encapsulated gas was excited to emit light by applying RF, and its emission spectrum was measured with an Ocean Optics Maya 2000 pro spectrophotometer. Lamps used for gas selection were determined with reference to the results of the electric field simulation, and appropriate gas was selected with reference to the wavelength and intensity of the emission spectrum from the enclosed gas.

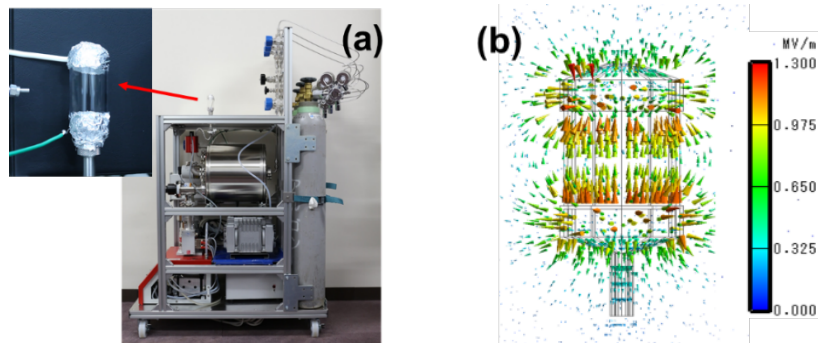


**Figure 1.** (a) photograph of prototype gas inclusion and lighting test equipment and (b) schematic illustration of electric field computer simulation of lamp with RF electrodes.

## RESULTS AND DISCUSSION

Each excitation gas was sealed under various conditions, and a light emission experiment was performed under application of RF system. Various emission spectra were observed under the kinds and/or conditions of parged gases when experiments were conducted. Due to the measurement of the spectrum, the light in the ultraviolet region occurred in a variety of ways, and the gas with the strongest intensity was SF<sub>6</sub>-N<sub>2</sub> mixed gas.

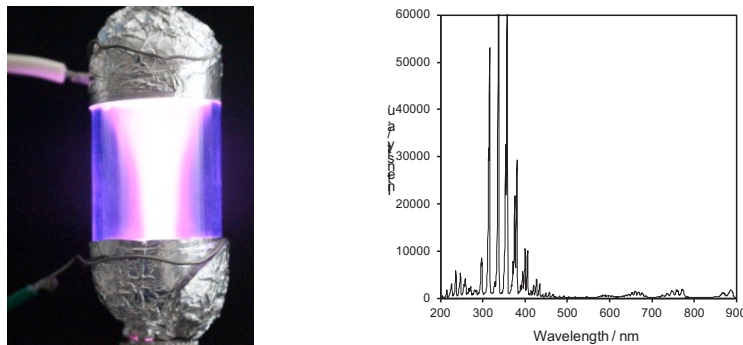


**Figure 2.** Photograph of electrodeless lamp with parged SF<sub>6</sub>-N<sub>2</sub> gas and emission UV/Vis spectrum of this lamp

Compared with the existing mercury lamp, it was able to show the same intensity of emission spectrum. However, unlike mercury luminescence (254 nm), luminescence was observed at 300-400 nm. Therefore, a fluorescent agent, having a high luminescence conversion ratio, meeting this requirement was required. We focused on quantum dots.

Quantum dots (QDs) are useful for various applications because of their photoluminescent characteristics, depending on their particle size, which could not be observed in bulk. In general, CdE (E=S, Se, Te) QDs, included in II-VI Group semiconductor nanoparticles, have been known to industry. However, the substitute QD materials have been required, because the use of Cd materials have been strictly regulated since 2016. We tried to synthesise efficient, low-toxic, environmentally-harmonized heavy metals-Free, low cost CuInS<sub>2</sub> (core) and CuInS<sub>2</sub>/ZnS (core/shell) QDs using microwave heating. We used multimode microwave chemical equipment (EYELA corp. Wavemajic) through batch process and the solution was microwave-heated with multimode. To compare conventional heating with microwave heating, the condition of reaction, such as the shape of flask, reaction temperature, metal precursors, solvent etc., was oriented to the condition in conventional heating process. Comparison was carried out with PL-spectra (excited wavelength: 450 nm), XRD, TEM, DLS, EDX. In both conventional and microwave heating process, the size of QDs were dispersed in the range of 3-7nm and crystal shape was observed. However, the core QYs in microwave heating was 9.1 % and full width at half maximum (FWHM) was 128 nm, while those in conventional heating was 6.2 % and FWHM was 151 nm, highlighting that synthesis in microwave heating is better than conventional heating in terms of high QYs and low O<sub>2</sub> molecular inclusion. The heating time was changed from 30 min to 5min due to microwave rapid-heating and higher quality core QDs (QYs: 11.2%, FWHM: 122 nm) could be synthesized in 1/6<sup>th</sup> of the heating time. In respond to this result, core/shell QDs were synthesized by microwave and conventional heating through a hot injection process. The quality of core/shell QDs is higher than that of core QDs. The quality of microwave-heated core/shell QDs is higher than that of conventionally-heated ones, even though lower blue shift could be seen in microwave-synthesized core/shell QDs (**Table 1**).

**Table 1.** QYs and HWHMs of CuInS<sub>2</sub> (core) and CuInS<sub>2</sub>/ZnS (core/shell) QDs characterized in this research (MW: Microwave; CH: Conventional heating)

Heating condition	Particle type	FWHM / nm	QYs / %
MW	core/shell	111	18.9
MW (rapid)	core	122	11.2
MW	core	128	9.1
CH	core/shell	117	17.3
CH	core	151	6.2

We ensured that it is possible to efficiently synthesize high-quality CuInS<sub>2</sub> (core) and CuInS<sub>2</sub>/ZnS (core/shell) using further optimization and flow process. The synthesized QDs were applied to the inner surface of the lamp and the emission was observed. Details will be reported within the presentation.

## REFERENCES

- [1] S. Horikoshi, M. Abe, and N. Serpone, *Photochem. Photobiol. Sci.*, Vol.8, pp. 1087–1104, 2009.

# Solid-state RF Energy: The Industry After the First Consumer Launch

**Dr. Klaus Werner**

RF Energy Alliance, Beaverton, Oregon 97003 USA  
[www.rfenergy.org](http://www.rfenergy.org)

**Keywords:** Solid state RF power amplifiers, RF energy applications, amplifier technology, roadmaps, consumer markets, RF Energy Alliance

## **ABSTRACT**

Solid-state radio frequency (RF) technology used for heating and power delivery applications has taken hold in the last couple of years in a number of markets and has given rise to the notion of RF Energy applications. The new technology is currently being designed into a number of different applications like microwave ovens, RF plasma lighting, automotive plasma ignition, and medical cancer treatments. Likewise for industrial use, where all kinds of heating, drying, curing, sintering or similar processes are currently being developed with solid-state RF energy rather than the legacy magnetron as the driving source.

With the launch of a commercial oven (IBEX One) and a high-end consumer system by Miele at Internationale Funkausstellung Berlin in autumn 2017, the long awaited “firsts” have finally happened. The consumer oriented solution is particularly significant, since it will break the chicken and egg problem of going to market with an “expensive” new technology.

This presentation will discuss the consequences of these launches for solid-state RF energy technology, the impacted markets and end users in more detail. Furthermore, the paper will highlight the recent RF Energy Alliance progress in developing specifications and guidelines for the advancement and adoption of solid-state RF generator subsystems for RF Energy applications.

# High Power Combining and Control Techniques for 2450MHz Solid-state Power Amplifiers

Rick Rigby<sup>1</sup>

<sup>1</sup>Ampleon USA, Smithfield, RI, USA

**Keywords:** Solid State, High Power, Phase calibration.

## INTRODUCTION

Frequently there is a requirement to generate high power CW sources for industrial processing and heating. This power level has traditionally been generated by magnetrons however there are significant advantages in using solid-state devices in this application. Since the power levels generated by a single transistor is currently a few hundred watts combining is needed to replace the 10s of kW generated by magnetrons. In this paper we will examine: Software and hardware techniques to mitigate amplitude and phase imbalance in the individual amplifiers; Control and calibration schemes to combine combined collections of amplifiers.

## EQUIPMENT AND PROCEDURE

In this demonstration, two 60dBm 2.45GHz RF generators were combined to generate 63dBm. Each of the 60dBm RF generators internally combines four 250W(54dBm) pallets to generate its 60dBm output.

First, consider the individual 60dBm generator: Figure 1a illustrates the combining of the outputs of four pallets inside a compact 60dBm generator. Each 60dBm generator contains an MCU to run control firmware. An IQ modulator chip is used to generate the 2.45GHz frequency at low power. The phase of the synthesized waveform can be adjusted with the quadrature input value which allows phase matching of the 60dBm module when used in a larger, combined system. Circuitry was included between the synthesizer and the driver amplifier to allow for phase and gain adjustment of each channel. During individual module testing, phase and gain are adjusted to match the four channels. These phase and gain values persist in non-volatile DAC's. Once each module has phase and gain matched, each module is calibrated to determine the in-phase DAC setting for requested output powers between 40.0dBm and 61.0dBm in 0.5dBm steps. This is repeated over the frequency range of the module, in this case 2.41GHz to 2.49GHz at 20MHz intervals. These calibration tables are persisted in non-volatile memory and restored on power-up.

Runtime user power requests are interpolated in power and frequency to program the correct in-phase DAC value.

Second, the combined multi-kilowatt system: To build-up a multi-kilowatt system several 60dBm modules were combined. Figure 1b illustrates the combining of multiple 60dBm systems to make up a 67dBm 2.45GHz RF generator system using a radial combiner. Our setup combined two 60dBm modules. When combining multiple generators to create a system generating more than 60dBm it is necessary to use several hardware lines between generators, and designate one generator as ‘master’, to provide the reference clock. The firmware could be modified so that the designated ‘master’ unit performed changing power or frequency provided there was a communication port between the modules such as RS232/485. In our setup we used a host computer application to orchestrate changing power and frequency settings. The hardware handshake lines are shown in Figure 2a. There is the reference clock line, and a SYNC line. As already mentioned, the reference clock line is the reference clock from the synthesizer circuit of the module designated as the ‘master’. This common clock creates a coherent system, IQ modulators in all modules are using the same clock. The SYNC line is an open-drain line used by all modules to coordinate a setup change. During normal operation the ‘master’ unit pulls the SYNC line high and all modules continuously monitor the SYNC line. When any module receives a command to change setup from the host computer, the module pulls SYNC low. Each modules RF output is gated by the SYNC line. When SYNC goes low, all RF outputs are turned OFF. Each module processes the setup command. When processing has finished and a module is ready to turn RF ON again, the module releases the SYNC line. When the last module to finish processing releases SYNC, SYNC goes high. This gates RF ON for all systems.



Figure 1. Internal four way microstrip combiner for 60dBm[1] (a) and radial combiner combining 60dBm systems for multi kilowatt output[1] (b).

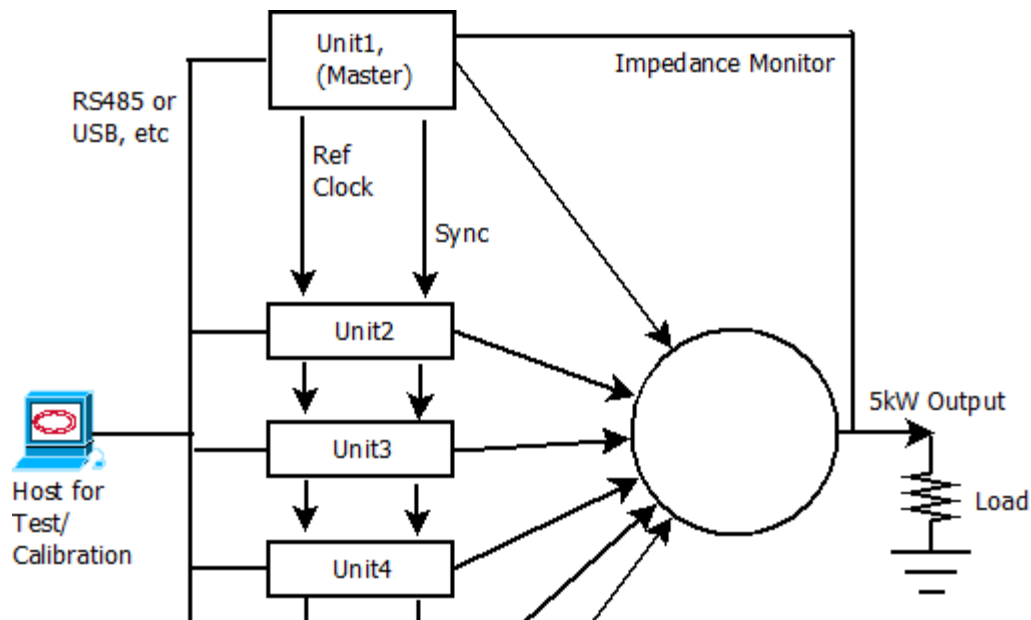


Figure 2a. Block diagram showing control signals between modules for a 67dBm system built from six 60dBm RF generators.

## RESULTS

We were able to calibrate and run a combined 63dBm system from a host computer using these techniques. A calibration table was built in 0.5dBm steps from 40.0dBm to 63.0dBm.

## DISCUSSION

Our results showed that operation of combined solid-state 2.45GHz pallets can be done using the techniques illustrated to provide calibrated solid-state system outputs greater than 60dBm. This technique can be used to further application development in areas where magnetron replacement with more compact and flexible systems operating at much safer DC voltages is desirable.

## CONCLUSION

We were able to verify that our design of a 60dBm RF generator with appropriate interface signals works well in combined solid-state systems yielding power outputs greater than 60dBm. This is a suitable way to use relatively low power solid-state 2.45GHz pallets to build systems with calibrated multi-kW power outputs.

## REFERENCES

- [1] R. Williams and B. Bartola, *Multi-kW Microwave Generators using LDMOS for Industrial Heating Applications*, IMPI 50, 2016.

# Microwave Assisted Manufacturing of Package-less Coffee-tablet: Magnetron Vs Solid State Sources

M. Garuti<sup>1</sup>, P. Veronesi<sup>2</sup>, E. Colombini<sup>2</sup>, M. Chenda<sup>3</sup>

<sup>1</sup>MKS Alter, Reggio Emilia, Italy

<sup>2</sup>University of Modena and Reggio Emilia, Italy

<sup>3</sup>Caffemotive, Trieste, Italy

**Keywords:** Solid state microwave generator, food product, coffee tablet

## INTRODUCTION

Coffee brewing machines use soft (bags) or semi-rigid (capsule) disposable containers to host loose or mildly pressed coffee powders, ready to use. The outstanding taste achievable by this technology has its counterpart in the higher cost per brewed cup, but more importantly, in the generation of large quantities of waste (for instance, spent capsules). Aim of this work is to describe a new microwave-assisted process suitable for the industrial production of filter- and capsule-less coffee doses, able to self-adapt to different loading conditions. The basis of the process is the use of localized heating to generate water vapor to bond granules [1], held under pressure, without any additive. If conducted by conventional means (injection of vapor, conventional heating of pressed powders), this process would result extremely time demanding and it would lead to the partial extraction of some of the active principles from the powdered bean. Microwave volumetric heating, limited on purpose to a few millimeters from the surface of pressed coffee powder, allows to generate enough steam to form a free-standing disc-shaped pellet, which can be used directly in brewing machines, coupling the advantages of capsule-coffee with the quality and environmental friendliness of freshly ground coffee

Based on these premises, a new microwave applicator, operating at 2.45 GHz, has been modeled, designed and tested on milled beans. Two different microwave sources have been used for validation tests, namely a magnetron generator and a solid state generator, and the advantages of the latter are addressed in this paper.

## METHODOLOGY

Dielectric properties of the load have been measured as a function of temperature and moisture in the 0.5-3 GHz range using an Agilent 85070 Dielectric probe kit. Measurements have been conducted under pressure, in order to generate over-saturated vapor only at the required pressure level, which will be set in the final applicator. Temperature dependent thermal properties have been used from literature [2] and used to model the microwave heating behavior of pressed disc-shaped loads, at 2-45 GHz

frequency. Figure 1 shows the initial model geometry, which has been completely parameterized in order to perform optimization on the key factors governing the heat generation pattern and efficiency, i.e. the microwave feed position, load position and applicator dimensions (inner radii). Microwaves are fed in the applicator by a coupling loop, through a coaxial port and the load is kept in position by a PTFE mold, whose end can be moved to ease loading, pressurizing and unloading of the product. Load geometry is constrained by compatibility with existing brewing machines, hence it has been set to a disc-shaped geometry, 56 mm of diameter and 9-11 mm of height.

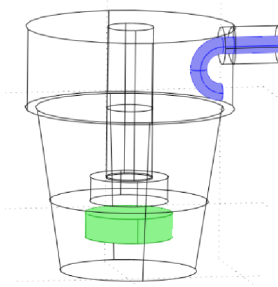


Fig. 1. Model geometry, with the disc shaped load (bottom) and coupling loop (top) highlighted.

Due to the process requirement (heating the outer shell of the load), optimization was conducted maximizing the average temperature of the outer shell (2 mm thickness) after 5 seconds of microwave heating at 500W and minimizing the variance of temperature in such zone. The first objective indirectly addresses energy efficiency, quantified also by the reflection coefficient, while the second one is used to estimate homogeneity of heating. Optimization was conducted using the Response Surface Method, to achieve a response surface able to predict the temperature distribution in the load as a function of the applicator geometry and load position, and to evaluate the robustness of the process under study.

Based on the modeling result, an easier coupling loop has been designed, and the introduction of a tuning metallic stub has proved essential to achieve a proper impedance matching at 2.45 GHz, as a function of different loading conditions.

## RESULTS

Qualitative 3D plot of the optimized solution is shown in Figure 2, demonstrating how heat is selectively generated in the outer shell of the load ( $|S_{11}| = 0.12$  in absence of tuning stub, at 2.45 GHz).

Based on the numerical simulation results, a functioning prototype has been built and tested using a magnetron source (maximum power = 1 kW). It was discovered that the total amount of power delivered did not match with theoretical calculation and was in excess of 1/3 approximatively. The use of a spectrum analyzer shown that the magnetron was running at a correct frequency and with an acceptable spectrum only when water was present inside the product: going forward on heating, spectrum became unexpectedly larger with several harmonics of important amplitude.

Alternatively, microwave power was provided by an MKS-Alter SG524 solid state generator, operating at 2.45GHz and capable of varying the frequency  $\pm 50$  MHz. achieving a satisfactory impedance matching during heating (average reflected power  $< 5\%$ ) without the need for any moving part (metallic stub). As the applicator is a resonant cavity, and because the product changes its dielectric properties with the temperature, thus moving the whole cavity resonance, the change in frequency allowed to adapt the impedance.

The system, in steady state conditions and using the solid state generator, is able to produce a single coffee pellet in less than 5 seconds, including loading and unloading operations, operating in parallel on 3 separate stations. Results, including operating frequency and reflected power vs time, will be presented as well.

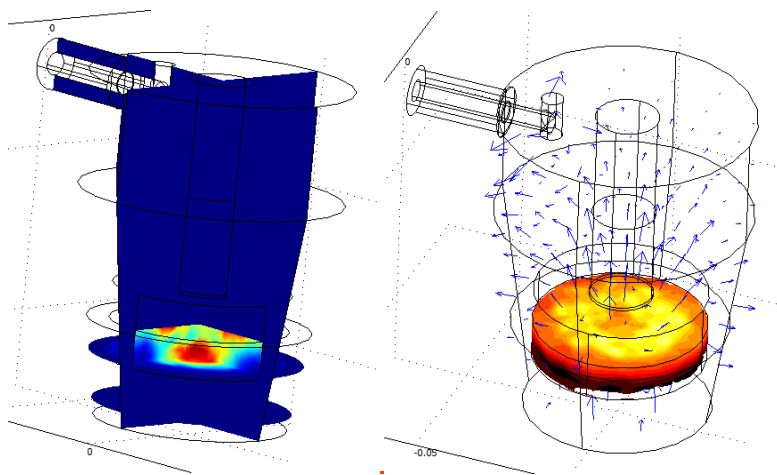


Figure 2: resistive heating plot showing localized heat generation (qualitative scale)

## CONCLUSION

The coupled use of design of experiment in a simulation environment allowed to rapidly design an efficient microwave applicator dedicated to the consolidation of powdered coffee to produce disc-shaped doses for use in current brewing machines. Self-generated steam pressure and rapid microwave heating, localized at the surface of the disc-shaped load, allows to create a compact outer shell which provides good mechanical properties, without altering the product flavor. The use of a solid state generator that allows automatic frequency tuning resulted in a saving of one forth of the total energy used.

## REFERENCES

- [1] Bhadra, R., Rosentrater, K. A. & Muthukumarappan, K. Measurement of sticky point temperature of coffee powder with a rheometer. *International Journal of Food Properties*. 16(5):1071-1079, 2013
- [2] V. Chandrasekar, R. Viswanathan, "Physical and thermal properties of coffee", *J. Agr. Eng Res.*, vol 73 pp 227-234, 1999
- [3] C. Leonelli, G.C. Pellacani, C. Siligardi, P. Veronesi, Microwave assisted burn-out of organic compounds in ceramic systems, in: *Key Engineering Materials*, vol 264-268, pp. 739-742, 2004

# Solid State Plasma Light source operated by a differential RF applicator

Dr. S. Holtrup<sup>1</sup>

<sup>1</sup>pinkRF, Nijmegen, Netherlands

**Keywords:** Solid state RF, RF lighting, microwave energy, solid state plasma lighting, plasma ignition, plasma operation

## INTRODUCTION

RF lighting technology is already known since mid of the 1990s. Until today most of RF lighting technology bases on magnetrons and cover a field of applications that requires high luminous intensities. Solid state plasma lights (SSPL) can extend the field of applications where lower luminous output is required. Although this type of lamps can operate with many different fillings suitable for specific requirements of industrial applications, like greenhouse lighting or UV light applications.

To drive a SSPL at low power levels, e.g. from several watts to 250 W, a bi-stable network is required [1]. The bi-stable network matches the two different main operation states of the lamp – ignition and operation. Therefrom the network received its name. For the ignition the fillings are in their initial state of matter, so the lamp can simply be described as a bulb filled with an inert gas. The ignition requires a high field strength, generated by the bi-stable network at a desired frequency. Once ignited, a plasma is formed in the bulb and creates a completely different load. The frequency is changed to provide best match for this load condition. Typically, these lamps are operated within the ISM band at 2.45 GHz. The bandwidth of this band is sufficient to match the SSPL with one static network for both conditions. The RF power is generated by a solid-state driver, that sets precisely the frequency at best match during operation. The power levels can be adjusted in PWM or CW mode for each state and diming likewise. The SSPL in this paper is built-up with a differential network, that delivers a higher ignition voltage across the bulb and is more robust against manufacturing tolerances. This is important to ensure the ignition of the lamp, because of the limited available power by means of the maximum power required in the specific application.

## EXPERIMENTAL APPARATUS

Two electrodes guide the electrical field towards the light bulb. This system builds up a differential pair and causes higher electrical field strength in between the electrodes and hence in the light bulb itself compared with asymmetrical designs. The differential signal is generated from an asymmetrical signal via a sleeve balun [1]. A high field strength

is necessary for the safe ignition of the lamp. Once the plasma discharge has been ignited, the impedance of the applicator changes. A specific matching circuit covers the matching in both cases – for ignition and operation. It is built in the applicator before the symmetrical network. The impedance at this point for both cases can be measured by using the Hot-S-parameter method [1]. Once knowing the impedances of the lamp, the network is developed to match both cases within the band of 2.4GHz to 2.5 GHz. To perform in both situations, a frequency-agile generator is required and therefore this lamp topology can only be supported by solid state RF.

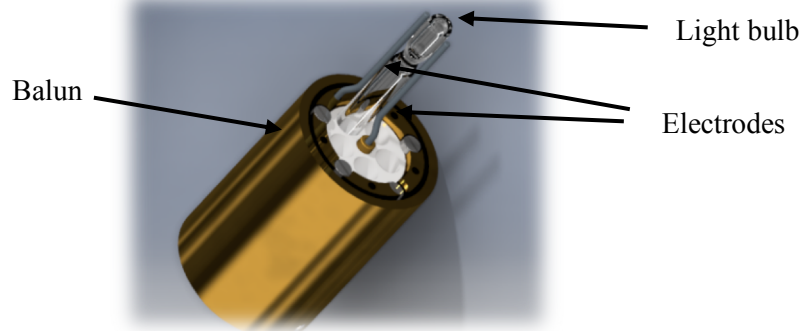


Figure 1. Schematic drawing of the light bulb incl. the electrodes along the glass rod.

**RESULTS**

A simulation of the ignition process is performed to determine the voltage across the light bulb, shown in Figure 2. This voltage must be higher than the critical breakdown voltage calculated with Paschen’s law to ignite the lamp. After the ignition the lamp turns into the operation mode creating a broadband spectrum, specific to its chemical composition of the constituents inside the lamp. These chemical substances are pretended

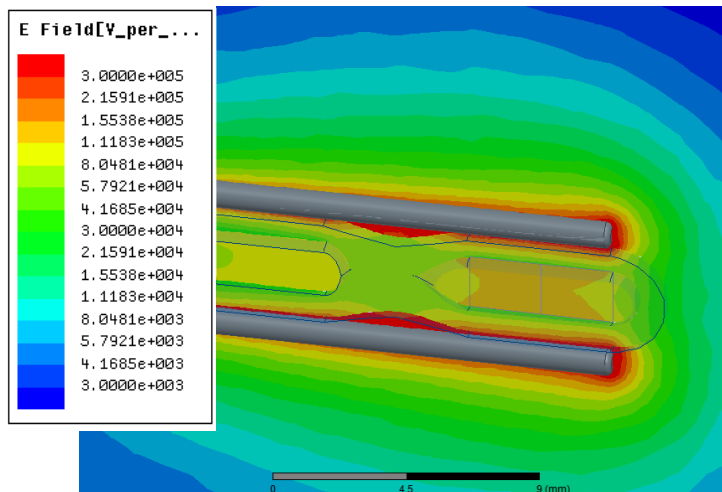


Figure 2. Simulated electrical field strength across the light bulb. A voltage of 500 V is simulated for an RF power level of 25 W.

by the application the lamp is used for. A UV light application has different requirements to the spectral light distribution as a greenhouse lighting application, for example. This causes although different impedances for different lamp types resulting in a specific matching circuit for each lamp type.

The operating lamp in Figure 3 is built for applications requiring a high UV content in the spectrum. The constituents were chosen to generate spectral lines mostly in the UVA and UVB range (approx. 300 nm to 400 nm) which were broadened by the high operating pressure in the lamp. In addition to the line broadening this high operating pressure leads also to a raise in the continuum radiation. This high pressure is caused by a high wall temperature at the light bulb of up to 900°C. To achieve this high temperature a relatively high amount of RF power has to be coupled into a tiny lamp. These extremely conditions lead to a high efficient plasma light source, that is principally adaptable to many kinds of applications and their special requirements.

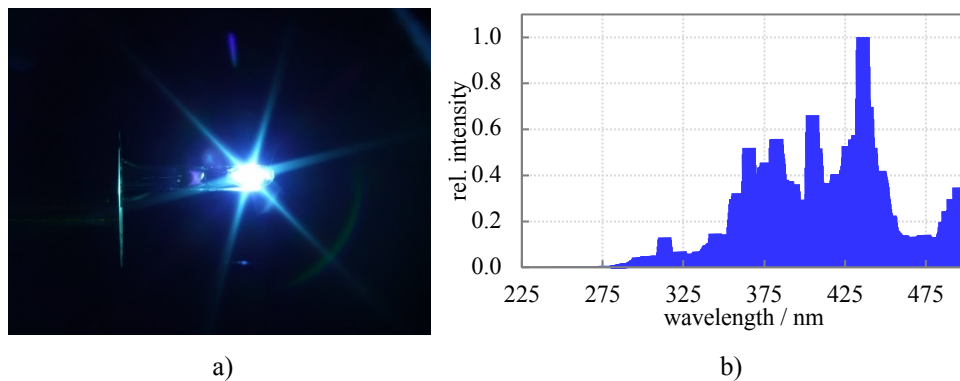


Figure 3. Operating solid state plasma light a) for applications requiring a high UV content in the spectrum and its rel. intensity vs. the wavelength b).

## CONCLUSION

This design enables broadband lighting sources with a very high estimated lifetime in a low to mid power range, e.g. several watts to some hundreds of watts. Varying the chemical components in the lamp lead to different spectral distributions and makes this kind of lamps suitable for various applications.

## REFERENCES

- [1] S. Holtrup, A. Sadeghfam, H. Heuermann and P. Awakowicz, Characterization and Optimization Technique for Microwave-Driven High-Intensity Discharge Lamps Using Hot S-Parameters, *IEEE Transactions on Microwave Theory and Techniques*, vol. 62, no. 10, pp. 2471-2480, Oct. 2014.
- [2] C. Schopp et al., Capacitively Coupled High-Pressure Lamp Using Coaxial Line Networks, *IEEE Transactions on Microwave Theory and Techniques*, vol. 64, no. 10, pp. 3363-3368, Oct. 2016.

# **Solid-State RF Energy – Advancements in Industrial Applications and Market Opportunities**

**Hannes Grubinger, Dave Lester, John Mastela, Manuel Romero, Klaus Werner, Roger Williams**

Ampleon, Huber + Suhner, MACOM, NXP Semiconductors, RF Energy Alliance,  
Richardson Electronics Ltd.

**Keywords:** Solid-State, RF Energy, Industrial, RF Energy Alliance

**Panel Title:**

Solid-State RF Energy – Advancements in Industrial Applications and Market Opportunities

**Abstract:**

An ever-increasing performance/price ratio coupled with unprecedented, precise RF signal control expands the practical use cases for Solid-State RF Energy (SSRFE) technology to include heating and power delivery scenarios. As a result, SSRFE technology is being developed for industrial applications that were previously considered impossible for RF tube based systems or dominated by cost-effective magnetrons.

The panel will focus primarily on industrial applications and market opportunities for SSRFE technology. Furthermore, the group will define a broad range of potential SSRFE applications, the go-to-market strategies and the cross-industry collaboration needed to quickly make inroads into the industrial market.

**Participants:**

- Hannes Grubinger, Huber + Suhner
- Dave Lester, NXP Semiconductors
- John Mastela, Richardson Electronics Ltd.
- Manuel Romero, MACOM
- Klaus Werner, RF Energy Alliance
- Roger Williams, Ampelon

# **CiMPAS – A Novel Approach for Fast Inline Microwave Pasteurization and Sterilization**

**Klaus-Martin Baumgaertner<sup>1</sup>, Daniel Baars<sup>1</sup>, Markus Reichmann<sup>1</sup>, Niko Voit<sup>1</sup>, Markus Dingeldein<sup>1</sup>, Uwe Bauer<sup>2</sup>, Mirko Kehr<sup>2</sup>, Eckehardt Ackermann<sup>2</sup> and Kevin Petersen<sup>3</sup>**

<sup>1</sup>MUEGGE GmbH, Reichelsheim, Germany

<sup>2</sup>Meyer Burger (Germany) GmbH, Hohenstein-Ernstthal, Germany

<sup>3</sup>Microwerk, Seattle, USA

**Keywords:** Food Pasteurization, Food Sterilization, Microwave Heating.

## **INTRODUCTION**

The food industry is experiencing a new transition in consumer behavior going from home-cooked meals or high-quality meal preparations to ready-to-eat meals and dining out. An issue is that many of these ready-to-eat meals offer inferior degrees of food quality due to lack of freshness, color, texture, flavor and even nutritional content. The consumer, however, is demanding a much healthier and more flavorful alternative.

In order to satisfy the consumer's demand for more convenience foods, it is essential for the food industry to offer a more sophisticated ready-to-eat meal alternative that provides the customer with greater nutritional value, taste, flavor, texture, color and appearance. An extra benefit is also added by extending the shelf life of these products, thus reducing a considerable amount of food waste and protecting the environment through efficient use of existing agricultural crop areas.

The major advantage of microwave heating compared to conventional heating is the almost homogeneous tempering of the entire volume of most edibles, being much more efficient than heating from surface to core in matters of process time, power consumption and avoidance of localized overheating. The groundbreaking Coaxially induced Microwave Pasteurization And Sterilisation (**CiMPAS**) developed by MUEGGE in co-operation with Meyer Burger (Germany) and Microwerk profits from this major advantage of microwave heating.

## **METHODS AND APPLICATIONS**

Microwave heating is gaining greater acceptance as an improved method for pasteurization and sterilization in the food industry. Currently, common industrial microwave heating systems rely on a microwave coupling into the processing chamber using horn antennas. In contrast, CiMPAS uses slotted coaxial antennas for targeted

deposition of microwave energy into the packaged, high-quality, ready-to-eat food product. This highly tailored microwave launching system is much closer to the packaged food products to be heated and requires less microwave energy. Moreover, microwave injection via the microwave launching system of CiMPAS can be specifically adapted to various kinds of food components to be processed at the same time, having different dielectric constants and dielectric loss factors which determine their ability to store electric energy and the particular conversion of microwave energy to thermal energy, respectively [1]. Consequently, the exposure time is significantly reduced, thereby helping to maintain the nutritional value of the food products in particular.

This paper will present the results of various microwave pasteurization examples performed with CiMPAS on packaged ready-to-eat food products. The food items were composed of different main and side dishes in trays of customized design. Homogeneous tempering of the edibles was proved within an extremely narrow temperature zone between 88°C and 91°C, a prerequisite for maintaining nutrient content. These experiments not only focused on proving homogeneity of the microwave heating process, but also demonstrated minimal changes to taste, flavor, texture and appearance of the food products.

The analysis of present data obtained by industrial microwave pasteurization with CiMPAS will assist the qualification of CiMPAS for microwave sterilization applications.

## **CONCLUSION**

CiMPAS, the groundbreaking processing system for inline pasteurization and sterilization of food by microwaves has already proven to meet the food industry's expectations for both fast and homogenous heating of packaged, high-quality, convenience food products by preserving nutrition, taste, flavor, texture, color and appearance, independent of the size and shape of the packaging and of the composition of each main and side dish.

## **REFERENCES**

- [1] J. Tang, Unlocking Potentials of Microwaves for Food Safety and Quality, *Journal of Food Science*, vol. 80, no. 8, pp. E1776-E1793, 2015.

# Ensuring Safe Consumption of Frozen Foods: A Call for Transformative Innovation

S. Gummalla<sup>1</sup>

<sup>1</sup>American Frozen Food Institute, Arlington, USA

**Keywords:** Frozen foods, *Listeria monocytogenes*, Food safety, Microwave cooking, Consumer behaviors.

## INTRODUCTION

The American Frozen Food Institute (AFFI) is the member-driven national trade association that advances all segments of the frozen food and beverage industry. We advocated public policy interests of the industry and serve as its voice before consumers, media, and policy makers. A primary objective of the institute is to foster industry development and growth through education and research programs and among these food safety is a priority. The presentation seeks to share the state of frozen food industry particularly from the lens of food safety issues, reveal ongoing efforts to mitigate public health risks, and discuss potential technology development opportunities to address food safety challenges.

## BACKGROUND

Frozen foods are at an important intersection in the industry's evolution, especially from the perspective of enhancing food manufacturing practices and meeting consumers' changing needs. From a food safety perspective however, frozen foods have in recent years been subject to frequent food recalls [1] and even attributed with a limited number of illnesses and outbreaks [2]. These events highlight the public health risks posed by the presence of *Listeria monocytogenes* and other pathogens in frozen foods and have raised significant concern among food manufacturers, regulatory agencies, and consumers alike. New and varied but potentially risk-prone consumer trends and behaviors; susceptibility of specific consumer segments to pathogens; the manner, by which consumers view and apply cooking instructions prior to consumption, have only heightened the call for action. As an example, smoothies prepared with frozen vegetables without first following food preparation/cooking instructions have the potential of exposing consumers to microbial hazards. Indeed, more and more consumers self-identify not following cooking instructions appropriately, mishandling frozen foods, or ignoring food labels in their entirety.

At the heart of this challenge is the trend towards more convenient foods and the perception that all frozen foods are innately ready-to-eat (RTE) food products. Consumer interventions specified through the cooking instructions on food packaging may be deemed by consumers as only rendering food palatable, rather than safe, for consumption. AFFI and frozen food manufacturers recognize that products in the not-ready-to eat (NRTE) state with validated cooking instructions are critical to offering consumers product choice, taste quality, nutrition, and convenience. Meeting marketplace demand and need for NRTE products however, is confronted by ambiguous regulatory policies [3] relative to presence of *Listeria* in frozen foods, lack of consistency in product labeling and industry messaging, new consumer behaviors and trends, and lagging technological advances to assist consumers.

Frozen foods and microwave cooking are inseparable in U.S. households and can play a central role in ensuring safe consumption of frozen foods. AFFI believes there is an opportunity for a concerted team effort from experts in food science, food packaging, food engineering, and other disciplines such as material chemistry and artificial intelligence, to develop more intuitive and targeted solutions to render microwavable foods safer and assist consumers determine when a food is safe for consumption. For instance, application of time-temperature indicators integrated within the microwave or the food itself may be able to confirm successful application of cooking instructions. Such indicators may have additional advantages when integrated with food packaging, to detect temperature abuse during transport through the frozen food supply chain from production to storage, transport, and consumer handling.

## **DISCUSSION**

This presentation will outline AFFI's holistic strategy and current efforts to combat food safety risks associated with frozen foods: scientific research, enhancing best manufacturing practices, consumer research, and proposed messaging and education initiatives. Key findings from recent consumer focus group and surveys relative to behaviors underscore the immediacy of much needed technological transformations to ensure safe consumption of frozen foods. This data and case stories to illustrate the challenges posed will be presented.

## **CONCLUSION**

AFFI's goals include identifying, initiating, and enlisting industry-academia collaboration bringing technical expertise from varied disciplines to define innovative food safety-oriented solutions targeted towards microwave applications for frozen foods.

## **REFERENCES**

- [1] U.S. Food and Drug Administration (USFDA) (<https://www.fda.gov/Safety/Recalls/>)
- [2] USFDA <https://www.fda.gov/Food/RecallsOutbreaksEmergencies/Outbreaks/ucm499157.htm>
- [3] USFDA Draft guidance on presence of *Listeria monocytogenes* in Ready-to-Eat foods <https://www.fda.gov/RegulatoryInformation/Guidances/ucm073110.htm>.

# Consumer Countertop Microwave Ovens Market Study

**Marie Jirsa <sup>1</sup>, Lea Anne Dea, Sumeet Dhawan, Anne Oslund, Jane Frieman**

United States,  
Tyson Foods Inc, Conagra Brands, Nestle and Campbell Soup Company

**Keywords:** microwaves, US survey of sales market data, trends, wattage

## INTRODUCTION

Consumer Microwave Ovens Market study examines the current sales of microwave ovens sold in the US. Looks at where ovens are sold. What manufacturer, models, wattage, size, features and price. This paper analyzes data as to what is currently being sold on the web at online stores such as Amazon vs. what is sold at appliance and department stores (both Regional and local), Electronic stores (such as Best Buy) Home Improvement: Home Depot and Lowes and discount stores such as Wal Mart and Target.

It also looks at what ovens are currently on the manufacturer websites. The data will be analyzed based on wattage, size, price, top manufacturers and features. The information will be used by companies to determine what wattage microwave to use when developing microwave preparation directions.

## METHODOLOGY

Microwave Ovens Sales data will be compiled by looking at web sites for online stores as well as visiting stores where microwave ovens are sold. Manufacturer websites will also be reviewed. Data will be compiled and analyzed.

# Transparent Observation Window for Microwave Oven

R.R. Jiang<sup>1</sup>, B.Q. Zeng<sup>1</sup>, J.L. Liu<sup>1</sup>, K.Q. Yang<sup>1</sup>, H. Wang<sup>1</sup>, J.H. Fan<sup>1</sup>, W.J. Cai<sup>1</sup>, X.Y. Yu<sup>2</sup>

<sup>1</sup>University of Electronic Science and Technology of China, Chengdu, Sichuan, China

<sup>2</sup>University of Electronic Science and Technology of China Zhongshan Institute, Zhongshan, Guangdong, China

**Keywords:** electromagnetic shielding, microwave oven, image quality.

## INTRODUCTION

Microwave oven doors are usually made of metal meshes, which shield microwaves and also permit observation of the cooking process through it. But the metal meshes usually distort the image. Alternatively, a transparent conductive film (TCF) can be used as an observation window and electromagnetic shield<sup>[1]</sup>. Indium tin oxide (ITO) is the most used TCF, but it cannot be used as an observation window of a microwave oven, because of the large surface current and strong electric field on the surface of the window.

## METHODOLOGY

A transparent metallic micro-mesh film was prepared by the self-forming network crack mask technique and lift-off method<sup>[1]</sup>. Films with low surface resistance ( $<0.2 \Omega / \square$ ) were fabricated, and had an optical transmission coefficient of about 55%. These films were incorporated in a window for a Midea M3-L233B microwave oven, as a replacement for the original grid window. To protect the TCF from scratching, a sandwich structure was used.

The microwave leakage was measured using a Holiday HI-1501 microwave leak energy tester. The electromagnetic shielding performance (S parameters) was measured over a frequency range of 2.4 –2.5 GHz using two waveguide-to-coaxial adapters and a vector analyzer (AV36580A).

In order to research the image quality of different microwave oven observation windows, we used a Canon 450D camera to take pictures of milk behind different microwave oven observation windows. Then we evaluated the image quality using an objective evaluation method with MATLAB.

## RESULTS

The measured S parameters were S<sub>11</sub>=-0.5dB (reflection coefficient) and S<sub>21</sub>=-49.5dB (transmission coefficient). The leakage power flux was tested for 30 mins at nine different positions on the microwave oven door with the normal metal grid window or the

TCF window under an 800ml water-load. The leakage power flux was also measured under no-load full-power operation for 30 mins, as shown in figure 1. Figure 1 shows that the leakage for the normal window was less than 0.2 mW/cm<sup>2</sup> and for the new TCF window 0.4 mW/cm<sup>2</sup>, which still satisfies the IEC safety standard<sup>[2]</sup>.

We evaluated the image quality with indices of peak signal to noise ratio (PSNR), fuzzy coefficient (K) and quality factor (Q)<sup>[3]</sup>. Photographs of milk being heated in a microwave oven with a normal metal grid window and a TCF window are shown in figure 2 and the measured image quality results in table 1.

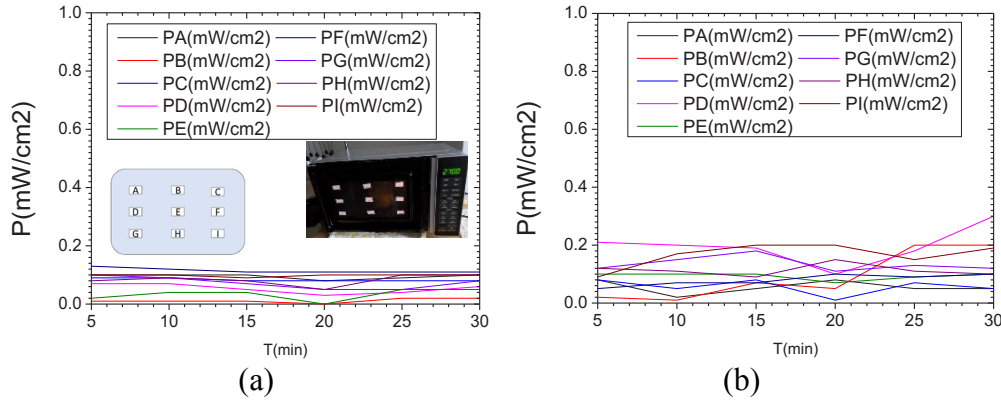


Figure 1. Leakage test of microwave oven doors under no-load full-power operation. The inset of (a) shows the nine test positions on the microwave oven door. The leakage power flux under no-load full power conditions for the normal grid window is given in (a) and for the TCF window in (b).



Figure 2. Photographs of milk being heated in a microwave oven with (a) the normal metal grid and (b) the transparent conductive film observation windows.

Table 1. Image quality of the normal metal grid and TCF microwave observation windows

	Normal metal grids	TCF
PSNR	19.5068	27.0227
K	1.9091	1.0248
Q	0.0651	0.1837

## DISCUSSION

A major problem for TCF windows is durability and survivability. For many TCF applications, the optical transpance is very important, which usually should be 80% or above. However at high optical transpance, the surface resistance is as high as  $\sim 10 \Omega / \square$ . But for microwave oven application, the optical transpance is not very important, but the surface resistance should be decreased to  $< 0.2 \Omega / \square$ ; otherwise the TCF window may be damaged.

## CONCLUSION

Metallic micro-mesh TCFs for microwave ovens had better image quality than normal grid windows, with the same electromagnetic shielding. The TCFs can also be applied to other high-power microwave energy fields which need high conductivity and excellent optical image performance.

## REFERENCES

- [1] B. Han, K. Pei, Y. Huang, X. Zhang, et. Al., "Uniform Self-Forming Metallic Network as a High-Performance Transparent Conductive Electrode", *Adv. Mater.*, vol. 26, pp. 873-877, 2014.
- [2] IEC 60335-2-25:2014, Amendment 1 - Household and similar electrical appliances - Safety - Part 2-25: Particular requirements for microwave ovens, including combination microwave ovens, 2014.
- [3] Z. Wang, H.R. Sheikh, and A.C. Bovik, Objective video quality assessment (Chapter 41 in The Handbook of Video Databases: Design and Applications), CRC Press, 2003, pp. 1041-1078.

# The Influence of Microwave Frequency on Heating Uniformity

Z.M. Tang<sup>1</sup>, T. Hong<sup>1</sup>, F.Y.Chen<sup>2</sup>, H.C.Zhu<sup>3</sup>, and K. M.Huang<sup>3</sup>

<sup>1</sup>China West Normal University, Nanchong, China

<sup>2</sup>State Key Laboratory of Electromagnetic Environment, Shanghai, China

<sup>3</sup>SichuanUniversity, Chengdu, China

**Keywords:** Microwave frequency; Heating Uniformity; selected frequencies; variable frequency.

## INTRODUCTION

Microwave heating has attracted extensive attention of the public because of its convenience and high efficiency. However, it usually leads to non-uniform temperatures. Because it is of great importance for the quality of products and heating efficiency, many methods have been suggested to improve microwave heating uniformity. These methods include the use of microwaves in combination with some other heating source, the use of microwave susceptors, and the employment of rotating turntables etc. One more interesting method is the variable frequency method [1]. However, most of these methods mentioned above do not provide sufficient theoretical explanations, especially with regard to the influence of frequency, we usually regard it as an ordinary and very old topic and have not paid enough attention to it. Obviously, it is not good for us to grasp these methods from the roots, so as to put forward a better heating method.

In this paper, to study on the influence of tiny shifts in frequency on the heating uniformity, systematical mathematic derivations as well as the theory of electromagnetic wave propagation in a multimode cavity are used. Then, the mathematical basis of such frequency effect is obtained and based on this, a new microwave heating method named frequency-selected method is proposed. Since this method works with selected frequencies, different frequency selecting schemes are compared, the characteristics of which are further deduced and concluded. Finally, finite element method is used to perform the proposed method and comparisons with the traditional variable frequency method are also made.

The results show that heating uniformity depends highly on tiny shifts in microwave frequency, and in order to use the frequency-selected method effectively, it is best to select frequencies by the comprehensive comparison of the scattering parameters ( $S_{11}$  parameters), the average of the electric field and the average temperature rise. Besides, the results also demonstrate that although the frequency varies in both the frequency-selected method and the traditional variable frequency method, mechanisms of them are different.

## METHODOLOGY

In a microwave heating system, the total electric field inside the cavity can be represented by a volum integral equation by the superposition principle. The theory of Fredholm equation and heat transfer equation are used to analytically demonstrate the dependence of heating uniformity on small shift of microwave frequency [2].

Then, a new microwave heating method named frequency-selected method is proposed, which is used to verify the influence of microwave frequency on heating uniformity. In this method the dielectric sample is not heated with fixed frequency but with variable frequencies selected from a certain frequency bandwidth. The procedure for frequency selecting is shown in Figure 1, in which Finite element method is used to perform the process. The selected frequencies are then used for heating, and each of them is picked out for heating at different periods of time. Moreover, the microwave frequency is assumed to be updated to a new one at the end time of each one second.

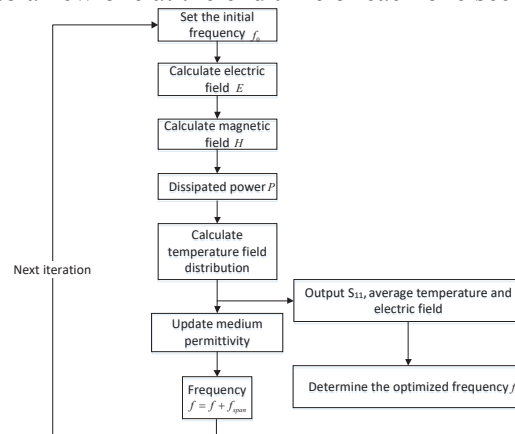


Figure 1. Flow chart for frequency selecting

## RESULTS

As is shown in Figure 2 and Figure 3, the heating performance are assessed from different aspects, including the temperature distribution on the top surface, the coefficient of variation (COV) spread as a function of heating time, as well as the rise of average temperature. In Figure 2 (a), there are two regions of concentrated high temperature on the top surface of the potato slice. In Figure 2 (b), there remain two concentrated hot areas slightly smaller than that of Figure 2 (a). Obviously, these two large hot areas become much smaller, and the temperatures of many other parts have different degree rises, resulting in a much more uniform temperature distribution as detailed in Figure 2 (c). However, figure 2 (d) shows that the two concentrated hot areas are as large as or even larger that of Figure 2 (a) when the ex-variable frequencies are used. That is to say, without the selected frequencies, variable frequency neither effectively improves the heating uniformity nor increases the average temperature. The results in Figure 3 are consistent with figure 2, although they are displayed in two different ways.

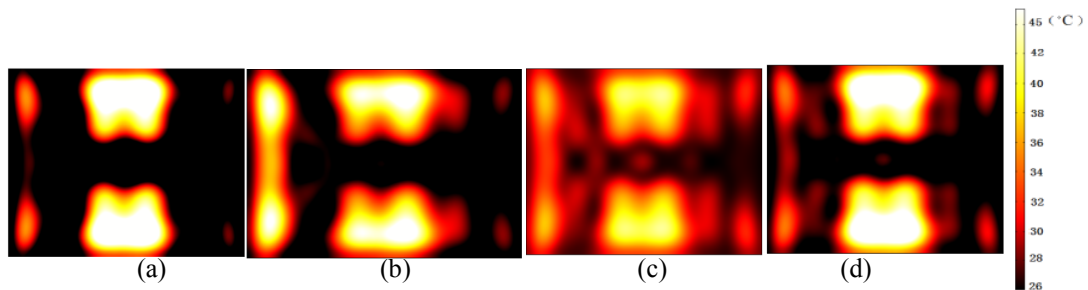


Figure 2. Temperature contours on the top surface after 30s of microwave heating, with (a) fixed frequency, (b) variable frequencies, (c) selected frequencies, and (d) ex-variable frequencies.

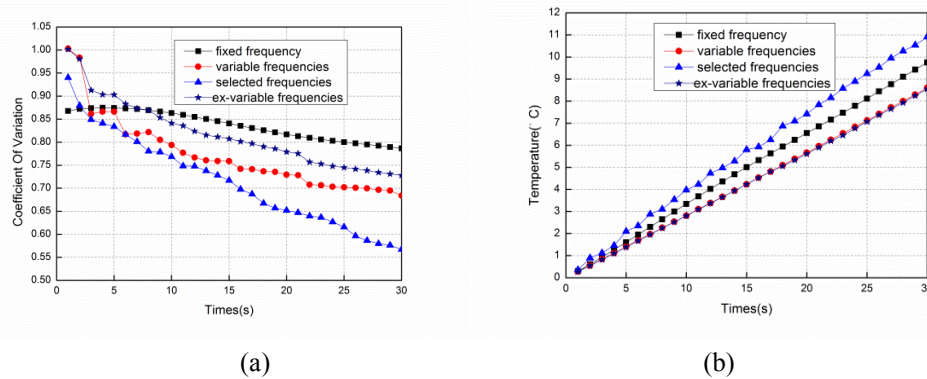


Figure 3. Comparison of COV and temperature histories, with fixed frequency, variable frequencies, selected frequencies, and ex-variable frequencies: (a) COV, (b) volumetric temperature histories ( $\Delta \bar{T}$ ).

### DISCUSSION

Heating uniformity depends highly on tiny shifts in microwave frequency, and heated with selected frequencies can improve heating uniformity effectively. Moreover, although the frequency varies in both the frequency-selected method and the traditional variable frequency method, mechanisms of them are different.

### CONCLUSION

The influence of tiny shifts in frequency on the heating uniformity is detailedly studied, the mathematic basis is obtained, and a more effective heating method is expected to be proposed based on the results of this study.

### REFERENCES

[1] C. Antonio and R. T. Deam, Comparison of linear and non-linear sweep rate regimes in variable frequency microwave technique for uniform heating in materials processing, *J. Mater. Process. Tech.*, vol. 169, no 2, pp.234-241, 2005.

[2] Z. Tang, T. Hong, F. Chen, H. Zhu, and K. Huang, Application of integral equation theory to analyze stability of electric field in multimode microwave heating cavity. *Eur. Phys. J. Appl. Phys.*, vol.80, no 1, pp. 10902, 2017.

# Millimeter Wave Interactions with High Temperature Materials and Their Application to Power Beaming

**Brad W. Hoff<sup>1</sup>, Martin S. Hilario<sup>1</sup>, Benmaan Jawdat<sup>1</sup>, Anthony E. Baros<sup>1</sup>,  
Frederick W. Dynys<sup>2</sup>, Jonathan A. Mackey<sup>2</sup>, Vadim V. Yakovlev<sup>3</sup>,  
Charles E. Andraka<sup>4</sup>, Kenneth M. Armijo<sup>4</sup>, Ender Savrun<sup>5</sup>, and Ian M. Rittersdorf<sup>6</sup>**

<sup>1</sup>Air Force Research Laboratory, Kirtland AFB, NM, USA

<sup>2</sup>NASA Glenn Research Center, Cleveland, OH, USA

<sup>3</sup>Worcester Polytechnic Institute, Worcester, MA, USA

<sup>4</sup>Sandia National Laboratories, Albuquerque, NM, USA

<sup>5</sup>Sienna Technologies, Woodinville, WA, USA

<sup>6</sup>Naval Research Laboratory, Washington, DC, USA

**Keywords:** Dielectric measurement, high temperature, dielectric substrates, ceramics, dielectric losses, power beaming

## INTRODUCTION

The Air Force Research Laboratory (AFRL) is involved in ongoing efforts to characterize dielectric properties of materials at high temperatures using millimeter wave radiation. A fundamental understanding of the complex dielectric properties of materials, and the dependence of these properties on frequency and temperature, is necessary to effectively utilize electromagnetic energy to controllably heat materials for applications such as power beaming [1-3].

## APPARATUS, METHODOLOGY, AND RESULTS

A “free space” dielectric measurement apparatus has been designed and developed to enable characterization of complex dielectric permittivity at high temperature (25 °C to 600 °C) in air and at frequencies in the W-band (75 GHz to 110 GHz) [1, 2]. A schematic of the measurement system is provided in Figure 1 (a). S-parameter sample values from the vector network analyzer (VNA) are converted to real ( $\epsilon_r'$ ) and imaginary ( $\epsilon_r''$ ) permittivity values as described by Hilario, et al. [2]. Complex permittivity data for an aluminum nitride-molybdenum composite sample (AlN:Mo = 95%:5% by weight) at 95 GHz is provided in Figure 1 (b).

## DISCUSSION

Complex dielectric property measurements made using high-temperature free-space methods are being used to guide development of high-temperature millimeter-wave-absorbing ceramic composites, such as AlN:Mo, for use in a mm-wave powered heat exchanger (HX) intended for future power beaming experiments. As part of the planned experiments, millimeter wave power will be transmitted to a remote station where the beamed power will be collected and converted to heat using a mm-wave absorbing ceramic HX. Generated heat will then be converted to electrical

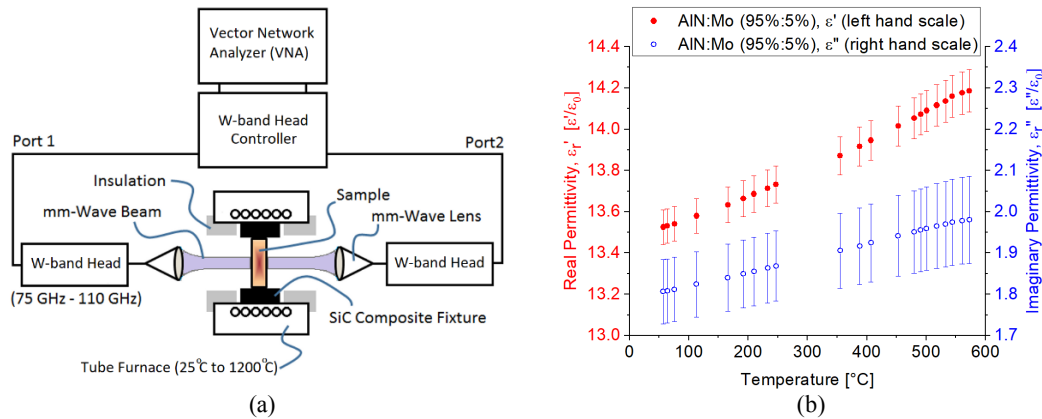


Figure 1. Schematic depiction of the high-temperature dielectric measurement apparatus (a) real and imaginary permittivity data for an AIN:Mo (95%:5% by weight) ceramic sample (b).

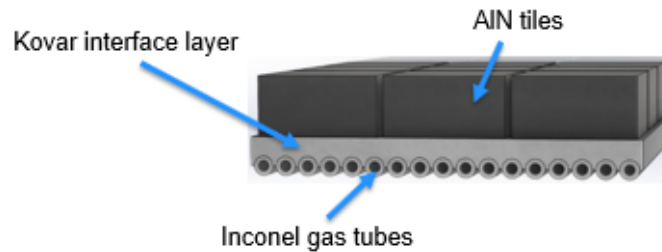


Figure 2. Conceptual drawing of a mm-wave powered heat exchanger sub-section. Ceramic tiles, Kovar baseplate, and the Inconel gas tubes are shown. Additional CTE grading layers between the ceramic and the base plate are not explicitly depicted here.

power using thermo-mechanical means. A conceptual drawing of a mm-wave powered heat exchanger sub-section is presented in Figure 2; AIN tiles, baseplate, and gas tubes are depicted there. Additional coefficient of thermal expansion (CTE) grading layers between the tiles and the base plate are not explicitly shown.

**ACKNOWLEDGEMENTS**

This work was funded by the Operational Energy Capability Improvement Fund (OECIF), by the Air Force Office of Scientific Research under FA9550-17RDCOR449, and by the Air Force Research Laboratory. The authors acknowledge helpful discussions with A. Sayir of the AFOSR.

**REFERENCES**

[1] B.W. Hoff, M. Hilario, B. Jawdat, D. Agrawal, M. Lanagan, J. Cheng, F. Dynys, “Characterization of high temperature dielectrics at millimeter wavelengths,” *Proc. of 12<sup>th</sup> Pacific Rim Conference on Ceramic and Glass Technology., Waikoloa, HI, May 2017.*  
 [2] M.S. Hilario, B.W. Hoff, B. Jawdat, M.T. Lanagan, A.W. Cohick, F.W. Dynys, J.A. Mackey, and J.M. Gaone, “W-band complex permittivity measurements at high temperature using free-space methods,” *IEEE Trans. Compon. Packag. Manuf. Technol.* (submitted).  
 [3] M.S. Hilario, B.W. Hoff, M.P. Young, and M.T. Lanagan, “W-band free-space dielectric material property measurement techniques for beamed energy applications,” *Proc. of 53<sup>rd</sup> AIAA Aerospace Sciences Meeting, 2015*, pp. 1–10.

# Solid-State RF-Energy Powered Atmospheric Pressure Ion Sources for Mass Spectrometry

**Ralf D. Dumler, Gregory S. Katzmann, Alberto Torreño Núñez  
Christian Berchtold and Arno Wortmann**

NovionX GmbH, Lindau, Germany

Solid-State RF-Energy offers exciting opportunities to develop new ion sources for ambient ionization mass spectrometry [1]. In the last two decades, manufacturers of semiconductors specializing in high frequency transistors have made excellent progress developing affordable transistors in the frequency range of 2,45 GHz in LDMOS and GaN designs. Different from traditional magnetron designs, the GaN and LDMOS transistors offer unique and improved abilities. NovionX GmbH introduces a unique power-controlled solid-state 2,45 GHz amplifier, designed to power a wide range of different ion sources for mass spectrometry. Ion sources can be easily connected to the solid-state RF Generator unit by means of a coaxial waveguide. Applications range from small molecule plasma ambient ionization, plasma ablation imaging to direct plasma pyrolysis of small molecules, photoionization and element analysis of aerosols. All this can be achieved with a single solid-state RF-Energy amplifier [2] and various interchangeable ion sources connected to atmospheric pressure inlet of a mass spectrometer. The new system provides fast detection and analysis for a wide range of different applications, as well as unparalleled flexibility.

## REFERENCES

- [1] Ambient Ionization Mass Spectrometry (New Developments in Mass Spectrometry), ISBN-13: 978-1849739269
- [2] K. Werner, H. Heuermann and A. Sadeghfam, "The Potential of RF Energy for the Ignition of Microplasmas", High Frequency Electronics, November 2012, pp. 38243

# Development of Resonant Cavity System, and its application to Low Permittivity Solvents

Hirromichi Odajima, Tadashi Okamoto and Aki Tomita

Pacific Microwave Technologies, Seattle, WA  
hodajima@pacificmicrowave.com

**Keywords:** Resonant Cavity, Solid state Oscillator, Solid state Amplifier, High Q,

## INTRODUCTION

To realize to focus MW energy same as convex lens for light, many engineering trials have been made, but so far they were not succeeded, even though resonant cavity is commonly understood well. The reason stayed at the use of magnetron. Magnetron cannot change frequency, so that only the idea to tuning up at resonance is limited to adjust physical size of cavity. But such a tuning by physical size is slow and not accurate to meet the fast change of dielectric property of heating material.

The solution to such a problem is the introduction of solid state oscillator and solid state amplifier. By the use of solid state devices, it becomes possible to change oscillating frequency fast enough to tuning up at frequency at resonance ( $f_r$ ).

In addition to the introduction of solid state devices, it becomes possible to optimize design of cavity and applicator by computer EMF (Electro Magnetic Field) simulation without making trial units and without doing many experiments.  
Cavity System

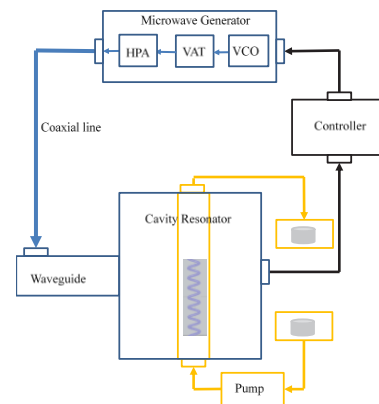


Fig. 1 Resonant

## METHODOLOY

Resonant cavity system using solid state devices we developed is shown in Fig.1. The MW generator is composed of VCO (Voltage Controlled Oscillator), VAT (Voltage controlled Attenuator) and HPA (High Power Amplifier). The MW is irradiated into the cavity via wave guide and iris after oscillating from the generator. Electric field (E-Field) in the cavity is detected by an antenna installed in it.

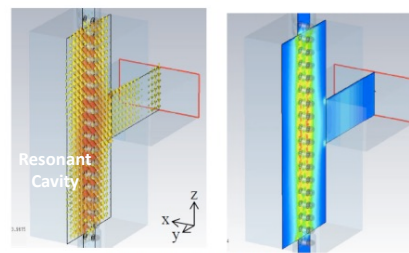
AFT (Automated Frequency Tuning) system tunes up oscillating frequency at  $f_r$  automatically based on the data detected by the antenna. Resonant mode of TM<sub>110</sub> or

TM010 is automatically kept generated always. Fig. 2 shows the example of computer EMF simulation that can show E-field strength and also temperature distribution of material to be heated up.

Heating up material by MW follows basically the next theoretical formula.

$$P = \pi f E^2 \epsilon \tan \delta$$

Traditional MW chemistry paid much efforts to improve its efficiency by the use of solvents that can absorb MW efficiently. Because of that, solvents having higher dielectric property are commonly used.



Left : E-field Distribution  
Right : E-field Energy Concentration

Fig. 2 EMF Simulation

Solvents having low permittivity such as Toluene and Xylene were widely used among chemical industry as those prices are relatively cheap, but those solvents were considered not suitable for MW chemistry, as MW absorption is low, and most of irradiated MW power is reflected from cavity. But giving consideration to the formula above, if E-field is high enough, and appropriate impedance matching is introduced to minimize reflection, it was considered possible to heat up low permittivity solvents efficiently.

By applying computer EMF simulation, it reveals that Q is higher than 200, and E-field in center of cavity reaches higher than 40kV/m, it is possible to heat up Toluene higher than 200C based on the conditions of MW power 250W, TM110 mode, and with impedance matching mechanism. Based on the EMF simulation, resonant cavity system was developed shown in Fig. 3.



Fig. 3 Resonant Cavity

## RESULTS

Using the system developed, applied experiments and confirmed that heating up low permittivity solvents up to very high temperature is really possible. Details are shown in Table 1.

Table 2 shows how high pressure is necessary to heating up various solvents without vaporization. Solvents having higher permittivity such as MeOH, Ethanol, Acetonitrile and IPA need pressure higher than 5MPa for 250C. However lower permittivity solvents such as Toluene and Xylene only needs 2.0MPa at max.

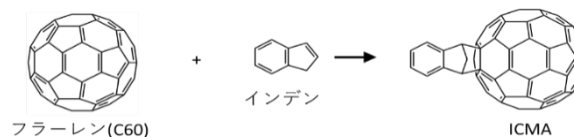


Fig. 4 Fullerene Derivative Conjugation

Based on those information, reactions using low permittivity solvent were tried. The reactions tried were Claisen rearrangement and Fullerene derivative conjugation

shown in Fig. 4. The reaction making Fullerene derivative ICMA is made of Fullerene and Indene, using Xylene as solvent, with 2.5MPa pressure, heating up to 270C by MW power of 250W, succeeded in producing ICMA with productivity of > x10 than traditional external heating process.

Table 1 Conditions of Heating up Toluene

1. System	
MW Oscilation	Solid state
Cavity Size	79□
Mode	TM110
Reactor	Helical Tube
Reactor Volume	10mL
Back Pressure Regulator	
Impedance Matching	
2. Conditions	
MW Power	250W
Frequency	2.4-2.5GHz
Flow Rate	15mL/min
Residence Time	40 sec
Pressure	2.5MPa
3. Result	
Temp.	>200°C

Table 2 Vaporized Pressure of Solvents

Solvents S	Vaporized P @250°C(bar)
MeOH	87.7
Ethanol	65.9
Acetonitrile	62.3
IPA	59.4
Acetone	56.2
t-Butyle Alcohol	50.8
Water	37.9
Hexane	34.1
DME	17.5
Toluene	16.7
p-Xylene	9.9
DMF	7.8
DMSO	5.0

source  
:  
Vapo  
urtec  
  
DIS  
CUS  
SIO  
N  
  
eson

ant Cavity and low permittivity solvent can realize high Q and high E-field in cavity, that can make possible to make MW assisted reactions at very high temperature under low pressure condition. By the use of low permittivity solvent, direct activation of substrate chemicals may have possibility.

## CONCLUSION

MW Resonant Cavity system and use of low permittivity solvents are going to open new chemical process windows for both R&D and production by “ultra super heating”.

## REFERENCES

- [1] Saori Yokozawa, et al : “Development of a Highly Efficient Single-Mode Microwave Applicator with a Resonant Cavity and its Application to Continuous Flow Syntheses”, RSC Advances
- [2] Hiromichi Odajima, Tadashi Okamoto, Akira Tomita : “Microwave Reactor Using Solid State Oscillator & Resonant Cavity, and its Applications to Chemical Synthesis”, at AMPERE 2017, Delft, The Netherlands, September, 2017
- [3] Joshua Barham, et al : “Selective, Scalable Synthesis of C60-fullerene/indene Mono-adducts using a Microwave Flow Applicator”, publish underway by The Journal of Organic Chemistry

# Use of Microwaves in Molecular Modeling to Study Protein Structures

Sai Kranthi Vanga<sup>1</sup>, Ashutosh Singh<sup>2</sup> and Vijaya Raghavan<sup>1</sup>

<sup>1</sup>McGill University, Sainte-Anne-de-Bellevue, QC, Canada

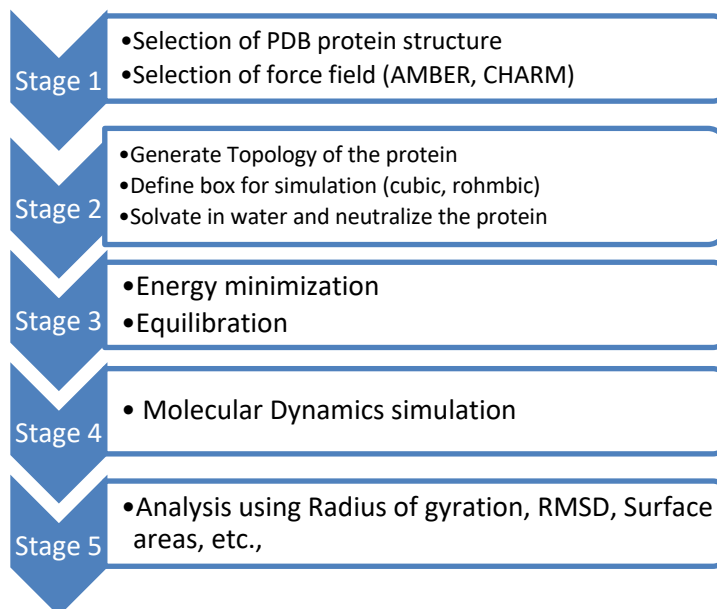
<sup>2</sup>University of Guelph, Guelph, ON, Canada

**Keywords:** secondary structure; oscillating waves; GROMACS; microwave.

## INTRODUCTION

In recent years, the need to understand the effects of various processing methods on proteins has become paramount with an exponential rise in cases of food allergies and other proteopathies. Computer simulations have been used to enhance the molecular scale understanding of the structural conformations of these proteins that can directly influence their functional properties. Though we use the microwave simulations to study the proteins and their secondary structure [1,2], the studies can extend to studying nanoparticles and nanotubes [3].

## METHODOLOGY



## RESULTS AND DISCUSSION

We are presenting the effect of microwave processing on food proteins, primarily allergens and antinutrients present in milk, peanut and soy. Simulating microwaves can help us study various structural properties including Radius of Gyration, Root mean square deviations (RMSD), Root mean square Fluctuations (RMSF) and solvent accessible surface area. Furthermore, simulation also aid in visualization of the structural deviations which might not be possible during a conventional experimental setup.

When oscillating electric field was applied with thermal treatment higher peaks observed at 363 K suggesting that these epitopes are becoming unstable and are deviating further compared to control as temperature is increasing. There were peaks observed at 363 K in epitope range 127-150 suggesting that in this region, epitopes might be more reactive compared to control. Furthermore, 348 K has higher peaks compared to 363 K for few residue groups which might be due to these specific residues moving into the core and becoming unavailable for reactions on the surface.

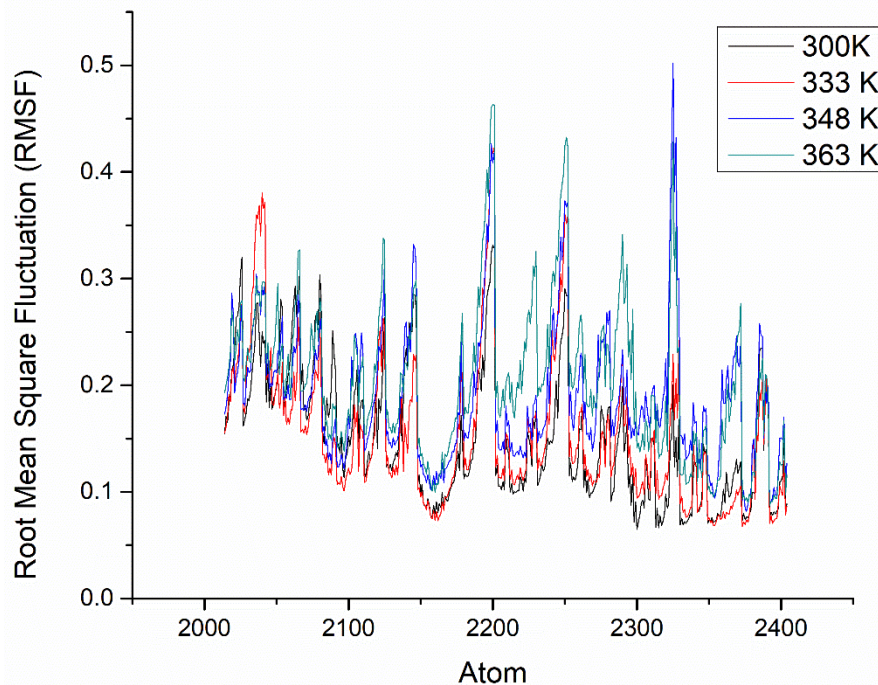


Figure 1. Root mean square fluctuations of Allergen Epitope (Residue: 127-150; atoms: 1950 - 2400) in beta-lactoglobulin due to microwave treatment (2450 MHz).

## CONCLUSION

The microwave studies showed significant changes in protein structures. In the case of peanut allergen Ara h 6, the treatment resulted in significant compression leading to reduction in solvent accessible surface area. In the case of beta-lactoglobulin, which is also an allergen in cow's milk microwave treatment resulted in its enhancement.

## ACKNOWLEDGEMENT

The authors would like to acknowledge the support of Natural Sciences and Engineering Research Council (NSERC), International Development Research Centre (IDRC) and Global Affairs Canada (GAC) for their financial support.

## REFERENCES

- [1] S.K. Vanga, A. Singh and V. Raghavan, Effect of thermal and electric field treatment on the conformation of Ara h 6 peanut protein allergen, *Inn. Food. Sci & Emer. Tech.*, vol. 30, pp.79-88, 2015.
- [2] A. Singh, S.K. Vanga, V. Orsat and V. Raghavan, Application of Molecular Dynamic simulation to study food proteins: A Review, *Crit. Rev. Food. Sci & Nutr.*, in press 2017
- [3] M. Zhou, Y. Hu, J. C. Liu, K. Cheng and G. Z. Jia, Hydrogen bonding and transportation properties of water confined in the single-walled carbon nanotube in the pulse-field. *Chem. Phys. Let.*, vol. 686, pp, 173-177, 2017.

# Development of Small Size Microwave Reactor using LTCC Cavity and Solid-state Device

M. Nishioka<sup>1</sup>, A. Suzuki<sup>2</sup> and M. Miyakawa<sup>1</sup>

<sup>1</sup> National Institute of Advanced Industrial Science and Technology, AIST, Miyagi, Japan

<sup>2</sup> Adamant Namiki Precision Jewel Co., Ltd., Tokyo, Japan

**Keywords:** LTCC, single mode, solid-state microwave generator, TM<sub>010</sub>

## INTRODUCTION

A portable chemical analyzer that contains a temperature-controlled chamber requires reduction of the warm-up time because the time reduction has a strong effect on the battery capacity. A microwave temperature-controlled chamber can reduce the time. Moreover, using a solid-state microwave generator, the analyzer can be designed to be small and lightweight. However, microwave applicator sizes are limited to the microwave wavelength (e.g. 12 cm for a 2.45 GHz microwave system). Therefore, we have been developing a small microwave reactor using a low-temperature co-fired ceramic (LTCC) [1]. The wavelength is shortened by the factor of the square root of the dielectric constants of the ceramics. The LTCC can be manufactured using complex 3D structures such as an antenna pattern or chemical fluid channel. As described herein, a small single mode applicator was constructed in the LTCC. Furthermore, the continuous flow microwave heating was demonstrated. The ultimate goal of this research is that all microwave components, including the microwave source and control circuit, be designed in the LTCC package and installed in the portable chemical analyzer.

## EXPERIMENTAL APPARATUS

Earlier, we studied the cylindrical TM<sub>010</sub> mode cavity (90 mm dia., 100 mm length) as the single mode applicator for the continuous synthesis of nanoparticles [2]. Instead of the previous cavity, the post-wall cavity manufactured from 40 sheets of LTCC was used. The dielectric constant and loss factor of the LTCC were, respectively,  $\epsilon' = 7.8$  and  $\epsilon'' = 0.002$ . The cavity diameter was reduced by a factor of  $\sqrt{\epsilon'}$ . Thereby, the LTCC cavity diameter was approx. 30 mm. Also, 32 posts of post-walls, which were made electrically conductive using silver paste, were formed along a circle (Fig. 1(a)). The top layer and bottom layer of the LTCC sheets were coated by Au (Fig. 1(b)). The area surrounding the top and bottom layers and the post-walls functioned as the cylindrical TM<sub>010</sub> cavity (Fig. 2(b)). To introduce the microwave energy and to monitor the TM<sub>010</sub> mode resonance formation, two ports of a loop antenna were formed near the post-wall in

the LTCC (Fig. 1(c)). At the center axis of the cavity, a through-hole (3.2 mm dia.) was fabricated for the flow tube installation.

Microwave characteristics of the LTCC cavity were measured using a vector network analyzer (E5071C; Agilent Technologies Inc.). A computational simulation (Comsol Multiphysics 5.0a; Comsol Inc.) was also used to confirm the  $TM_{010}$  resonance frequency.

A frequency-controlled solid-state microwave generator (100 W; Tokyo Keiki Inc.) was used for fluid heating. The generator was operated to maintain the  $TM_{010}$  resonance automatically by adjusting the generator frequency using a control board (Ryowa Electronics Co. Ltd.). Water used as the fluid model flowed through the flow tube (silicone tube id 1 mm) at the rate of 1 mL/h to 60 mL/h maintained by a syringe pump (Nexus 3000; Chemyx Inc.). Temperature differences between the inlet and outlet of the LTCC cavity were measured using 0.5 mm dia. thermocouples (T-35; Sakaguchi EH VOC Corp.) installed in the tube.

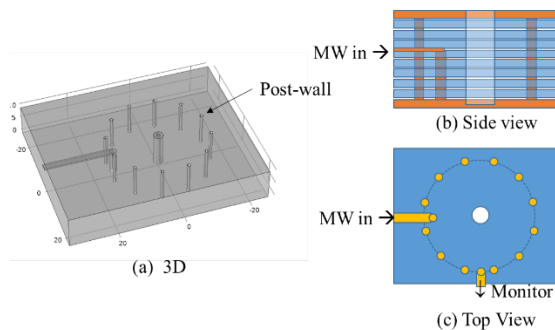


Fig. 1 Design of the LTCC cavity.

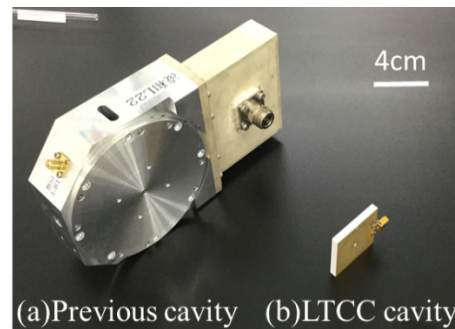


Fig. 2 Photograph of LTCC cavity.

## RESULTS

The 25 g LTCC cavity was  $4\text{ cm} \times 4\text{ cm} \times 0.5\text{ cm}$  ( $8\text{ cm}^3$ ). These values are smaller than those described in earlier reports (dimensions,  $10\text{ cm} \times 10\text{ cm} \times 2\text{ cm}$ ; volume,  $200\text{ cm}^3$ ; weight, 1.3 kg). According to the network analyzer measurement, the resonance frequency of the LTCC cavity was 2.408 GHz, which is consistent with  $TM_{010}$  resonance frequency from the simulation analysis. Then the flow tube was installed through the LTCC cavity. Water was filled into the tube. The resonance frequency was shifted to 2.391 GHz. The -17 MHz shift represented that the LTCC cavity resonance was affected by the fluid in the tube.

Fluid heating by the LTCC cavity was accomplished using the microwave irradiation. Our microwave heating system detected the  $TM_{010}$  resonance frequency automatically and irradiated the corresponding microwave frequency. When water of 3 mL/h flowed through the tube, the time profile of the temperature at the tube outlet (distance between cavity bottom plate and thermocouple was 5 mm) resembled that depicted in Fig. 3. The 18 W microwave irradiation raised the temperature + 4 °C. The

relation between the flow rate and microwave power is shown in Fig. 4. Results demonstrate that the small LTCC cavity performed to control the fluid temperature.

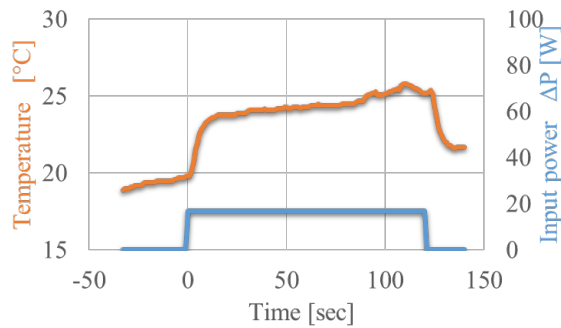


Fig. 3 Temperature profile (3 mL/h).

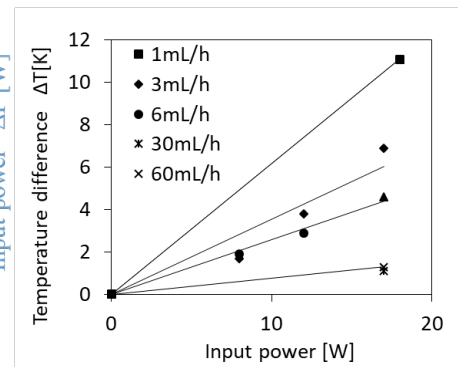


Fig. 4 Flow rate dependence.

## CONCLUSION

To develop the small microwave fluid temperature controller, LTCC and solid-state microwave device technology were combined. An LTCC cavity (4 cm × 4 cm × 0.5 cm) was demonstrated with water used as the model fluid. With a flow rate of 1 mL/h to 60 mL/h conditions, the water temperature was controllable using the developed system.

The LTCC technology can embed all components of a microwave system, including the microwave source and the control system. For future studies, one-chip microwave fluid temperature control equipment will be designed.

## REFERENCES

- [1] D. Belavic, M. Hrovat, G. Dolanc, M. Santo Zarmik and K. Makrovic, Design of LTCC-based ceramic structure for chemical microreactor, *Radioengineering*, vol. 21, issue 1, pp. 195-200, 2012.
- [2] M. Nishioka, M. Miyakawa, H. Kataoka, H. Koda, K. Sato and T. M. Suzuki, Continuous synthesis of monodispersed silver nanoparticles using homogeneous heating microwave reactor system, *Nanoscale*, vol. 3, pp. 2621-2626, 2011.

# Exploiting microwave activated combustion synthesis for metallurgy

E. Colombini<sup>1</sup>, A. Garzoni<sup>2</sup>, R. Rosa<sup>1</sup>, A. Casagrande<sup>2</sup>, P. Veronesi<sup>1</sup>, C. Leonelli<sup>1</sup>

<sup>1</sup>Department of Engineering “Enzo Ferrari”, University of Modena and Reggio Emilia, Via Vivarelli 10, 41125 Modena, Italy

<sup>2</sup>Department of Industrial Engineering, University of Bologna, Viale Risorgimento 4, 40137 Bologna

**Keywords:** Combustion Synthesis, Microwave Activation, Powder Metallurgy, Simulation

## INTRODUCTION

Microwave ignition of combustion synthesis (CS) reactions between metal powder reactants, in a single mode applicator, has been studied by the present authors since 2006 [1]. Several systems were investigated, both by experiment and simulation [1][2].[3] Process intensification is now considered the most promising development path for the chemical process industry and modern chemical engineering in order to face recent challenges of enhanced process safety, conservation of natural resources, reduction of environmental impact and energy consumption. From this perspective, the CS technique, using smaller equipment, energy consumption limited to the ignition step and complete conversion of the reactants into products, should be considered a promising technique to pursue such key process intensification objectives in advanced materials and inorganic chemical compound manufacturing.[1][3][4][5]. CS ignited by conventional heating techniques usually show an inversion of the heat flow before and after the exothermic reaction. As soon as the powders reach the ignition temperature, the heat released during the reaction tends to rapidly raise the temperature of the reactants undergoing the CS reaction, and subsequently the heat flow is directed from the reaction zone towards the surrounding environment. Thus, as soon as the reaction occurs, it is no longer possible to continue to transfer heat from an external conventional heating source to the reaction zone. On the contrary, microwaves heating in the ignition of CS reactions is expected to lead not only to a more rapid temperature increase of the whole reaction zone, but also to a continuous energy transfer to the reactants and products during and after the ignition, with consequent heat generation.[6]

## METHODOLOGIES

Simulation by Comsol Multiphysics 3.5a and Concerto software was carried out to investigate the rapidly occurring combustion reactions and to gain deeper insight on the development of specific temperature profiles, which can be used to control product microstructures. Disc-shaped specimens were fabricated from mixed metal powders, weighted according to the stoichiometry of the compound (e.g. NiAl 50%at-50%at, FeCoNiCuAl each element at 20%at.), mixed either manually in an agata jar or in a

planetary ball mill, and molded applying between 100-200 MPa of uniaxial pressure. All the experiments were conducted in reproducible setups, using rectangular (WR-340) single mode cavities at 2.45GHz at powers from 0.3 to 6 kW).

Different systems were analyzed, including pure  $\beta$ -NiAl intermetallic phase synthesis with external auxiliary absorbers, like SiC, and then using such intermetallic phases to join titanium alloys.[1] The importance of having at least one ferromagnetic reactant was further investigated, processing Fe+Al, Co+Al and Ni+Al in predominantly electric or magnetic field regions of the applicator [7]. In parallel, exploiting the selectivity of heating, microwave assisted CS was used to minimize the extension of heat affected zones when joining dissimilar materials, i.e Inconel and Titanium, [3] or CVD-SiC. [8]

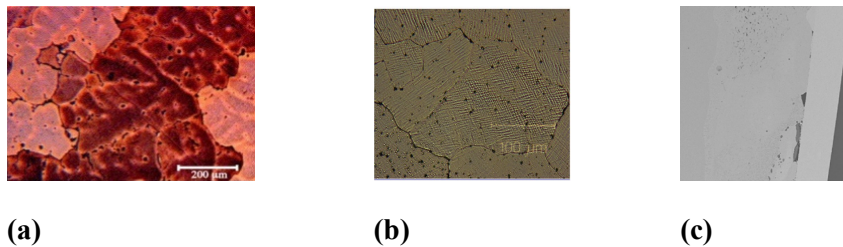


Figure 1: Microstructures of  $\beta$ -NiAl (a), NiAl activated in B (b), NiAl as joining between Inconel and Ti (c)

## RESULTS

Recently, the research focused on multi-principal element systems, known also as High Entropy Alloys. High entropy alloys (HEAs) are composed of five or more principal constituent elements at similar atomic percentage. High Entropy Alloys were successfully synthesized by microwave activated combustion synthesis, with significantly lower energy consumption than the state of the art alternative synthetic routes (induction heating, arc melting, mechanical alloying). Based on the achieved results, [9][10] new compositions of HEAs have been developed, namely FeNiAlCuMn, SiC reinforced FeCoNiCrAl alloys and Si-modified Mn<sub>25</sub>Fe<sub>x</sub>Ni<sub>25</sub>Cu(50-x) alloy.[11][12]

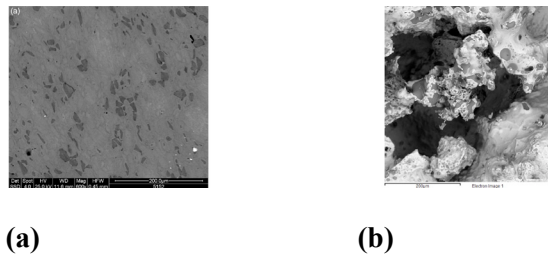


Figure 2: An Example of SiC modified HEA (a, b) and Micrograph (SEM) of the inner of the pellet

## DISCUSSION

The microwave assisted powder metallurgy route for HEAs retained the sample shape formed by uniaxial pressing, thus opening the possibility for near net shape manufacturing of HEA components, provided that proper post-heat treatment is performed. The sample composition was homogeneous in all cases, without the typical dendritic segregation produced by traditional technologies. However, post-treatment is needed to compensate for some lack of homogeneity, like local depletion of some elements, which can be attributed to the sluggish diffusion, typical of many high entropy alloys. Finally, CS has been applied also to mineral ore reduction, using metallothermic reactions, leading to the synthesis of iron-based alloys. CS performed favorably compared to carbothermal reduction, when a low carbon content of the products is required.

## REFERENCES

- [1] G.Poli, R.Sola, P.Veronesi, Microwave-assisted combustion synthesis of NiAl intermetallics in a single mode applicator: Modeling and optimisation. *Mat. Sci. and Eng.: A*, vol. 441, no. 1–2, pp. 149-156, 2006
- [2] R. Rosa, P. Veronesi, C. Leonelli, A review on combustion synthesis intensification by means of microwave energy, *Chem. Eng. and Proc.*, vol. 71, pp. 2– 18, 2013
- [3] E. Colombini, et al., Microwave ignited combustion synthesis as a joining technique for dissimilar materials: Modeling and experimental results, *Int. J. Self Propag. High Temp. Synth.* vol. 21, pp. 25–31, 2012
- [4] P. Veronesi, et al., A. Microwave assisted combustion synthesis of non-equilibrium intermetallic compounds. *J. Microw. Power Electromagn. Energy*, vol. 44, pp. 46–56, 2010
- [5] R. Rosa, R., P. Veronesi, Functionally graded materials obtained by combustion synthesis techniques: A review. In *Functionally Graded Materials*; Reynolds, N.J.M., Ed.; Nova Science Publishers: New York, NY, USA, 2012; Chapter 2, pp. 93–122.
- [6] P. Veronesi, et al., Enhanced reactive NiAl coatings by microwave-assisted SHS. *COMPEL* vol. 27, pp. 491–499, 2008
- [7] R. Rosa, et al., Microwave ignition of the combustion synthesis of aluminides and field-related effects, *Journal of Alloys and Compounds*, vol. 657, pp. 59-67, 2016
- [8] R. Rosa et al., Microwave assisted combustion synthesis in the system Ti–Si–C for the joining of SiC: Experimental and numerical simulation results, *Journal of the European Ceramic Society* vol. 33, pp. 1707–1719, 2013
- [9] P. Veronesi, Microwave processing of high entropy alloys: A powder metallurgy approach, *Chemical Engineering and Processing*, vol. 122, pp. 397–403, 2017
- [10] P. Veronesi, Microwave-Assisted Preparation of High Entropy Alloys, *Technologies* vol. 3, pp. 182-197, 2015
- [11] E. Colombini et al., SPS-assisted Synthesis of SiCp reinforced high entropy alloys: reactivity of SiC and effects of premechanical alloying and post-annealing treatment, vol. 61, no. 1, pp. 64-72, 2018
- [12] P. Veronesi et al., Microwave assisted synthesis of Si-modified Mn<sub>25</sub>Fe<sub>x</sub>Ni<sub>25</sub>Cu<sub>(50-x)</sub> high Entropy alloys, *Materials Letters*, vol. 162, pp. 277–280, 2016

# Dry Microwave Chemistry Enabled Fabrication of Pristine Holey Graphene Nanoplatelets with Rich Zigzag Edges

Huixin He

Department of Chemistry, Rutgers University, Newark, NJ 07102, USA

**Keywords:** Dry microwave chemistry, graphene, holey graphene, edge

## INTRODUCTION

Holey graphene, referred to as graphene with nanoholes in their basal planes, recently attracted increasing research interests from both fundamental and practical application point of view.[1] The existence of nanoholes in these bulk 3D materials not only increases accessible surface area, but also provides desired “short-cuts” for efficient mass transport across graphene basal planes and ultimate access to/ from inner surfaces, which is very different from the intrinsic perfect graphene sheets. Most importantly, generating nanoholes naturally transform a large number of in-plane atoms into edge atoms. These atoms have different electronic states and chemical functionalities from their basal planes, which render holey graphene materials unique properties and capabilities. Recent years have witnessed wide range applications from molecular sensing to electrochemical energy generation and storage, demonstrating the critical advantages of holey graphene-based materials toward practical applications. However current approaches for scalable production of holey graphene materials require graphene oxide (GO) or reduced GO (rGO) as starting materials.[2] Thus generated holey graphene materials still contain a large number of defects on their basal planes, which not only complicates fundamental studies, but also influences certain practical applications due to the largely decreased conductivity, thermal and chemical stability.

## METHODOLOGY

This work reports a novel, rapid, and eco-friendly mass production approach. In this approach, dry microwave chemistry was exploited to fundamentally solve the problems in traditional methods, so that controllable generation of nanoholes can be achieved while leaving other parts of the graphene basal plane largely intact. Furthermore, the hole edges can be controlled to be rich in zigzag geometry, which is the preferred edge structure for catalytic and spintronic applications.

## RESULTS

The near pristine nature of their basal planes and the zigzag edges were clearly observed *via* atomic resolution Transmission Electron Microscope (TEM) and further supported by other techniques, including the studies of the localized  $\pi$ -edge states associated with zigzag geometry *via* electron paramagnetic resonance (EPR) measurements.

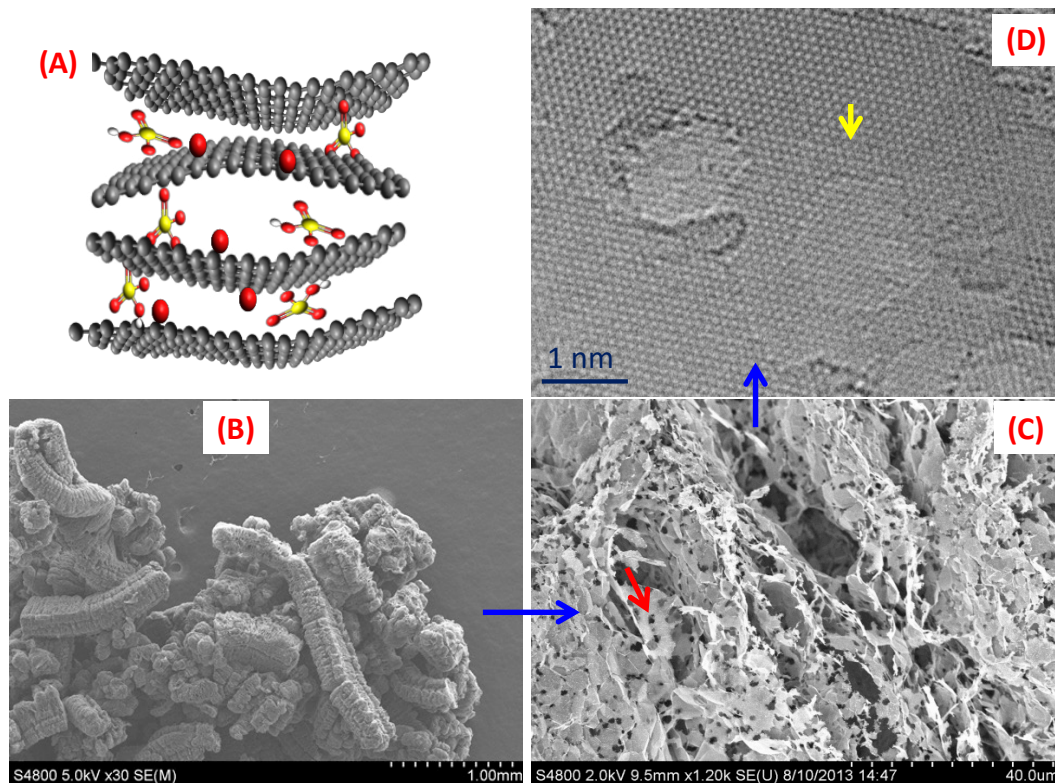


Figure 1. (A) A schematic drawing showing the slightly oxidized GIC (SO-GIC). The dry powder is of SO-GIC is used as the starting material for microwave irradiation. (B) Short microwave irradiation in air induces concurrent exfoliation of the SO-GIC and hole generation. Scanning Electron Microscope (SEM) images of the exfoliated SO-GIC (B, C). The red arrow pointed to a large hole in (C). (D) High resolution TEM shows that nanoholes were also generated while leaving the rest of the basal plane almost defect free. The yellow arrow pointed zigzag edges of the holes.

## DISCUSSION

There are no scalable approaches reported to date for mass production of highly conductive and chemically stable pristine holey graphene without involving metal-containing compounds and at low cost for practical bulk applications. Furthermore, the traditional methods are challenging in controlling the hole edges with dominated zigzag geometry. From thermodynamic point of view, armchair should be the major ones. We attribute the unexpected results presented in this work to the unique contactless Joule heating mechanism provided by microwave heating applied in this approach compared to

traditional convection heating approaches and also the structure of the slightly oxidized graphite as the starting materials for the microwave chemistry.

## CONCLUSION

In summary this work reports a simple and scalable approach to fabricate pristine holey graphene nanoplatelets which are rich in zigzag edges. The approach exploits dry microwave chemistry providing several non-competeable advantages over the previously reported methods for large scale production and broad application.

## REFERENCES

- [1] Sun, H. T.; Mei, L.; Liang, J. F.; Zhao, Z. P.; Lee, C.; Fei, H. L.; Ding, M. N.; Lau, J.; Li, M. F.; Wang, C.; Xu, X.; Hao, G. L.; Papandrea, B.; Shakir, I.; Dunn, B.; Huang, Y.; Duan, X. F. *Science* vol. 356, pp. 599-604, 2017.
- [2] Han, X. G.; Funk, M. R.; Shen, F.; Chen, Y. C.; Li, Y. Y.; Campbell, C. J.; Dai, J. Q.; Yang, X. F.; Kim, J. W.; Liao, Y. L.; Connell, J. W.; Barone, V.; Chen, Z. F.; Lin, Y.; Hu, L. B. *Acs Nano* vol. 8, pp.8255-8265, 2014.

# Microwave-assisted Preparation of Polyphosphoric Acid in a Continuous Flow Reactor

Chun Zhang, Huacheng Zhu, Yang Yang and Kama Huang

Sichuan University, Chengdu, China

**Abstract:** Microwave selective and rapid heating techniques in conjunction with greener reaction media are significantly reducing energy consumption and reaction times in material synthesis and several organic transformations. Poly-phosphoric acid(PPA) is a liquid mixture solution with high added value, which is widely used in petrochemical and electronic materials manufacturing. Traditional single batch reactor for preparing of PPA is time-consuming, high energy consumption and low polymerized degree, the largest barrier of which is the scaling up from a laboratory scale to a production scale.

In this paper, a highly temperature-controlled continuous flow tubular reactor system was developed in the optimized waveguide type monomode microwave cavity.

The structure of microwave monomode heating system is shown in Figure 1. The microwave-assisted preparation of PPA is performed in monomode microwave heating laboratory system composed of microwave generator with intelligent power control unit, fiber-optic probe for temperature measurements. The tubular reactor is placed in the middle of the waveguide, where the electric field is the strongest by adjusting the position of tunable short circuit.

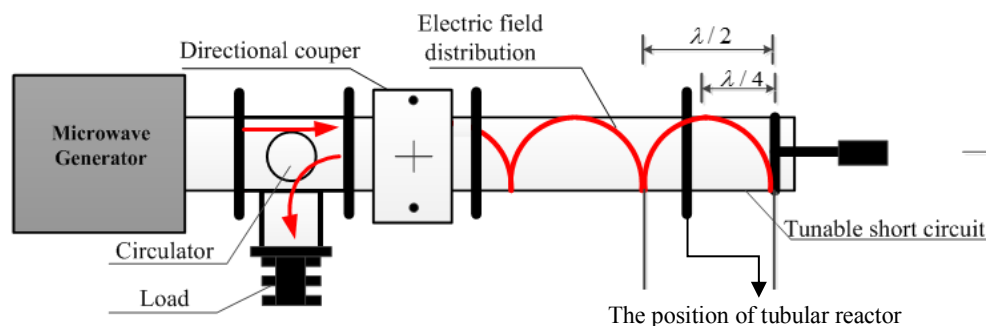


Fig.1 The structure of microwave system

Because phosphoric acid is highly corrosive, special continuous-flow processing system needs to be designed, as shown in Figure2. An upward anti-flash hood

connected to the quartz reactor and cooling water applied both to the vapor and the condensed phosphoric acid. An empty flask followed by a multi-neck flask and a conical flask are placed after the upper condense pipe and the same one below. The rubber tube connected the conical flask and the multi-neck flask is used to keep the balance of the system pressure.

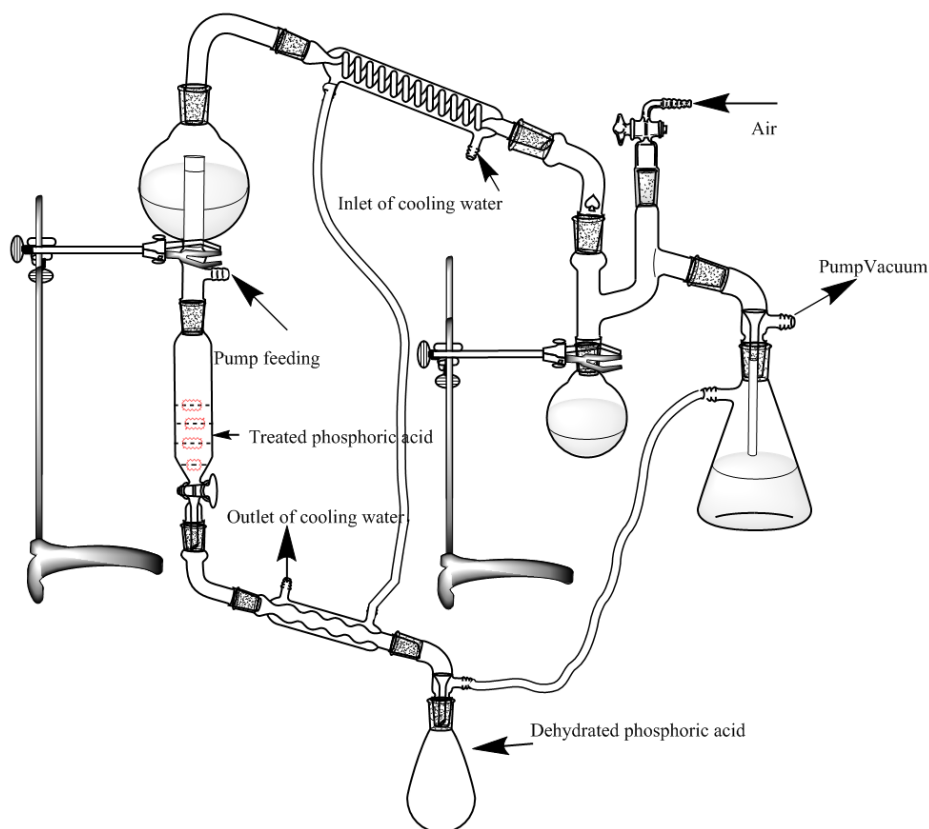


Fig.2 The set-up of continuous-flow processing system

An amount of 100g orthophosphoric acid (85%) as primary material is automatically feed into the quartz reactor by peristaltic pump and heated by microwave. Temperature was measured in this whole process of concentrating, which can be maintained at the target temperature by adjusting the feeding rate or reducing MW power to a required level calculated by PID controller.

For the sake of better concentrating efficiency, different microwave power input(Fig.3(a),(b)), reduced pressure by vacuum air pump in the system(Fig.3(c)), and inlet flow velocity of phosphoric acid was studied (Fig.3(d)). From Fig.3(a) and (b), we can conclude that increasing microwave input power can shorten the time and increase the concentration. A slightly negative pressure environment is also conducive to the evaporation of water as shown in Fig.3(c). Fig.3(d) shows the mean value of absorbed microwave power to maintain the temperature at 250°C for variant flow velocity.

The optimal dehydration process conditions were obtained through a series of contrast experiments.

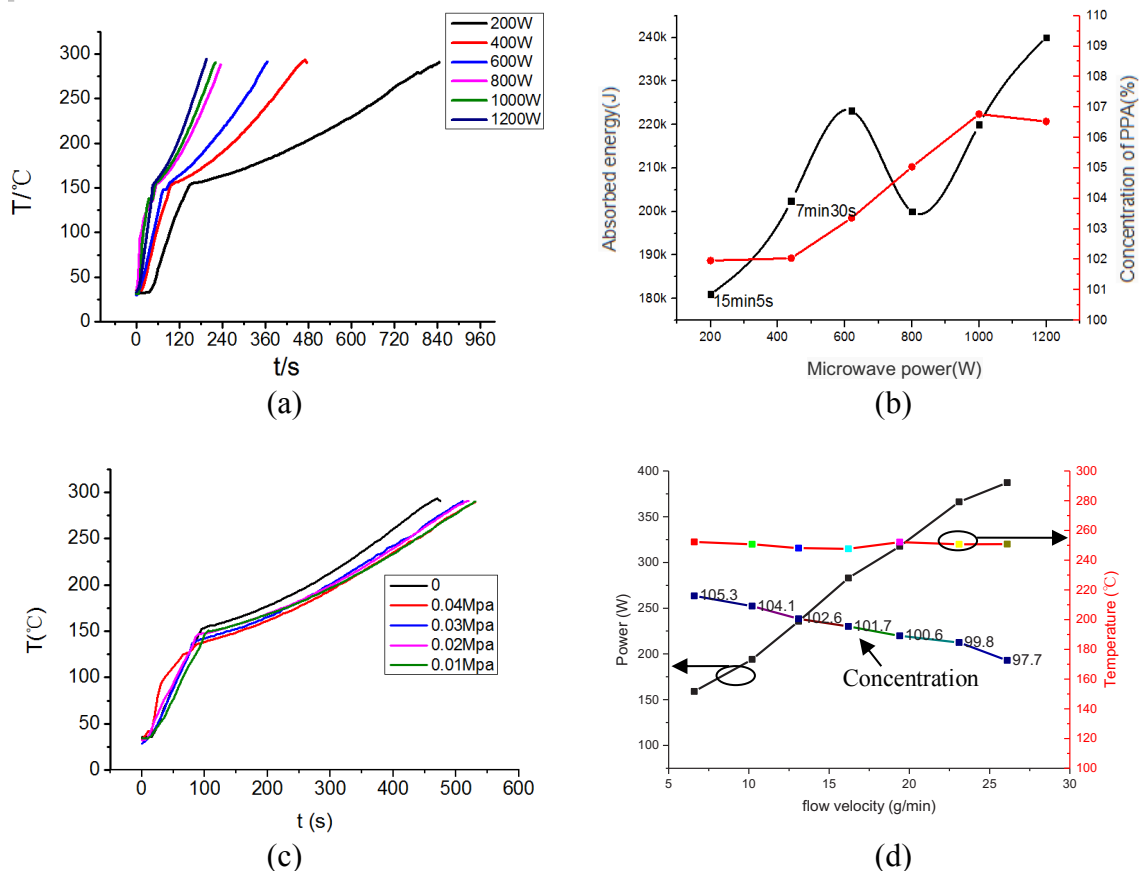


Fig.3 Experimental result

A microwave-assisted continuously condehydration of orthophosphoric acid for preparation of PPA was investigated at the laboratory scale. It has been shown that MW irradiation can be efficiently applied for PPA preparation due to the high absorbing capacities of the starting material and the process products. Under the conditions of optimized power and temperature control, our results can be considered as a reference point for scale-up experiment scale-up and have shown a successful performance of MW orthophosphoric acid dehydration on an industrial-scale which will be beneficial in terms of process times and energy efficiencies for its much higher process rates.

# Using Evanescent Field Applicators for Shallow Microwave Heating

Graham Brodie, Grigory Torgovnikov and Peter Farrell

The University of Melbourne, Australia

**Keywords:** Microwave, Shallow Heating, Dielectric Resonator

## INTRODUCTION

Microwave heating is determined by the field distribution in a dielectric material. These field distributions depend on the frequency of the microwave fields, the geometry of the applicator, the geometry of the heated material, and the dielectric properties of the material [1]. In many cases, the objective of microwave heating is a uniform temperature distribution; however, in some application, such as the treatment of asphalt, timber, soil or weeds, shallow surface heating is desirable to reduce energy requirements.

Evanescent fields are non-propagating electromagnetic fields, which decay exponentially with distance, even in the absence of any dielectric material which could absorb the energy. Evanescent fields exist in wave guides, which are operating below cut-off wavelengths [2]; however, there are several other methods of generating evanescent fields. In particular, evanescent fields are associated with total internal reflection in dielectric wave guides (optic fibre) [3] or slow wave structures [4, 5]. In this case a dielectric material was used.

Assuming a wave is being transmitted along an electrically dense dielectric material (like plastic, glass or ceramic) such that the field is incident onto an interface with a less electrically dense material (like air). When the electromagnetic field is propagating parallel or nearly parallel to the interface, total internal reflection in the electrically dense material occurs; however, there is an evanescent field created in the less electrically dense material, which can be described by:

$$E_e = E_o e^{-\hat{z} \cdot \frac{2\pi}{\lambda_o} \cdot \sqrt{n_1^2 \sin^2 \theta_i - n_2^2}} \cdot e^{j\left(\hat{x} \cdot \frac{2\pi}{\lambda_o} \cdot \frac{n_1}{n_2} \cdot \sin \theta_i - \omega t\right)} \quad (1)$$

Where  $E_o$  is the field amplitude,  $\lambda_o$  is the wavelength in free space,  $w$  is the angular frequency of the wave,  $\hat{z}$  is the unit vector perpendicular to the surface of the dielectric material, and  $\hat{x}$  is the unit vector along the surface of the dielectric material in the direction of field propagation. In a non-magnetic material, the refractive index of material  $i$  is  $n_i = \sqrt{\kappa_i}$ , where  $\kappa_i = \frac{\epsilon_i}{\epsilon_o}$  and  $\theta_i$  is the incident angle onto the internal surface of the dielectric material, measured relative to the normal to the surface (i.e. for waves propagating parallel to the surface,  $\theta = 90^\circ$ ).

Equation (1) describes an evanescent electromagnetic wave, propagating along the surface of the electrically dense dielectric material, where the speed of the wave is slowed by a factor of  $\frac{n_1}{n_2}$  because of the dielectric behaviour of the material interface.

In the case of a dielectric block, which is housed in a metal applicator housing, with only one surface of the dielectric material exposed, there will be a standing wave

generated inside the dielectric block with an evanescent field on the exposed surface of the dielectric that can be described by:

$$E_e = E_o e^{-2k\sqrt{n_1^2 \sin^2 \theta_i - n_2^2}} \cdot \sin\left(\frac{l\pi y}{a}\right) \cdot \sin\left(\frac{m\pi z}{b}\right) \cdot \sin\left(\frac{n\pi x}{c}\right) \cdot e^{-j\omega t} \quad (2)$$

Where a, b, and c are the dimensions of the metal housing for the dielectric block inside the applicator; and l, m, and n are the mode numbers of the resonant field;  $\omega$  is the angular frequency of the wave and t is time.

## METHODOLOGY

A dielectric evanescent field applicator (Figure 1), operating at 2.45 GHz and based on a block of alumina, with dimensions of 355 mm by 140 mm by 13 mm, was designed, fabricated and tested for soil heating. Hortico Potting Mix was used for the tests. The soil had a moisture content of 32% (on a dry weight basis), a density of 586 kg m<sup>-3</sup> and a significant percentage of organic particles of different sizes. The soil was placed into polypropylene containers with dimensions of 120 x 250 x 300 mm.

The applicator was arranged with the exposed ceramic surface facing upward and the soil containers were placed on top of the applicator, for easy experimental arrangement. It was assumed that the very thin walls and floor of the polypropylene soil containers would not adversely affect the heating pattern.

Temperatures in the soil were measured by thermocouples: at depths of 10, 30, 50, 80 and 100 mm below the applicator; at distances of 30, 60, 90, 120, 150, 180, 210 mm from the beginning of the applicator; and at the distances of 37.5, 75, and 112.5 mm, in both directions from the centre plane of the applicator, after applying 55.5 kJ of microwave energy.



Figure 1: Evanescent field applicator, based on an alumina dielectric resonator, seated into the applicator housing and fed from a standard WR340 wave guide (left) an overview of the applicator design and (right) a photograph of the alumina block inside the applicator housing.

## RESULTS AND DISCUSSION

The temperature distribution (Figure 2) was of the form shown in equation (3) ( $R^2 = 0.88$ ), suggesting that the applicator housing supports multi-modal resonance, when the alumina block is place. This is due to the much shorter wavelength of the microwave fields inside the dielectric block, compared with the wavelength in air.

The temperature along the applicator length is naturally attenuated at a rate  $e^{-2ax}$  as the microwave energy is absorbed by the soil; however, the vertical decay in temperature is governed by:  $e^{-2dz}$ . The parameter, d, in the temperature profile model is about 13.5 times faster than the natural attenuation due to the soil, defined by parameter a, because it

is determined by the evanescent field decay rather than natural attenuation in a lossy medium.

$$T = T_a \cdot \left[ A_1 \sin^2 \left( \frac{\pi y}{a} \right) + A_2 \sin^2 \left( \frac{3\pi y}{a} \right) \right] \cdot \left[ A_3 \sin^2 \left( \frac{\pi x}{c} \right) + A_4 \sin^2 \left( \frac{2\pi x}{c} \right) \right] \cdot e^{-2ax} \cdot e^{-2dz} + T_o \quad (3)$$

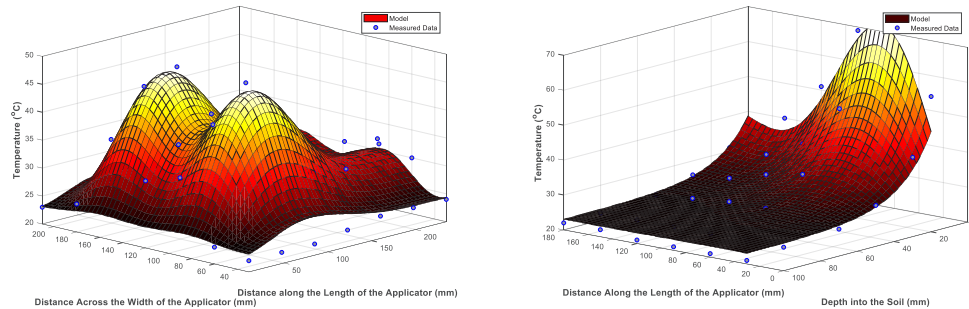


Figure 2: (left) Horizontal temperature distribution 10 mm below the soil surface, and (right) Vertical temperature distribution through one of the modal peaks at 90 mm from the start of the applicator

This type of applicator seems to be much more effective where only shallow surface heating is required. Multi-modal resonance in the applicator provides better heating uniformity across the width of the applicator than could be achieved using other systems, such as a horn antenna.

## REFERENCES

- [1] G. Brodie, "The influence of load geometry on temperature distribution during microwave heating," *Transactions of the American Society of Agricultural and Biological Engineers*, vol. 51, pp. 1401-1413, 2008.
- [2] K. I. Sinclair, G. Goussetis, M. P. Y. Desmulliez, A. J. Sangster, T. Tilford, C. Bailey, *et al.*, "Optimization of an Open-Ended Microwave Oven for Microelectronics Packaging," *IEEE Transactions on Microwave Theory and Techniques*, vol. 56, pp. 2635-2641, 2008.
- [3] N. J. Cronin, *Microwave and Optical Waveguides*. Bristol: J W Arrowsmith Ltd, 1995.
- [4] D. A. Dunn, "Slow wave couplers for microwave dielectric heating systems," *Journal of Microwave Power*, vol. 2, pp. 7-20, 1967.
- [5] Y. N. Pchel'nikov, "Features of slow waves and potentials for their nontraditional application," *Applications of Radiotechnology and Electronics in Biology and Medicine*, vol. 48, pp. 450-462, 2003.

# The Influence of Microwave Soil Treatment on the Toxicity of Arsenic in Wheat (*Triticum aestivum* L.)

Humayun Kabir, Graham Brodie, Dorin Gupta and Alexis Pang

The University of Melbourne, Dookie, Australia

**Keywords:** Microwave, Soil heating, Arsenic, Remediation, Wheat yield

## INTRODUCTION

Arsenic (As) is the most devastating toxic heavy metal in the environment, raising global concern for sustainable agriculture due to its ultimate toxicological effects, persistence in nature and ability of bio-accumulate in the ecosystem [1]. Different physical, chemical, and biological remediation technologies to avoid As pollution have already been introduced, but none of these methods satisfies full-scale remediation requirements. Microwave (MW), a form of electromagnetic radiation with wavelengths ranging from 1m to 1mm with frequencies between 300 MHz to 300GHz [2], is currently being used for diversifying waste treatment to reduce heavy metals [3] and increase crop growth and yield [4]. However, in As remediation, MW soil treatment is a new thought. Therefore, a glasshouse pot experiment was conducted to explore the toxicity of As on wheat plants as a function of concentration of As in the soil and MW soil treatment.

## METHODOLOGY

A two factorial, completely randomized block design glasshouse pot experiment was conducted with four replicates of each treatment combination at the Dookie Campus of the University of Melbourne, Australia. The soil, classified as clay loam, was collected from the wheat paddock of the Dookie farm (-36° 37' S; 145° 70' E) at a depth of 0–15 cm. Samples of 8.5 kg of soil were placed in unperforated plastic pots (27 cm diameter). These were treated with five levels of As (0, 20, 40, 60 and 80 mg kg<sup>-1</sup> soil) as aqueous solution prior to applying three levels of MW energy (0, 127.06 and 254.12 kJ kg<sup>-1</sup> soil). A 6 kW MW chamber consists of 6 magnetron (1 kW each) with the frequency of 2.45 GHz was used for 0, 3 and 6 minutes to achieve the soil temperature of 0, 60 and 90°C respectively, which correspond with the MW energy levels used for soil treatment.

Twelve seeds of the Gregory wheat variety were sown in each pot on 6<sup>th</sup> of June, 2017. Mono ammonium phosphate (MAP) fertilizer was applied (equivalent to 150 kg ha<sup>-1</sup>) to each pot as a starter dose for wheat production. Different growth parameters were measured during the growing period and the final dry biomass yield and grain yield were measured at crop maturity.

## RESULTS

The results show that, the MW soil treatment had a significantly beneficial effect on growth and yield parameters of wheat. For example, plant height, plant vigor, SPAD value, tiller number, biomass yield and grain yield increased significantly in MW treated pots compared with the control pots, even at the higher rate of As application (Figure 01). However, MW 6 minutes treatment showed significant increase in growth and yield compare with the control and MW 3 minutes treatment. Furthermore, some lower doses of As (20 and 40 mg kg<sup>-1</sup> soil) presented a positive response to some growth and yield parameters, although these decreased at higher As concentration (60 and 80 mg kg<sup>-1</sup> soil). Additionally, early wheat growth was more susceptible to As toxicity, compared with the mature stage. The high microwave treatment mitigated these early growth impacts.

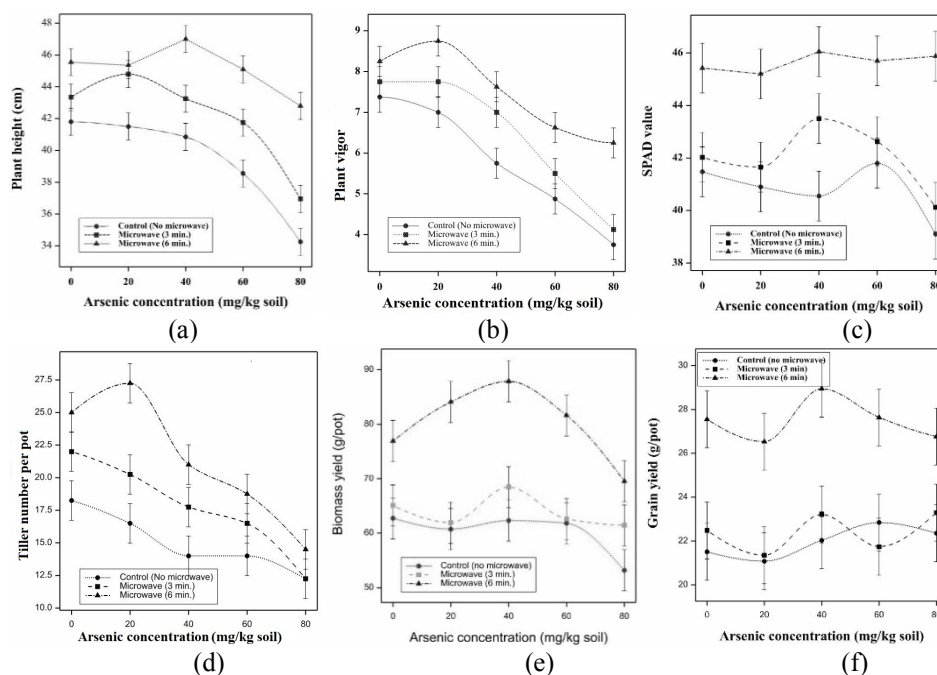


Figure 01: Effect of MW soil treatment on wheat plant growth and yield in As contaminated soil (a) plant height at maximum tillering, (b) plant vigor at early seedling, (c) SPAD value at maximum tillering, (d) tiller number at maximum tillering, (e) biomass yield at final harvest and (f) grain yield.

## DISCUSSION

It is well known that, high soil As has an adverse effect on plant growth and development due to its phytotoxicity. In this study, the results showed that the MW soil treatment had a significantly beneficial effect on growth and yield of wheat even at the higher rate of As application. More availability of nutrient and organic carbon from dead microorganisms results the higher amounts of substrate in the soil, which may enhance microbial activity, ultimately increasing the soil fertility and final crop growth [5].

Humification of soil organic matter, increases of soil organic carbon and macromolecular organic substances with higher numbers of functional groups [6], and synthesis of organometallic and coordination compounds result from the MW irradiation. These possibly reduce the bioavailability and adsorption of As and ultimate result in better plant growth. In addition, displacement of soil phosphate by arsenate increased the availability of phosphate to the plant, which results in the increased plant growth at low concentration of As. This decreased again at the higher As level. As is not an essential element for plants, but small amounts of As can stimulate plant growth and increase plant biomass [7]. Furthermore, at the early growth stage, As had more effect on the plant growth whereas, at the mature stage As showed less effect because of better establishment of plants at mature stage.

## CONCLUSION

MW soil treatment (6 minutes) significantly increased the growth and yield of wheat plants, even at the higher level of As compare with the control and MW 3 minutes treatment. Low concentrations of As to some extent enhanced the plant growth, which decreased significantly with increasing As concentration. As has more adverse effects at earlier growth stages than at the mature stage of wheat crop growth. Finally, MW soil treatment may have potential to reduce As toxicity to wheat plants. However, though this was the first As and MW interaction experiment so far, further detailed laboratory and glasshouse pot experiments need to explain the reasons for better plant growth in MW treated soil along with As contamination.

## REFERENCES

1. Naidu, R., et al., *Managing arsenic in the environment: from soil to human health*. 2006: CSIRO publishing.
2. Banik, S., S. Bandyopadhyay, and S. Ganguly, *Bioeffects of microwave—a brief review*. *Bioresource technology*, 2003. **87**(2): p. 155-159.
3. Dauerman, L., et al. *Microwave treatment of hazardous wastes: feasibility studies*. in *Microwave Conference, 1992. APMC 92. 1992 Asia-Pacific*. 1992. IEEE.
4. Brodie, G., *Applications of Microwave Heating in Agricultural and Forestry Related Industries*, in *The Development and Application of Microwave Heating*. 2012, InTech.
5. Zhou, B.W., et al., *Effect of microwave irradiation on cellular disintegration of Gram positive and negative cells*. *Applied Microbiology and Biotechnology*, 2010. **87**(2): p. 765-770.
6. Kim, M.C. and H.S. Kim, *Artificial and enhanced humification of soil organic matter using microwave irradiation*. *Environmental Science and Pollution Research*, 2013. **20**(4): p. 2362-2371.
7. Onken, B. and L. Hossner, *Plant uptake and determination of arsenic species in soil solution under flooded conditions*. *Journal of Environmental Quality*, 1995. **24**(2): p. 373-381.

# Investigation of Radio Frequency Heating as A Dry-blanching Method for Carrot Cubes

Chuting Gong<sup>1</sup>, Yanyun Zhao<sup>2</sup>, Yubin Miao<sup>3</sup>, Hangjin Zhang<sup>1</sup>, Jin Yue<sup>1</sup>,  
Shunshan Jiao<sup>1\*</sup>

<sup>1</sup>SJTU-OSU Innovation Center for Environmental Sustainability and Food Control, Key Laboratory of Urban Agriculture (South), School of Agriculture and Biology, Shanghai Jiao Tong University, 800 Dongchuan Rd., Shanghai 200240, China

<sup>2</sup>Department of Food Science and Technology, 100 Wiegand Hall, Oregon State University, OR, USA

<sup>3</sup>School of Mechanical Engineering, Shanghai Jiao Tong University, 800 Dongchuan Rd., Shanghai 200240, China

**Keywords:** Radio frequency (RF), Blanching, Enzyme activity, Quality, Carrots

## INTRODUCTION

Blanching is a key step in fruits and vegetables dehydration process to protect color and texture by inactivating enzymes. Conventional blanching generally uses hot water or steam as heating medium, which would result in adverse effects on color, texture and nutritional value. Radio frequency (RF) heating had been proposed and studied as a new blanching method recently for fruits and vegetables. RF heating was applied to inactivate oxidative enzymes (PPO and LOX) in model system and apples, apples can be adequately blanched because of thermal effect of RF treatment and quality of apples was comparable to that blanched by conventionally hot water [1]. Besides, RF heating was investigated for blanching of potato cuboids and the corresponding quality change was also evaluated, the results indicated RF heating holds great potential for blanching of vegetables [2, 3]. This study investigated RF heating as a dry-blanching method for carrot cubes. RF blanching treatment protocol was developed and RF blanching effect and associated quality change (texture, vitamin C, color, etc.) were also evaluated by comparing with conventional blanching method (2 % NaCl, 95, 2.0 min).

## METHODOLOGY

RF heating unit (12 kW, 27.12 MHz) was used in this study. The carrot cubes (5.0×5.0×5.0 mm<sup>3</sup>) were prepared, placed in different type of containers and blanched by RF heating for 3.0-7.0 min with electrode gap of 8.0-8.6 cm. Temperature profile during RF heating was recorded by placing fiber optic sensors in five different positions and RF heating uniformity was evaluated by using temperature uniformity index (TUI) [4], peroxidase (POD) enzyme activity was measured based on guaiacol method, vitamin C content was determined by spectrophotometric method, sample color and texture were measured by chromascope and texture analyzer, respectively. Data were analyzed by analysis of variance (ANOVA) and test at significant level of 0.05 using the statistical SPSS software.

## RESULTS

RF heating uniformity increased with RF electrode gap increasing, different types of containers affected RF heating uniformity as well, and samples filled in round shape container had better RF heating uniformity. Besides, the enzyme activity (POD) of carrots with thickness of 6.8 cm was reduced by 90-95% after RF blanching for 2.0-7.0 min at different electrode gaps (8.0-8.6 cm). Hardness, chewiness and springiness of carrot cubes decreased after RF blanching. The redness of the samples blanched by RF was higher than those blanched by conventional method which is more preferred. The loss rate of vitamin C of samples blanched by RF was significantly ( $p>0.05$ ) lower than that blanched by conventional method.

Table 1. The water activity, color (redness), hardness and vitamin C content of carrot cubes blanched by RF and conventional hot water.

Treatments	Water activity	a* (redness)	Hardness	Vitamin C (mg/100g)
Fresh samples	0.91±0.01 <sup>a</sup>	37.14±0.03 <sup>a</sup>	68.56±0.01 <sup>a</sup>	12.89±0.09 <sup>a</sup>
Conventional blanching (95°C, 2.0 min)	0.83±0.02 <sup>b</sup>	32.01±0.05 <sup>e</sup>	22.13±0.10 <sup>e</sup>	6.91±0.31 <sup>d</sup>
RF blanching (8.0 cm, 3.0 min)	0.68±0.01 <sup>c</sup>	36.88±0.05 <sup>c</sup>	31.63±0.06 <sup>d</sup>	8.51±0.31 <sup>b</sup>
RF blanching (8.3 cm, 5.0 min)	0.71±0.02 <sup>c</sup>	36.11±0.08 <sup>d</sup>	40.11±0.29 <sup>c</sup>	7.68±0.05 <sup>c</sup>
RF blanching (8.6 cm, 7.0 min)	0.80±0.01 <sup>b</sup>	37.03±0.05 <sup>b</sup>	45.87±0.26 <sup>b</sup>	7.92±0.15 <sup>bc</sup>

The superscripts in the same column with different alphabet are significantly different ( $p<0.05$ )

## DISCUSSION

The results indicated that RF dry-blanching obtained better blanching effect because of lower blanching temperature and faster heating rate comparing to conventional method. Owing to dielectric and volumetric heating characteristics of RF treatment, carrots treated by RF dry-blanching had expected color with relatively high redness retention and less shrinkage in texture. Besides, instead of using hot water as heating medium, RF dry-blanching obtained better retention of water-soluble nutrient such as vitamin C.

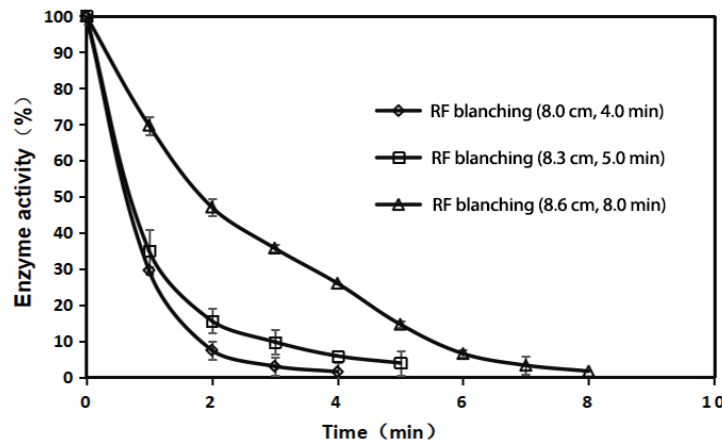


Figure 1. Enzyme activity-time profile of carrot cubes obtained from RF heating between different electrode gap.

## CONCLUSION

This study demonstrated that RF dry-blanching method is an effective blanching method for carrot cubes, and the quality of samples can be well maintained. Improvement of RF heating uniformity during RF blanching should be further investigated in the future study to reduce the adverse effects on product quality.

## REFERENCES

- [1] Manzocco, L., Anese, M., & Nicoli, M. C. (2008). Radiofrequency inactivation of oxidative food enzymes in model systems and apple derivatives. *Food Research International*, 41, 1044–1049.
- [2] Zhang, Z., Guo, C., Gao, T., Fu, H., Chen, Q., & Wang, Y. (2018a). Pilot-scale radio frequency blanching of potato cuboids: heating uniformity. *Journal of the Science of Food and Agriculture*, 98, 312–320.
- [3] Zhang, Z., Wang, J., Zhang, X., Shi, Q., Le, X., Fu, H., & Wang, Y. (2018b). Effects of radio frequency assisted blanching on polyphenol oxidase, weight loss, texture, color and microstructure of potato. *Food Chemistry*, 248, 173–182.
- [4] Alfai, B., Tang, J., Jiao, Y., Wang, S., Rasco, B., Jiao, S. & Sablani, S. (2014). Radio frequency disinfestation treatments for dried fruit: model development and validation. *Journal of Food Engineering*, 120(1), 268-276.

# Industrial Microwave Assisted Pressurized Induction Heating (MAPIH) Thermal Processing System – An Application of Microwavable Brown Rice Preparation

**Kuang-tse Chin<sup>1</sup>, Hong-I Chang<sup>2</sup>, Chung-Jen Chen<sup>3</sup>, Yi-Chieh Tsai<sup>3</sup>, Jhao-Rong Huang<sup>3</sup>, and Yeun Chung Lee<sup>4</sup>**

<sup>1</sup> BOTTLE-TOP Machinery Co., Ltd. Nantou, Taiwan.

<sup>2</sup> National Formosa University, Yunlin, Taiwan

<sup>3</sup> Food Industry Research & Development Institute, Hsinchu, Taiwan.

<sup>4</sup> National Taiwan University, Taipei, Taiwan.

**Keywords:** microwave assisted, induction heating, microwave tray, precooked brown rice, thermal processing

## INTRODUCTION

Conventional thermal processes have been available in food industry for more than a century, some of their products are still of questionable quality. One of the major quality detracting attributes is long heating time; thus, microwave have been considered as a solution. Recently, a microwave assisted thermal sterilization (MATS) system, developed at Washington State University (WSU), has been licensed to the Food Chain Safety Company [1]. Some engineering considerations and the potential for application in the meat industry, have been reviewed [2]. Microwave assisted systems would be a great innovation in the food industry. A continuous Industrial Microwave Assisted Pressurized Induction Heating (MAPIH) Thermal Processing System was developed by BOTTLE-TOP in Taiwan [3]. The MAPIH is an individual package thermal process system that could be used for high temperature cooking and sterilization. In this paper we present some primary results of developing and evaluating shelf stability of brown rice in a microwavable tray. Brown rice is considered to have more health benefits than white rice, but it is more difficult to cook and less palatable. Microwavable products would provide better taste and convenience to consumers. The experimental works were carried out in the MAPIH simulator which is a single batch system designed for product development as well as small scale in-store processing.

## METHODOLOGY

The MAPIH simulator consisted of a rotatable semi-hermetic induction heating cavity and a microwave power source. A 1 kW induction heating coil plate was set inside the heavily constructed cavity, which was closed by a polytetrafluoroethylene (PTFE) cover. Above the cavity was a 1 kW 2.45GHz microwave source. The microwaves radiated from a rectangular waveguide (TE10 mode) antenna into the cavity. An 8mm thick CPET tray ( $\Phi=133\text{mm}$ ,  $H=21.5\text{mm}$ ) was used in the experiments. The tray was heat sealed with a 0.07mm thick laminated plastic film (PET/PE/LLDPE/PE). Brown rice was pre-soaked for 15 hours and then filled and sealed in the tray. Comparative studies were conducted with: steam retorted samples; MW/IH 2 min; MW/IH 1 min+IH 6 min; MW/IH 2 min+IH 2 min; and (MW/IH) 2 mi+(IH) 4 min, where MW: microwave heating, IH: induction heating, MW/IH: combined. Temperature was measured during the process using FPI-HR-2 with FOT-L-SD Temperature Sensors (FISO Technologies, Quebec, Canada). In some experiment Kromagen Magenta K120-NH ink (TMC Hallcrest, Flintshire, UK) was used as a temperature indicator. The thermally sensitive dye showed a distinct pink color at around 120 °C. Some samples were tested by TA-XT2 Texture Analyzer (Stable Micro System, Surrey, England) to compare texture qualities objectively. Organoleptic test were the main method used in quality evaluation. In the sensory evaluation, coded samples were presented to the panelists and scored for color, texture, flavor, and overall acceptability on a 9-point hedonic scale. Samples were stored in incubators (LTS-580CH, Yscco, Hsinchu, Taiwan) at 18 °C and 80% relative humidity for 10, 15, and 30 days for shelf stability tests. After storage, samples were tested by sensory evaluation and standard bacteriological analysis.



Figure 1. The MAPIH simulator, and assembly of processing cavity.

## RESULTS AND DISCUSSION

Brown rice was well cooked under pressure in the MAPIH simulator. Fig 2 shows the temperature history during microwave heating; 115 °C was the highest temperature reached at this experiment. Fig. 3 shows the temperature distribution of brown rice in the tray after different process operations. Heated under (MW/IH) 2 mi+(IH) 4 min gave a very uniform temperature profile. The heating process also resulted in the most palatable products right after processed and after various storage times. The bacteriological analysis indicted negative results. The primary study has shown the MAPIH simulator and pressurized process might be a good method for preparing shelf stable brown rice products.

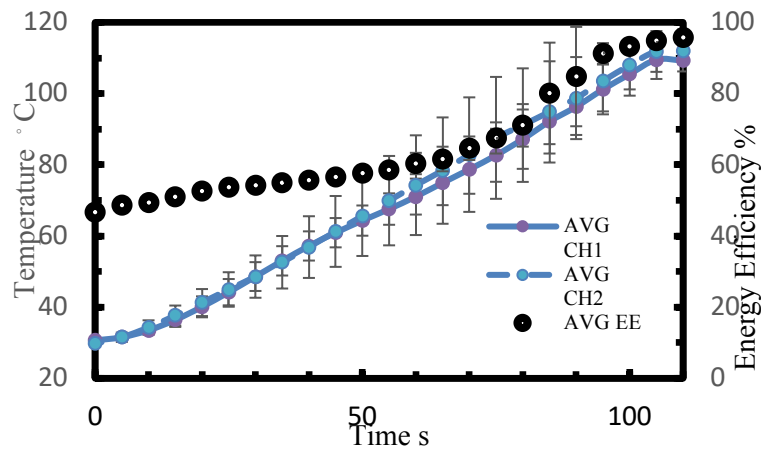


Figure 2. Temperature history of brown rice during microwave heating and energy efficiency during the process.

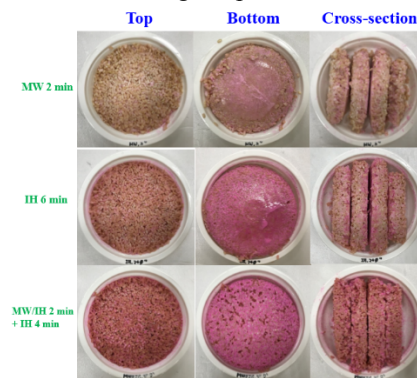


Figure 3. Temperature profile shown by thermal sensitive dye after various heating procedures.

**CONCLUSION**

In the study we used the MAPIH simulator to prepare shelf stable and microwavable brown rice successfully. The thermal process system might have the potential to extend to other products

**REFERENCES**

[1] J. Tang, Microwave sterilization for packaged meals. *Food Engineering Magazine* October, pp-159-160, 2013.  
 [2] G. V. Barbosa-Cánovas, I. Medina-Meza, K. Candoğan, D. Bermúdez-Aguirre, Advanced retorting, microwave assisted thermal sterilization (MATS), and pressure assisted thermal sterilization (PATS) to process meat products. *Meat Science*. 98(3), pp.420-434, 2014.  
 [3] <http://www.bottop.com/microwavec.html>

# Improving Plant's High Temperature Tolerance and Pest Resistance by Microwave Effective Stimulation

K. Kadomatsu, N. Suzuki, S. Horikoshi

Sophia University, 7-1 Kioi-cho, Chiyoda-ku, Tokyo, 102-8554, Japan

**Keywords:** microwave, plants, high-temperature tolerance, pest resistance

## INTRODUCTION

In a previous study, our laboratory discovered that irradiation by weak microwaves of *Arabidopsis thaliana* (model plants) during the vegetative growth stage accelerates the development of inflorescence stems and subsequent growth, and induces heat stress tolerance. In this study, the useful effects of microwave stimulation were observed using strawberry. We found that microwave irradiation was able to enhance high-temperature tolerance during fruit production and pest resistance in strawberry, and some more detailed mechanisms of this process were investigated.

## METHODOLOGY

Strawberry plants (cultivar: Houkouwase), in the reproductive growth stage, were irradiated with 2.45GHz, 30 W of microwave power, for 1 hour in a multimode device. Then, plants were transplanted onto a planter containing commercial culture soil and grown on the rooftop (outdoor). To diminish the influence of differences in the conditions of sunshine and wind in different positions, each planter was regularly relocated in the experiment. We investigated stem length, number of leaves, fresh weight of fruits and number of flowers and fruits per plant after microwave stimulation treatment.

To confirm the results obtained from the analyses of strawberries, experiments were also carried out using *Arabidopsis thaliana* (cultivar: Columbia-0) which is used as a model plant. For *Arabidopsis thaliana*, plants were grown on culture soil (Jiffy 7, peat pellet) in an artificial growth chamber (Nihon Medical Instruments Manufactory, LH-60FL 12-DT) (21 ° C., 16 hr photoperiod). Microwave stimulation treatment was applied at 14 days after seeding. In the leaf preference test using the larvae of the cabbage butterfly, the plants which were subjected to

the microwave stimulation treatment and the untreated plants were placed apart from each other by about 10 cm. The larvae were placed at the center thereof to observe which plant the larvae choose. In addition, an egg preference test on microwave stimulated plants and untreated plants was performed using adults of Mongolia butterfly. Furthermore, from the viewpoint of molecular biology, genes related to jasmonic acid synthesis (plant hormone involved in wound response and pest resistance) were analyzed using Real-time PCR method.

## RESULTS AND DISCUSSION

**High temperature resistance:** Microwave-treated strawberries tended to produce fruits for a longer period compared with the untreated strawberries. This difference between microwave treated- and untreated-plants may be due to the enhanced tolerance to high-temperature by microwave stimulation treatment. Indeed, when the temperature during the fruiting period was examined, the temperature was above 25 ° C, which is higher than the optimum temperature for the growth of strawberry, 20 to 23 ° C. In general, strawberries will not fruit when the temperature rises during the day. Therefore, tolerance to high-temperature is improved by microwave stimulation treatment, resulting in longer period of fruit production.



**Figure 1.** Pictures taken on the same day (right) Microwave, and (left) Control.

**Pest resistance:** Observation of strawberry leaves for a long period revealed that the plants that were subjected to microwave stimulation tended to have less damage caused by insects on leaves than the control plants. The number of leaves that suffered from insect feeding damage in the microwave stimulated plants was reduced to about half of that in the untreated plants.

We also investigated the number of leaves and the leaf area. No difference was found in the number of leaves. But it was found that the leaf area of the microwave stimulated plants was larger than that of the untreated control plants. A similar tendency was also observed in cauliflower and rocket. Therefore, to confirm the positive effects of microwave stimulation on defense against pests, *Arabidopsis thaliana*, grown in the laboratory, was used to investigate the presence or absence of feeding damage by the larvae of the

experimental cabbage butterfly. When placing the larva of the cabbage butterfly at the center between the microwave stimulated leaves and untreated leaves, the larvae tended to choose control leaves (Fig. 1). When the plants were subjected to microwave stimulation treatment, it was confirmed that feeding damage on leaves was reduced.

Generally, it is known that plants exhibit various protective reactions against injury, such as the production of jasmonic acid. Analysis of the genes related to the biosynthesis of jasmonic acid confirmed an increased expression of ACX2, ACX4, AOS and its response gene MGL. This suggests that jasmonic acid is involved in the attenuation of feeding damage via microwave stimulation treatment. Other defense reactions including production of secondary metabolites and reactive oxygen species, will be also considered in future studies.

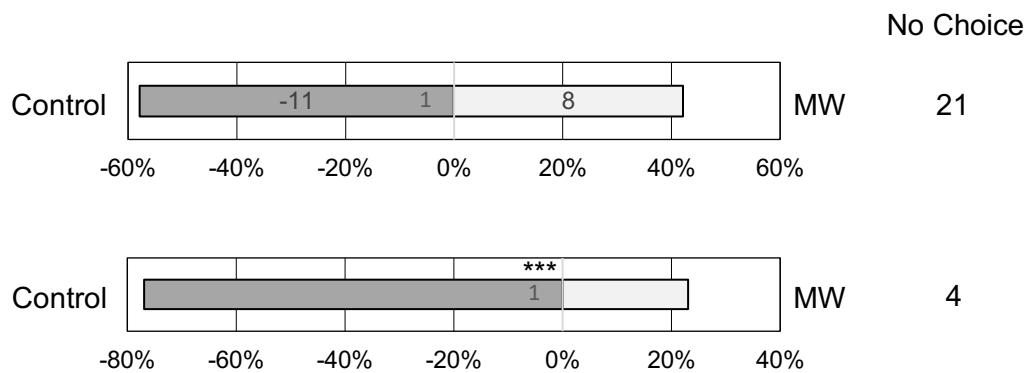


**Figure 2.** Results of preference test to *Arabidopsis thaliana* by larvae of cabbage butterfly. \*\*\* :Student binominal test at  $0.001 < P < 0.01$

**CONCLUSION**

We figured out that microwave stimulation is the useful strategy to enhance tolerance of plants to high temperature during fruit production and pest resistance. It will be applicable to harvest the heat-sensitive fruits such as strawberry under the high temperature. In addition, enhanced pest resistance via microwave irradiation may be due to the activation of jamonic acid synthetic pathway and its downstream signaling. Other mechanisms including production of secondary metabolites and reactive oxygen species were shown to be also involved in pest resistance. Therefore, the effects of microwave irradiation on these other mechanisms in plants will be investigated in future studies.

# Radiofrequency Inactivation of *Enterococcus faecium* NRRL B-2354 in Cumin Seeds

Long Chen<sup>1</sup>, Jeyamkondan Subbiah<sup>1,2\*</sup>

<sup>1</sup>Department of Biological Systems Engineering, University of Nebraska-Lincoln,  
Lincoln, NE 68583, USA

<sup>2</sup>Department of Food Science and Technology, University of Nebraska-Lincoln,  
Lincoln, NE 68588, USA

**Keywords:** RF heating, cumin seeds, pasteurization, *E. faecium*

## ABSTRACT

A large number reported outbreaks of *Salmonella* in spices has been reported in the United States and around the world. Radiofrequency (RF) heating is a novel thermal processing technology, which volumetrically heats the food products resulting in a shorter come-up time. This feature can be used to develop a high-temperature short-time pasteurization method to assure food safety with minimal deterioration in food quality. In this study, cumin seeds were inoculated with *Enterococcus faecium* NRRL B-2354 (*E. faecium*) and evaluated as a potential surrogate for RF processing in cumin seeds. A small bag of 20 g cumin seeds was inoculated with *E. faecium* and placed in the cold spot of 450 g cumin seeds packed in a rectangular tray sealed by Press'n film with a venting nut at the center. The whole tray with inoculated pack at the center was subjected to RF heating in a 6 kW 27.12 MHz RF system for 70, 80 and 90s, respectively. The cold spot was determined by temperature profiles from six fiber optic sensors at different locations of sample during the same RF heating process. The results showed that there were 1.86±0.24, 3.38±0 and 6.23±0.17 log reductions for 70, 80 and 90 s RF heating, respectively. Comparing with previous results of RF inactivation of *Salmonella* spp., this study concluded that *E. faecium* is a good surrogate for RF processing in cumin seeds. RF heating is a promising pasteurization technology for spices.

# Development of a Computer Simulation Model for a 915 MHz Single-mode Microwave Heating System Applied in Thawing Process

Roujia Zhang<sup>1</sup>, Donglei Luan<sup>1</sup>, Xichang Wang<sup>1</sup> and Yifen Wang<sup>1,2</sup>

<sup>1</sup>Engineering Research Center of Food Thermal-processing Technology, Shanghai Ocean University, Shanghai 201306, China

<sup>2</sup> Biosystems Engineering Department, Auburn University, Auburn, AL 36849, USA

**Keywords:** microwave thawing, single-mode, computer simulation, heating pattern, electric field distribution, temperature distribution

## INTRODUCTION

Thawing processes are more and more significant in food industry along with the wide application of freezing technique in food preservation. Microwave (MW) heating generates heat throughout the whole volume of frozen food which has the potential to reduce thawing time significantly and improve products' quality remarkably [1]. However, non-uniform temperature distribution (i.e. heating pattern) of food is still the major problem during microwave heating processes. This non-uniform heating will be severe when high microwave power is applied in an industrial scale system because the heat generation in food is proportional to the square of the electric field intensity. For a thawing process, microwave heating is more complicated than a common heating process due to the big difference in dielectric properties of food between frozen and thawed states. Therefore, a uniform electric field distribution is the key point in designing MW heating systems especially for thawing processes on an industrial scale. A 915 MHz single-mode (stable electric field distribution with varying frequency) microwave heating system was developed in our laboratory to study heating uniformity of such a system and collect engineering data of electric field distribution for industrial system design.

## METHODOLOGY

The 915 MHz single-mode microwave heating system consisted of waveguides, a top horn applicator, a MW heating cavity ( $2200 \times 495.3 \times 247.7 \text{ mm}^3$ ) a conveyor belt and two 915 MHz MW suppressors (Fig. 1). In this system, the operating frequency of the magnetron that generated the MW energy was at  $915 \pm 13 \text{ MHz}$ . Several standard WR975 rectangular waveguide elements (the inner cross-sectional dimension was  $247.7 \times 123.8 \text{ mm}^2$ ) were used to transmit microwaves from the generator to the horn applicator.

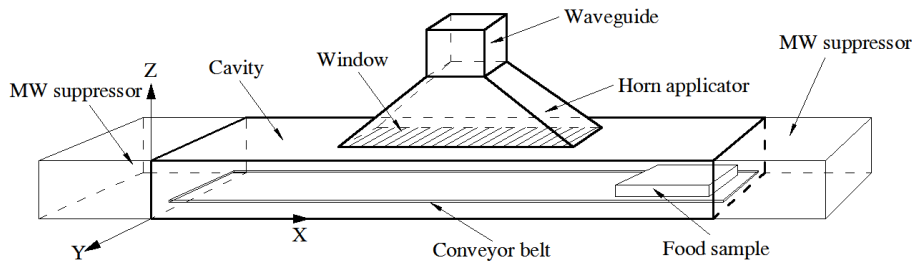


Figure 1. The 915 MHz single-mode microwave heating system

In this study, frozen surimi was used as a real food sample to verify the heating pattern obtained from the computer simulation model. The dielectric properties of surimi were measured using a dielectric properties measurement system which consisted of a network analyzer (E5071C, Agilent Technologies), a high-temperature probe, a programmable circulator and a sample holder. The computer simulation model was developed based on the MW heating system using QuickWave version 7.5 (QW3D, Warsaw, Poland). The FDTD method was used to numerically solve the coupled electromagnetic and heat transfer equations during MW heating. To validate the developed computer simulation model, the temperature distribution at top, middle and bottom layers of the surimi slab were captured by an infrared camera (FLIR, Wilsonville, Oregon, USA) just after the thawing process. A fiber optic temperature measuring system (Ptsensor, Xi'an, Shanxi, China) was used to measure the real-time temperature profile of the tested frozen surimi during MW heating [2].

**RESULTS**

Heating patterns of both simulation and validating results are summarized in Fig. 2 with the same color bar from 0.0 to 20.0 °C.

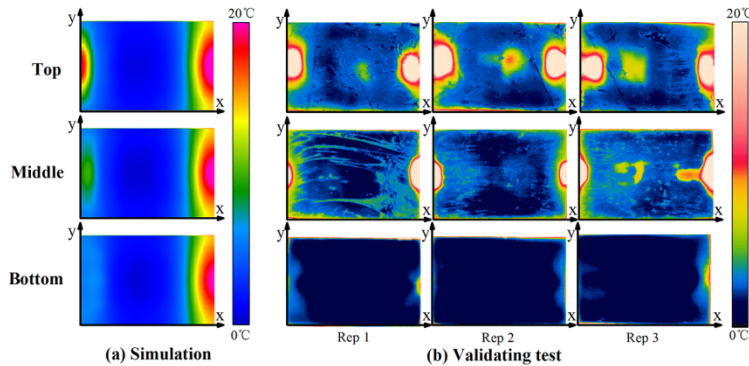


Figure 2. Temperature distribution of surimi slab (a) simulation, (b) validating test

In this study, the heating pattern affected by varying frequency was investigated using the developed computer simulation model. The electric field distribution at the middle layer

in  $z$  (thickness) direction within the single-mode microwave heating cavity at different frequencies are shown in Fig. 3.

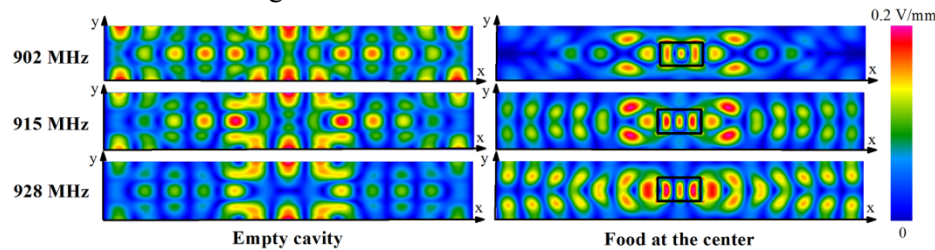


Figure 3. Electric field distribution with and without the loaded food in the heating cavity at different frequencies

## DISCUSSION

In triplicate validating tests, the heating patterns of the surimi at different layers were highly consistent which indicated that the heating pattern in the single-mode MW heating system was stable and repeatable. Heating patterns obtained from computer simulation agreed well with the validating ones. Results from both simulation and validating tests showed that the heating pattern was symmetrical in  $x$  axis, and hot spots remain located at the two edges in  $x$  direction. However, the temperature at the right edge was a little higher than the left one. That's because the surimi was moving towards the left direction while the highest electric field intensity arose at the center of the microwave heating cavity. When the surimi was moving out of the heating cavity, the right side was heated more than the left side by higher electric field intensity. For the electric field distribution results in Fig 3, the electric field distribution was similar to each other within the empty cavity, which indicated that it was insensitive to varying frequency. With loaded food, good repeatability of the electric field distribution was also observed among different frequencies. Thus, stable and repeatable heating pattern of loaded food would be obtained within this single-mode microwave heating system. The single-mode microwave heating design will play an important role in industrial scale microwave heating system.

## CONCLUSION

The heating pattern obtained from simulation agreed well with that of the validating tests, which indicated the accuracy of the simulation model. Within a single-mode microwave heating cavity, either with or without loaded food, the electric field distribution was stable and repeatable with varying frequencies. This validated computer simulation model could be utilized in designing microwave heating cavity and food products during industrial applications.

## REFERENCES

- [1] Wen X, Hu R, Zhao JH, Peng Y, Ni YY. 2015. Evaluation of the effects of different thawing methods on texture, colour and ascorbic acid retention of frozen hami melon (*Cucumis melo* var. *saccharinus*). *International Journal of Food Science & Technology*, 50(5), 1116-1122.
- [2] Wang Y, Wig TD, Tang J, Hallberg LM. 2003 a. Dielectric properties of foods relevant to RF and microwave pasteurization and sterilization. *Journal of Food Engineering*, 57(3), 257-268.

# Microwave Heating of a Thin Composite Part: a Parametric Study

H. Tertrais<sup>1</sup>, A. Barasinski<sup>1</sup>, and F. Chinesta<sup>2</sup>

<sup>1</sup>GeM-Ecole Centrale Nantes, 1 Rue de la Noë, 44321 Nantes, France

<sup>2</sup>ESI Chair at PIMM, ENSAM ParisTech, 151 Bd de l'Hôpital, 75013 Paris, France

**Keywords:** Composites processing, influential parameters, microwave heating, simulation, proper generalized decomposition

## INTRODUCTION

As composite material tends to be more and more present in transportation industries (automotive and aeronautic), the optimization of their manufacturing process is crucial. In order to reduce the long cycle time and high energy cost of the traditional processes, microwave heating appears to be an appealing candidate as it relies on volumetric heating [1]. Complex physics involved in the process is far from being controlled and that is why a simulation tool has been developed in order to solve the electromagnetic and thermal equations in a multi-layered composite part. While experimental studies have been carried out, to develop the process [2], no 3D simulation tool is available today, so the approach detailed in the paper is therefore new.

In order to get a deeper control over the process, a parametric analysis is carried out. The sensitivity of the electric field and temperature distribution is studied with respect to the material properties and the boundary conditions; results related to the latter are presented in the paper. The sensitivity study helps the end-user to appreciate the crucial parameters involved in the heating process and their impact on the homogeneous heating of the part.

## METHODOLOGY

A coupled code has been developed to simulate the microwave heating of a thin composite material. The code is based on the in-plane-out-of-plane separated representation within the Proper Generalized Decomposition (PGD) framework [3-4]. The PGD method has been developed to solve thermal, mechanical or rheological problems, but never applied to electromagnetic heating. This technique allows for capturing complex geometry of the material in the thickness as the material is made of plies whose characteristic in-plane dimension is orders of magnitude higher than the one related to the thickness. The separated representation is a solution to the need for a high-resolved mesh in the thickness while avoiding any major impact on the computational cost.

The electromagnetic model consists of solving the weak equation below assuming that the electric field is written as the sum using the PGD method.

$$\int_{\Omega} \frac{1}{\mu} (\nabla \times \mathbf{E}) \cdot (\nabla \times \bar{\mathbf{E}}^*) d\Omega - (2\pi f)^2 \int_{\Omega} \left( \varepsilon - i \frac{\sigma}{2\pi f} \right) \mathbf{E} \cdot \bar{\mathbf{E}}^* d\Omega + \int_{\Omega} \frac{1}{\bar{\varepsilon}\bar{\varepsilon}\mu} (\nabla \cdot (\varepsilon \mathbf{E})) (\nabla \cdot (\varepsilon \bar{\mathbf{E}}^*)) d\Omega - \int_{\partial\Omega} \frac{1}{\bar{\varepsilon}\bar{\varepsilon}\mu} (\nabla \cdot (\varepsilon \mathbf{E})) \cdot (\mathbf{n} \cdot (\bar{\varepsilon} \bar{\mathbf{E}}^*)) d\Gamma = 0$$

$$\mathbf{E}(x, y, z) \approx \sum_{i=1}^N \mathbf{X}_i(x, y) \circ \mathbf{Z}_i(z)$$

where  $\mathbf{E}$  is the electric field,  $f$  is frequency,  $\mu$  is magnetic permeability,  $\varepsilon$  is dielectric permittivity, and  $\sigma$  is conductivity. The temperature is solved using the same technique:

$$\rho C_p \frac{\partial T}{\partial t} = \nabla \cdot (\boldsymbol{\lambda} \cdot \nabla T) + \frac{1}{2} \sigma |\mathbf{E}|^2$$

$$T(x, y, z, t) \approx \sum_{i=1}^M X_i(x, y) Z_i(z) \theta_i(t)$$

where  $T$  is the temperature,  $\rho$  is the density,  $C_p$  the heat capacity and  $\boldsymbol{\lambda}$  the thermal conductivity.

**RESULTS**

The parameter study is realized on a simple test case as depicted in Fig.1. The part is a plate made of a homogeneous isotropic composite material placed in a mold made of ceramic material, which is transparent to microwave. Operating frequency is set to 2.45 GHz. The mesh of the domain is composed in the in-plane direction ( $x, y$ ) and is made of 3600 Q4 elements. In the vertical direction ( $z$ ), the mesh is non-regular in order for it to be refined in the composite area. The out-of-plane mesh is therefore composed of 200 linear node elements which size goes from 0.06 mm to 0.34 mm.

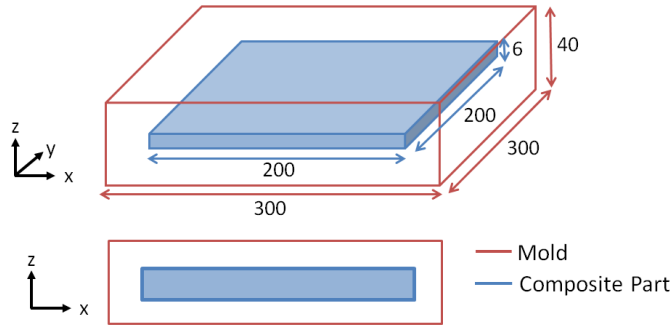


Figure 1. Test case geometry composed of the composite and the mold. Dimensions are in mm.

When processing a composite part in a microwave cavity, the waves propagate in free space, and the electric field gets a certain pattern on the surface of the tool. This study follows the impact of the position of the mold in the cavity. For one specific disposition, the boundary conditions have a certain pattern. If this disposition changes, one can wonder how much it would impact the electric field distribution on the mold and temperature field distribution in the composite part.

To study this scenario, an oven cavity is modelled using COMSOL Multiphysics software. The electric field is simulated in the cavity and the boundary conditions are transferred to the simulation tool developed. The study takes into account 3 cases: mold

centered in the cavity, 3-cm offset in the  $x$ -direction and 3-cm offset in both the  $x$ - and  $y$ -directions. Figure 2 depicts the temperature distribution for the three cases.

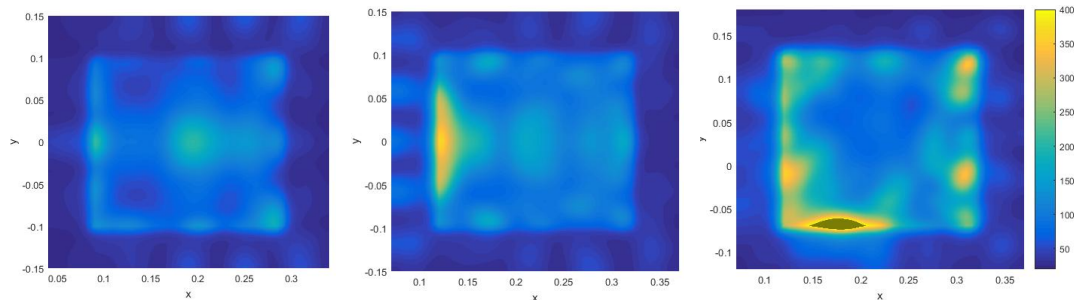


Figure 2. Temperature distribution in °C in the middle cross-section in the  $xy$ -plane for centered (left), 3-cm offset along the  $x$ -axis (middle), and 3-cm offset along the  $x$ - and  $y$ -axes (right).

A variation in the electric field distribution due to the misplacement of the composite part impacts the temperature. In the centered case, the heating of the part can be considered well homogenised and no hot spot can be seen. On the contrary, the two cases that follow are impacted by the misplacement of the part in the oven cavity. Hot spots appear on the edges of the composite part and local temperature reach up to 400°C after a heating of 20 min, that would damage the part.

## CONCLUSION

A numerical approach to solve the microwave heating of a composite part has been briefly exposed. Using this tool, a parametric study has been presented. It looked at a process of microwave heating in a closed cavity and the placement of the part in the cavity has been studied. This type a study can result on recommendations to end users concerning the manipulation of the parts when dealing with microwave heating.

Further work is to extend the parametric analysis to other quantities of interest such as the stacking for multilayered composite parts and study the impact of adding a conductive layer between the mold and the part to homogenize the heating.

## REFERENCES

- [1] G. Hug, *Behavior Analysis of Carbon-Epoxy Laminates under High-Speed Loading: Manufacture of the Same Materials by Means of Microwave Curing for Comparison*, Ph.D. Thesis, Arts et Métiers ParisTech, 2005.
- [2] M. Kwak, P. Robinson, A. Bismarck and R. Wise, “Curing of composite materials using the recently developed HEPHAISTOS microwave”, In: *18th International Conference on Composite Materials*, 21-26 (2011)
- [3] B. Bognet, A. Leygue, F. Chinesta, A. Poitou and F. Bordeu, “Advanced simulation of models defined in plate geometries: 3D solutions with 2D computational complexity”, In: *Computer Methods in Applied Mechanics and Engineering*, 201, 1-12 (2012)
- [4] F. Chinesta, R. Keunings and A. Leygue, *Proper Generalized Decomposition for Advances Numerical Simulations. A Primer*, Springer, 2014.

# Effect of Microwave Absorber and Power Level on Microwave-assisted Pyrolysis of Pine Sawdust

Candice Ellison and Dorin Boldor

Louisiana State University Agricultural Center, Baton Rouge, LA, United States

**Keywords:** Microwave pyrolysis, biofuels, lignocellulosic biomass

## INTRODUCTION

Pyrolysis is a thermochemical conversion process in which biomass is decomposed at elevated temperatures in the absence of oxygen and can be used to produce energy-dense liquid fuels and other chemicals from renewable biomass sources. Research efforts have focused on increasing the liquid product yields and composition, while also increasing the overall process efficiency [1]. Compared to conventionally heated pyrolysis reactors, which incur losses to heating elements, the reactor itself, and the surroundings, dielectric heating can increase process efficiency as heat is generated directly within the material, provided good coupling of microwaves with the material. As woody biomasses are generally poor absorbers of microwaves, a microwave absorber is typically added to the feedstock to catalyze dielectric heating [2]. In this study, residual pyrolysis char is used as the microwave absorber as it is readily available as a byproduct of pyrolysis and has been shown to be a good microwave absorber [3]. This study aims to determine the effect of char/biomass mixture and microwave power on pyrolysis reaction temperature, product yields, and overall process efficiency.

## METHODOLOGY

This study investigates the effect of microwave absorber and microwave power on pyrolysis temperature and biomass pyrolysis product conversion in a microwave reactor. Two char/biomass mixtures (0 and 10% wt char) and four microwave power levels (600, 900, 1200, and 1500W) were studied. Samples consisting of 20g pine sawdust mixed with char were loaded into a quartz U-tube and placed at the center of a waveguide applicator supplied by a 2.45 GHz, 6 kW microwave source. Pyrolysis temperature was measured through 1.5 cm diameter openings in the waveguide walls by an infrared camera. For each experiment, liquid, gas, and residual char product yields were quantified and samples collected for compositional analysis. Karl Fisher titrations were conducted on liquid samples to quantify the water content. Heating values of liquid and char products were measured by bomb calorimetry and the energy content of syngas was calculated based on gas composition as determined by gas chromatography.

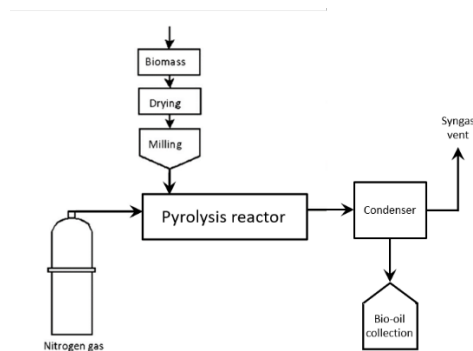


Figure 1. Schematic diagram of the pyrolysis system.

**RESULTS**

Without the aid of microwave absorber, pine biomass failed to reach pyrolysis temperatures, only reaching 200°C at 1500 W. Addition of char to pine sawdust, was found to considerably increase microwave absorption in the feedstock as observed by the increase in temperature and rate of pyrolysis. Final pyrolysis temperatures increased by about 400 °C with addition of 10% char compared to pyrolysis of pine without char. Final pyrolysis temperature increased from 125 to 200 °C for 0% char mixtures when microwave power was increased from 600 to 1500 W, respectively. For 10% char mixtures, pyrolysis temperature increased from 415 to 665 °C in the same power range.

Pyrolysis product yields and overall energy balance were significantly affected by char mixture and microwave power level. Pyrolysis char, liquid, and syngas yields were also correlated to pyrolysis temperature. For pyrolysis feedstocks with 0% char, water-free bio-oil yield increased with increasing microwave power to a maximum of 25% bio-oil for pyrolysis at 1500 W microwave power. For feedstock mixtures with 10% char, bio-oil yield increased to a maximum of 25% at 900 W, then decreased at greater power levels due to increased secondary thermal cracking reactions yielding greater syngas. Residual char yields decreased to a minimum of 13% for pyrolysis temperatures greater than 480 C, above which char yield remained constant, indicating complete pyrolysis.

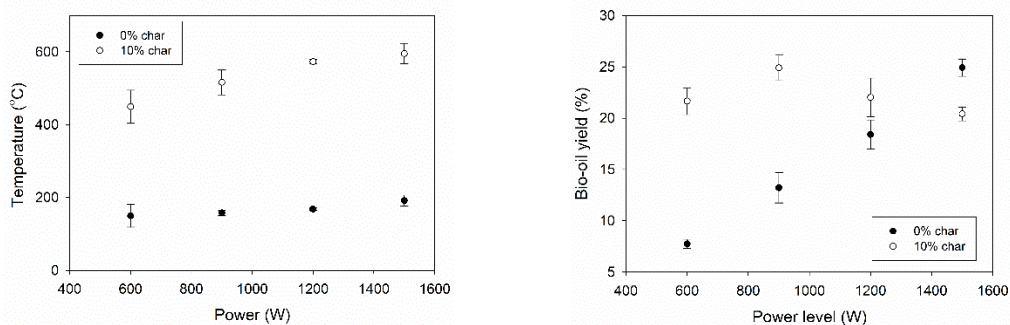


Figure 2. Final pyrolysis temperature measured by infrared camera and water-free bio-oil yield as a function of power level for each char mixture.

## DISCUSSION

Maximum bio-oil yields were produced from pyrolysis at 1500 W without addition of char, and at 900 W for 10% char mixtures. Addition of biochar to the feedstock decreased the microwave power needed to produce the greatest bio-oil yields. While both feedstocks attained the same maximum bio-oil yield of 25%, the pine feedstock with 10% char mixture required less microwave power input. The overall energy balance of the system was low or negative for samples without char addition, while samples with 10% char attained a maximum net energy conversion of 66 MJ/kg at 1200 W microwave power.

Interestingly, the temperatures at which each feedstock yielded the maximum bio-oil yield were drastically different: 191 °C for the 0% char feedstock and 516 °C for the 10% char feedstock. This phenomenon could be due to differences in the rate of heating, which is known to affect product yield distribution.

## CONCLUSION

Biochar was found to be a good microwave absorber for microwave-assisted pyrolysis of pine biomass and increased the process efficiency by reducing the power required to attain maximum bio-oil yields.

## REFERENCES

- [1] Yin, C., Microwave-assisted pyrolysis of biomass for liquid biofuels production. *Bioresource Technol.*, vol 120, pp. 273-84, 2012.
- [2] Beneroso, D., et al., Microwave pyrolysis of biomass for bio-oil production: Scalable processing concepts. *Chemical Engineering Journal*, vol. 316, pp. 481-498, 2017.
- [3] Ellison, C., McKeown, M. S., Trabelsi, S., Boldor, D., Dielectric Properties of Biomass/Biochar Mixtures at Microwave Frequencies. *Energies* (19961073), vol 10, no 4, pp. 1-11, 2017.

# Research Progress of Microwave Rapid Hardening for Ultra-large Artificial Marble Blocks

Haibing Ding<sup>1</sup>, Liang Tang<sup>1</sup>, Weisong Li<sup>1</sup>, Zhimin Huang<sup>2</sup>, Dengfeng Lu<sup>1</sup>, Ke Tang<sup>1</sup>, Ren Xiao<sup>1</sup>, Nanyang Liu<sup>1</sup>

<sup>1</sup>Key Laboratory of High Power Microwave Sources and Technologies, Institute of Electronics, Chinese Academy of Sciences, Beijing, China

<sup>2</sup>Guangxi Academy of Sciences, Nanning, China

**Keywords:** Microwave Hardening; Artificial Marble Blocks; Engineering Prototype; Preliminary Test;

## INTRODUCTION

Artificial marble is mainly comprised of scraps and powder of natural marble and limestone, sand, and resin. In a conventional production process, extruded artificial marble blocks harden in normal atmosphere, taking up to 10-15 days, which hinders productivity improvement. In this paper, microwave, at the frequency of 915MHz, is used to rapidly harden ultra-large artificial marble blocks with a typical dimension of  $3.2 \times 1.6 \times 0.95 \text{m}^3$  in industrial production. After optimizing the distribution of power loss density and thermal structures, a microwave hardening prototype, with maximum output power of 160 kW, has been applied in trial production. The prototype already finished hardening over 3000 artificial marble blocks, and performed stably, reliably and safely. Microwave hardening process takes less than 1 hour, which is much shorter than natural hardening of 10-15 days.

## MECHANISM

$$\lambda_{1/2} = \frac{3\lambda_0}{8.686\pi\sqrt{\varepsilon_r'}\tan\delta}$$

The effect of microwave on a dielectric is associated with the microwave frequency and dielectric constant. Artificial marble is one kind of non-conductor. When microwave enters the artificial marble blocks, energy from the microwave is continuously absorbed and converted to internal energy, as the field strength and power gradually decay. The microwave half power penetration depth  $\lambda_{1/2}$  describes the ability of the microwave to penetrate into the marble [1].

$\lambda_0$  is the wave length of the microwave on the surface of dielectric.  $\varepsilon_r'$  is the real part of the relative dielectric constant.  $\delta$  is the loss angle of dielectric. The dielectric constant and loss angle of dielectric were tested using transmission line method as per

reference [2]. Constants, including thermodynamic constants such as density, specific heat capacity and thermal conductivity, are tested under normal atmospheric pressure and temperature.

Table 1. Physical constants of artificial marble

Constants	Units	Value
Relative dielectric constant	-	7.7~8.0
Tangent of dielectric loss angle at 915MHz	-	0.03
Tangent of dielectric loss angle at 2450MHz	-	0.05
Specific heat capacity	kJ/kg/K	1.02
Thermal conductivity	W/K/m	1.20
Density	kg/m <sup>3</sup>	2680

When the frequency is 915 MHz and 2450 MHz, the microwave half power penetration depth  $\lambda_{1/2}$  is 0.43 meters and 0.16 meters. Using simulation software to simulate at different frequencies, 915 MHz is more effective to penetrate the artificial marble.

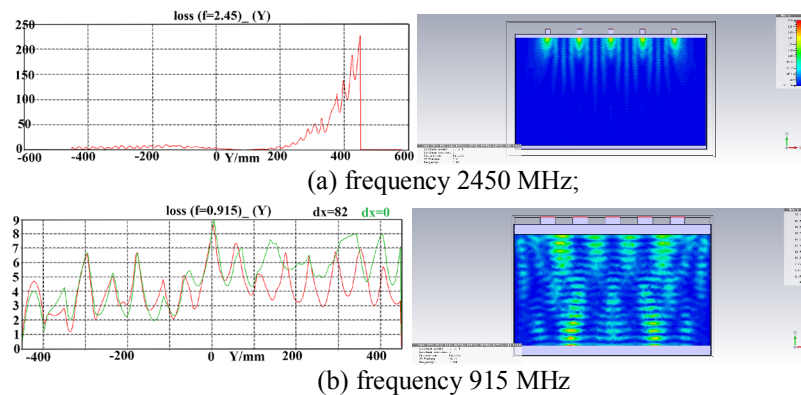


Figure 1. Simulation results of the density of power loss:

The engineering prototype has total power up to 160kW. Microwave of 915MHz is fed into the curing chamber by 15 ports. Optimization of the power loss density is achieved by changing the dimensions of the chamber and the distribution of the 15 ports. Voltage standing wave ratio (VSWR) of each port is in the range of 1.1 to 1.9. Fig. 1 gives the simulation results of the density of power loss at two frequencies. To improve the temperature uniformity of marble blocks under dynamic thermal balance, a thermal structure model was built and simulated.

**RESULTS**

Engineering prototype of artificial marble blocks hardening machine, shown in Fig. 2, consists of one multimode resonant chamber, eight microwave generators using industrial magnetron generating 915MHz microwave, and an optimized microwave waveguide feeding system connecting the generators to the chamber. Each marble blocks weighs about 10 to 12 tons. Two rail flatbeds move horizontally in and out. A hydraulic

lifter moves up and down. Microwave hardening process takes less than one hour and is much shorter than natural hardening of 10-15 days.



Figure 2. Engineering prototype of artificial marble blocks hardening machine

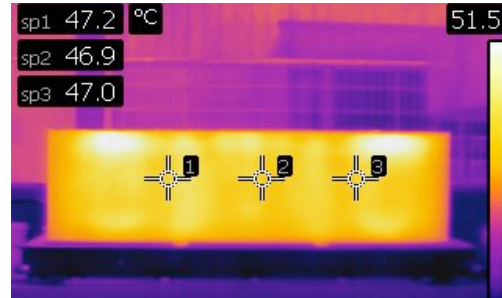


Figure 3. Image of artificial marble block temperature distribution using infrared camera

Optimum hardening, control of the rate of heating and uniformity of the temperature distribution by adaptively changing the power level of 15 microwave ports, is based on experimental production data. The temperature difference of the marble blocks will affect the product consistency, weaken mechanical strength, and increase the internal stress. Marble blocks will even crack and break because of large temperature difference. The temperature difference is less than 4.5 degrees Celsius in microwave hardening progress. An infrared camera image of an artificial marble block after hardening process is shown in Fig. 3.

## CONCLUSION

According to the test reports from China National Quality Supervision and Testing Center for Stone Products (Guangdong), the product qualities of microwave hardened artificial marble satisfy the standard of artificial stone industry. The uniformity is improved, glossiness is improved by 10%, and the linear coefficient of expansion decreased by 30%.

## REFERENCES

- [1] PENG Z, HWANG J-Y, MOURIS J, et al, Microwave Penetration Depth in Materials with Non-zero Magnetic Susceptibility. *ISIJ International*, 2010, 50(11): 1590-1596.
- [2] Roelvink J, Trabelsi S, Nelson S O, Determining Complex Permittivity from Propagation Constant Measurements with Planar Transmission Lines. *Measurement Science and Technology*, 2013, 24(10):105001-105008.
- [3] Feng T, Ding HB, Gao DP, Zhang ZC, Numerical Simulation and Experiment of Hardening Behaviors in Unsaturated Polyester Resin Artificial Marble Blocks Under Microwave Radiation. *IEEE Transactions on Plasma Science*, 2016, 44(10): 2485-2492.

# Rapid Microwave Assisted Delignification of Biomass Using Deep Eutectic Solvents

**Pranjali D. Muley<sup>1\*</sup>, Daniel Kuroda<sup>2</sup>, Jian Shi<sup>3</sup>, Sue Nokes<sup>3</sup>, Dorin Boldor<sup>1\*</sup>**

<sup>1</sup>Department of Biological & Agricultural Engineering, Louisiana State University and Agricultural Center, Baton Rouge, LA, USA 70803

<sup>2</sup>Department of Chemistry, Louisiana State University, Baton Rouge, LA USA 70803

<sup>3</sup>Department of Biosystems and Agricultural Engineering, University of Kentucky, Lexington, KY USA 40546

**Keywords:** Biomass deconstruction, Deep Eutectic Solvents, Microwave Processing.

## INTRODUCTION

Deep eutectic solvents (DES) are natural ionic solvents with special properties. Formed by compounds that are solid at room temperature and form a non-aqueous liquid when mixed due to depression in melting point. These non-aqueous liquids stay in liquid state when cooled down to room temperature. Deep eutectic solvents are most commonly synthesized by mixing quaternary ammonium salts and metal chloride or hydrogen bond donor such as urea [1]. DES's have shown to have similar chemical and physical properties as that of ionic liquids. However, since DES are synthesized from cheaper materials such as Choline Chloride, Urea, Oxalic, lactic, Malic, Formic acid etc. they are much cheaper than traditional ionic solvents [2]. DES has evolved as a promising solvent for biomass deconstruction. Biomass deconstruction is an important step for separation of lignin and cellulose. Separated cellulose can be used for bioethanol production while lignin can be used in synthesis of various materials and chemicals. DES's are also found to be non-toxic and a greener alternative to ionic liquids. Due to rapid and volumetric heating microwave based chemistry has significant advantages over conventional heating techniques. In this report we investigate the application of microwave heating to synthesize DES as well as for biomass deconstruction using various deep eutectic solvents.

## METHODOLOGY

In this study we investigated three different DES's namely; oxalic acid: choline chloride (1:1), lactic acid: choline chloride (2:1) and Formic acid: Choline chloride (2:1). The DES's were synthesized in a 2450MHz microwave batch Ethos E reactor (Milestones Inc.)(figure 1). Briefly, known ratio of Choline chloride and acid were mixed in a

microwave safe beaker. The powdered mixture was heated in the microwave until the solids melted to form a clear liquid. The reactor used was a 2450 MHz Ethos EX microwave extraction system with fiber optic temperature sensor and pressurized Teflon beakers (Milestones Inc. Shelton, CT, USA). This process took less than a minute for all DES's. The DES was then cooled to room temperature. Pinewood sawdust (particle size < 250 microns) was milled and dried. 1.5 g of biomass was added to 30 g of DES and the mixture was added to a pressurized Teflon beaker with a magnetic stirrer. The mixture was heated at different temperatures (110, 120, 130, 150, 170 °C) and times (1, 5, 10, 15, 20 min). The solution was cooled to room temperature and filtered. The dissolved liquid was precipitated to obtain lignin while the residue was further washed and dried. A modified version of the standard analysis techniques issued by TAPPI (Technical Association of the Paper and Pulp Industry) was performed on the dried biomass to calculate lignin content. These tests can also be applied for large scale samples, however, to accommodate smaller sample volumes in this study, a modified version was used.

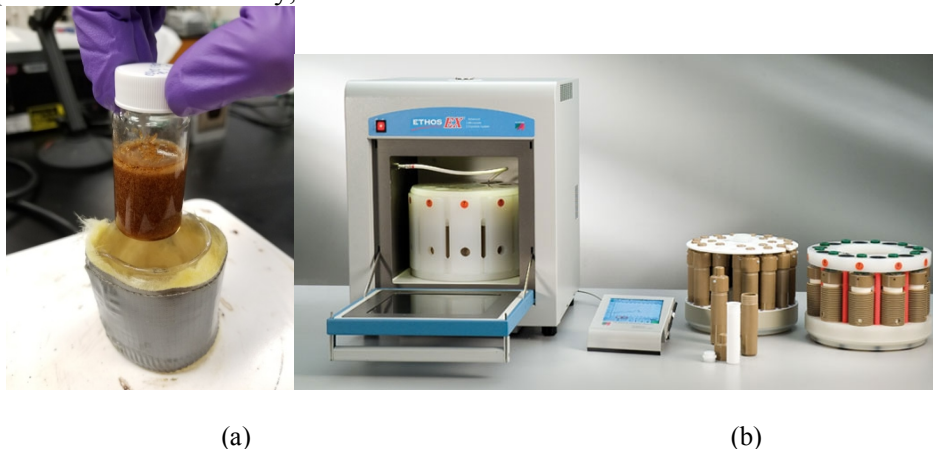


Figure 1. Schematic diagram of the microwave system (a) processed mixture of biomass and deep eutectic solvent and (b) Ethos E microwave digester

## RESULTS

Oxalic acid: choline chloride DES was found to dissolve more biomass compared to formic acid and lactic acid. As the temperature increased, amount of biomass dissolved also increased. However this trend reversed as the temperature reached 160°C. Higher biomass dissolution was obtained as the processing time was increased. Optimum time and temperature for biomass deconstruction using oxalic acid – choline chloride DES was 160°C and 15 min. Delignification increased as the deconstruction temperature increased. Highest delignification was obtained at 160°C for oxalic acid: choline chloride DES (Figure 2).

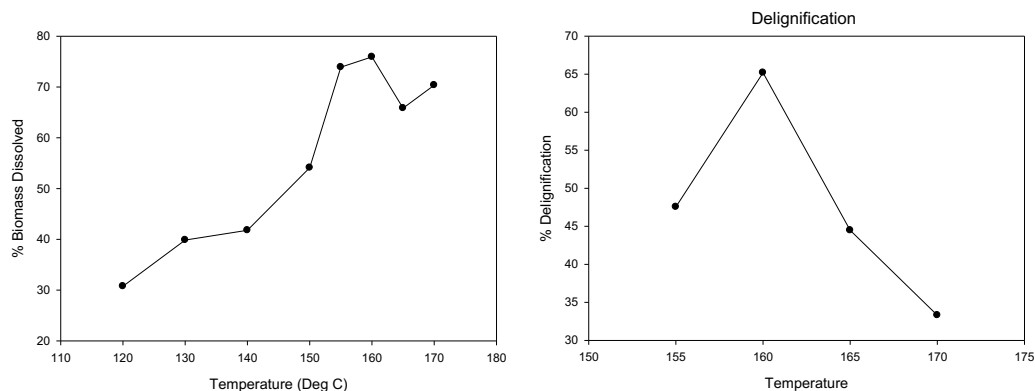


Figure 2. Percent biomass dissolved and delignification of biomass at different temperatures for biomass processing using oxalic acid: choline chloride DES.

## DISCUSSION

Biomass deconstruction using conventional heating requires 8 – 12 hours of processing time. Same degree of deconstruction was obtained using microwave processing within 20 min. of processing time. This could be mainly due to direct volumetric heating of biomass- DES mixture. Advantage of using DES over ionic liquid includes selective deconstruction. DES was observed to selectively dissolve lignin [1,3]. Hence TAPPI analysis of residue showed high content of cellulose. While dissolved material when precipitated contained mainly lignin. Increase in both time and temperature increased the rate of dissolution.

## CONCLUSION

We successfully demonstrated the use of microwave reactor for biomass deconstruction using deep eutectic solvents. Microwave processing significantly reduced the time required for biomass deconstruction from few hours to matter of minutes. Oxalic acid DES was found to be most suitable for biomass deconstruction. The optimum time and temperature conditions for this DES was 160 °C and 15 min.

## REFERENCES

- [1] Francisco, M., van den Bruinhorst, A., & Kroon, M. C. (2012). New natural and renewable low transition temperature mixtures (LTTMs): screening as solvents for lignocellulosic biomass processing. *Green Chemistry*, 14(8), 2153-2157.
- [2] Pena-Pereira, F., & Namiesnik, J. (2014). Ionic liquids and deep eutectic mixtures: sustainable solvents for extraction processes. *ChemSusChem*, 7(7), 1784-1800
- [3] Tang, X., Zuo, M., Li, Z., Liu, H., Xiong, C., Zeng, X., ... & Lin, L. (2017). Green processing of lignocellulosic biomass and its derivatives in deep eutectic solvents. *ChemSusChem*.

# Microwave-Freeze-Drying of Fruit Foams for the Production of Healthy Snacks

Mine Ozcelik\*, Sabine Ambros, Ulrich Kulozik

*Chair for Food and Bioprocess Engineering, Technical University of Munich, 85354 Freising, Germany*

**Keywords:** Foam-mat drying, raspberry foam, freeze drying, microwave freeze drying, energy efficiency

## ABSTRACT

Due to increasing health awareness, healthy snack products have recently become more attractive for many consumers. Foams made out of fruit purees can subsequently be dried and consumed as snacks. Such dried foams can disintegrate very quickly upon contact with the saliva in the mouth, leading to a spontaneous flavor release. This "Aroma-Flash" is perceived as a positive sensory experience. Foams produced by microwave-assisted freeze drying have a more porous and cellular structure, which makes them favorable compared to the foams obtained by conventional drying of fruit puree. It is well known that freeze-drying (FD) is one of the leading methods to obtain high quality products. However, it requires long drying times, which result in high energy consumption and thus, proportionally high production costs. To make such fruit snacks affordable for the consumer, a gentle but simultaneously fast drying process has to be applied. Since a volumetric heating of a product can be achieved via electromagnetic radiation, the addition of microwave (MW) energy to a freeze-drying process can lead to a rapid and also an energy-efficient drying without deteriorating the product.

The aim of this study was to investigate the effect of MW-assisted freeze drying on the drying behavior of raspberry foams. Potato protein as plant origin protein is applied as a foaming agent and the polysaccharides maltodextrin and pectin are used as stabilizers. Raspberry foams were dried by MW-assisted freeze drying under various MW power input levels at a constant chamber pressure. During the MW-assisted drying, the product temperature was controlled via pulsed MW application. Freeze-drying experiments was performed as a reference.

The drying behavior was evaluated based on the drying kinetics, temperature distribution, absorbed microwave energy, and energy efficiency for the tested conditions.

The results showed that MW-assisted freeze-drying showed a 3 to 4-fold decrease in total drying time, and energy consumption was reduced by ~85% with highly satisfactory foam characteristics, as compared to FD. In this regard, microwave-assisted freeze drying could be a promising alternative to conventional freeze drying as it offers a more efficient process with comparable product quality.

# Sterilization of Raw Milk with Radio-Frequency Heating Technology: Quality, Safety and Shelf Life Evaluation

A.R. Di Rosa<sup>1</sup>, F. Leone<sup>1</sup>, G. Battaglia<sup>2</sup>, T. Veccia<sup>2</sup> and V. Chiofalo<sup>3</sup>

<sup>1</sup>Department of Veterinary Science, University of Messina, Italy

<sup>2</sup>Officine di Cartigliano S.p.A. – RF Division, Cartigliano, Italy

<sup>3</sup> Department of Chemical, Biological, Pharmaceutical and Environmental Sciences, University of Messina, Italy

**Keywords:** Radio-Frequency; milk, quality, safety, shelf-life.

Food industries use thermal treatments as a common strategy to inactivate microorganisms and enzymes, and guarantee safe products, avoiding the utilisation of preservatives and solving several shelf life problems. Commercial sterilisation usually relies on pressurised hot water or steam, transferring the heat from the outer surfaces of a foodstuff to its interior, often leading to long process times and to surface' dehydration phenomena and overheating. Recent researches into radio frequency heating technology has discovered that food products can be sterilised using time-temperature regimes, which are much milder than those required with conventional techniques, resulting in a minimal modification of food sensory and nutritive attributes. Moreover, radio frequency heating can be applied to foodstuffs that are already bottled or packed. In the present work, raw milk was sterilised, through a combination of steam and radio frequencies ( $\Delta T = +15^{\circ}\text{C}$ ), at various temperatures (75-125°C). Alongside the chemical composition (lipids, proteins, lactose, etc.), pH, acidity and total mesophilic count (TMC) were evaluated, in order to study the impact of this technique on milk quality and safety, during a storage period of 55 days at +4°C. According to the obtained results, pH and acidity were strictly homogeneous among the samples subjected to the very different temperatures; moreover, numerical values conform to those expected for good quality milk, despite the prolonged storage period. Regarding the TMC, under the threshold of 110°C, results are comparable with those obtained for fresh milk with a shelf life of 6-8 days; on the other hand, above this temperature, TMC values were always  $\leq 1$  cfu/mL. Interestingly, TMC tends to decrease over time, suggesting a

loss of vitality of the bacteria that survived the pasteurisation. In conclusion, radio frequency heating appear as a suitable technique for the production of Extended Shelf Life (ESL) milk, which can retain optimal physico-chemical and microbiological proprieties for prolonged time, compared to the other products present on the market.

# Are Enzymes Used in Foods Affected by Microwaves? – Exploring with a semiconductor microwave generator

Satoshi Horikoshi<sup>1</sup>, Kota Nakamura<sup>1</sup>, Nick Serpone<sup>2</sup>

<sup>1</sup> Sophia University, 7-1 Kioi-cho, Chiyoda-ku, Tokyo, 102-8554, Japan

<sup>2</sup> Università di Pavia, Via Taramelli 12, Pavia 27100, Italy.

**Keywords:** Enzyme; Papain; Catalase; Microwave-stimulated enzyme reaction

## INTRODUCTION

Recent years have witnessed the many possibilities of microwave usage in the biochemical field; in particular, the use of microwaves in peptide synthesis has been widely used in the industry. And further, enhancement of enzyme reactions by microwave is also expected. Enzymes are also used as catalysts in chemical reactions and biological reactions, and if activated they could be developed into various applied techniques. Although many reports investigating the effect of microwaves on food enzymes have appeared, to our knowledge no experiments have been conducted that compare microwave heating (MW) and conventional heating under strict temperature control. Moreover, while controlling microwaves, investigations that examine the effect(s) of electric field versus magnetic field unique heating of the microwaves are rather scant. Accordingly, to clarify these questions, we used a semiconductor generator [1,2] that permitted a facile control of the generated microwaves. In our study, we used a microwave device that provided strict control according to microwave engineering with which the effect of microwaves on food enzymes could be investigated. In particular, we examined the effect(s) of the microwaves' electromagnetic energy on an *in-vivo* (beef proteins) process and on the *in-vitro* papain-assisted hydrolysis of casein. Moreover, the enzymatic reaction using a Tannase enzyme to degrade albumen (a model food) was also carried out.

## METHODOLOGY

Experiments using a microwave-heating device for the hydrolysis of casein by the papain enzyme were conducted by connecting a prototype single-mode applicator to a 2.45 GHz semiconductor generator. The solution in the reactor was stirred using a micro-stirring bar and then subjected to a 4-Watt microwave electric field heating (*E*-field), to a 4-Watt magnetic field heating (*H*-field), and to conventional heating using a water bath.

**RESULTS & DISCUSSION**

**Papain:** Hydrolysis of proteins in beef by the papain enzyme rubbed onto the surface of beef samples, taken as a model of an *in-vivo* process, was examined (**Figure 1**) by conventional heating at 40 °C for 15 min in an electric furnace (**Figure 1b**); the surface softened compared to the original sample (**Figure 1a**). Under microwave heating at 40 °C for 15 min, however, the beef surface appeared to have melted (**Figure 1c**) suggesting an increased activity of the papain enzyme when exposed to microwaves. By contrast, control experiments showed no changes when subjecting the beef sample to microwave heating or conventional heating without the papain enzyme. This clearly demonstrates an accelerating effect of the enzyme-assisted hydrolysis of the beef’s proteins by the microwaves’ electromagnetic wave energy.

**Figure 2** reports UV spectral results of the hydrolysis of casein by papain in aqueous media subjected to microwave and conventional heating (water bath; WB). The maximal absorption of casein- decomposed amino acid recorded at 275 nm showed no significant differences in the hydrolysis rate of casein when heating at various times by microwaves’ *E*-field and *H*-field heating or WB heating. Evidently, in this case the microwaves had no specific effect on papain in the hydrolysis of casein.

Protease enzymes such as papain typically hydrolyze proteins, while at the same time they may undergo self-digestion with the amount in solution decreasing with reaction time. To demonstrate the latter, an aqueous solution containing only the papain enzyme was subjected to heating at 60 °C by the three heat sources. UV spectral results at 245 nm (**Figure 3**) confirmed that the extent of self-digestion of the enzyme was significantly lower under *E*-field and *H*-field heating than under WB heating. Results also showed that the self-digestion of papain was affected more by the microwaves’ *H*-field than by *E*-field heating as evidenced by the nearly negligible changes in UV absorption at 245 nm under *E*-field conditions. The self-digestibility ratio of papain increased with time under *H*-field conditions, while it decreased under *E*-



**Figure 1.** Observations of surface changes of beef samples after applying papain to the beef and maintaining it at 40 °C for 15 min: (a) control experiment with no papain used on the beef, (b) beef sample after heating in an electric furnace with papain on the surface, and (c) beef sample with papain subjected to microwave heating.

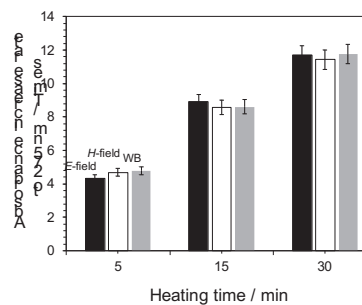


**Figure 2.** Time course of the papain-assisted hydrolysis of casein at 60 °C on heating with microwaves at the maximal position of the *E*-field density, maximal position of the *H*-field density and with WB heating.

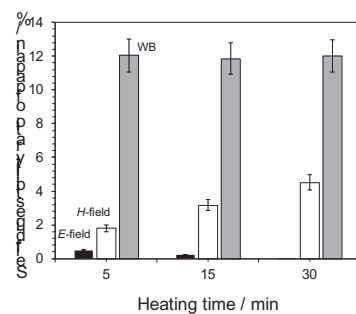


**Figure 3.** Self-digestibility ratio of papain (ratio of UV absorption at 245 nm at 5, 15 and 30 min against 0 min) with *E*-field heating, *H*-field heating and WB heating.

field heating. Clearly, the microwaves had less effect on the extent of self-digestion of the papain enzyme than WB heating, and particularly so under *E*-field heating conditions.

Further, decomposition products of casein and self-digested products of papain were analyzed using MALDI-TOFMS mass spectrometry, SDS-PAGE electrophoresis, and a protein sequencer.

### **PROPOSAL MECHANISM CONCLUDING REMARKS**

Papain applied to beef clearly promoted the hydrolysis of meat proteins by microwave heating relative to conventional heating. However, a similar distinction could not be seen in the *in-vitro* process involving the papain-assisted hydrolysis of casein. On the other hand, compared to conventional heating the microwaves had an inhibitory effect on the self-digestion of papain. To understand such apparent contradictions on the influence of microwaves over conventional heating on the enzyme-assisted hydrolysis of casein, our previous research on the acid hydrolysis of cellulose to produce glucose in the presence of AC-SO<sub>3</sub>H catalyst particles subjected to microwave heating and conventional heating might prove helpful [4]. Results of this study showed that microwave heating promoted the selective overheating of the AC-SO<sub>3</sub>H catalyst; a rapid hydrolysis of cellulose by microwave selective heating of the catalyst was expected. However, even though selective heating of the catalyst occurred, we found no difference in reaction efficiency in the acid-catalysed acid hydrolysis of cellulose, whether heated by microwave selective heating or by conventional heating. We attributed this observation to the fact that the hydrolysis of cellulose did not take place at or near the catalyst active site, but rather the reaction occurred in the solution bulk causing the effect of the microwaves to be diminished. Thus, we hypothesize that the hydrolysis of casein by the papain enzyme occurs in the solution bulk rather than at the active site of the papain enzyme. That is, the rate-determining step of the hydrolysis occurs in the solution bulk, wherein the microwaves affect the papain enzyme (self-digestion) so that it reduces the extent to which it can participate in the hydrolysis reaction. On the other hand, why did the microwaves promote the hydrolysis of beef proteins? The papain enzyme was directly adsorbed on the beef, which leads us to infer that the microwaves have a greater effect on the solid-solid reaction occurring on the surface of the beef sample than in the case where the reaction occurs in a solution phase – the process involving casein being an obvious case.

### **REFERENCES**

- [1] S. Horikoshi, K. Nakamura, M. Kawaguchi, J. Kondo, N. Serpone, *RSC Adv.* 6, 48237–48244, 2016.
- [2] S. Horikoshi, T. Nakamura, M. Kawaguchi, N. Serpone, *J. Mol. Cat. B:Enzym.* 116, 52–59, 2015.
- [3] S. Horikoshi, T. Watanabe, A. Narita, Y. Suzuki, N. Serpone, *Sci. Rep.* 8, 5151, 2018.
- [4] S. Horikoshi, T. Minagawa, S. Tsubaki, A. Onda, N. Serpone, *J. Catal.* 7, 231–244, 2017.

# A Novel Method of Radio Frequency (RF) Tempering Irregular-shape Frozen Food

Feng Li<sup>1</sup>, and Yang Jiao<sup>1,\*</sup>

<sup>1</sup> Engineering Research Center of Food Thermal-processing Technology, Shanghai Ocean University, Shanghai, China

**Keywords:** Radio frequency, meat, temper, irregular shape, heating uniformity

## INTRODUCTION

Radio frequency (RF) has been validated as an effective methodology in the frozen food tempering industry [1]. With its distinct property of volumetric heating, RF could save 80-90% tempering time and prevent quality degradation, especially drip loss [2,3]. Although there are a few commercial RF tempering systems available, some technical problems still need to be tackled before it will be fully accepted by the food industry. One of the major problems is the uneven heating for frozen food with various components and irregular shapes. Our previous results have explored the influence of sizes and shapes to the tempering properties, and demonstrated that sharp outer and inner edges both significantly influence tempering uniformity. However, the existing strategies for solving the problem are mostly focused on varying the shape and size of the material and the electrode plates, which is not applicable to irregular shape products[4]. New RF tempering uniformity improvement method needs to be developed.

## METHODOLOY

In this study, crushed ice, ethanol (95%) and glycerol (70%) were selected as the target surrounding medium for food immersion. Fresh lean beef sample was minced and stuffed into a 220\*140\*50 mm<sup>3</sup> cuboid container to make cuboid and step shape. Crushed ice was obtained from an ice maker, Ethanol (95%) and glycerol (70%) solutions were also prepared and all put into separate containers (285×190×60 mm<sup>3</sup>) stored at -18 °C together with all samples.

Before the experiments, frozen beef samples were removed from the container and individually immersed into the surrounding medium. Experiments were conducted in a 27.12 MHz 12 kW pilot-scale RF heater (Labotron 12, Sairem, France) with an electrode gap of 115 mm and input power of 3 kW. Experiments stopped when the center temperature of the sample reached -4 °C, which took 4.5 min for RF and RF + crushed ice, and 8 min for RF + ethanol and RF + glycerol tempering experiments. Tempering

uniformity was evaluated by assessing the sample heating pattern captured using an infrared camera right after RF tempering.

## RESULTS

The dielectric properties of ethanol, glycerol at -20 °C and distilled water at 0 °C (not available at -20 °C) in the frequency range of 1-2500 MHz were shown in Figure 1. The dielectric properties of medium indicates their potential of being utilized as the surrounding medium to improve the tempering uniformity. From the comparison, ice could be a perfect medium because of its low loss factor and relatively low dielectric constant.

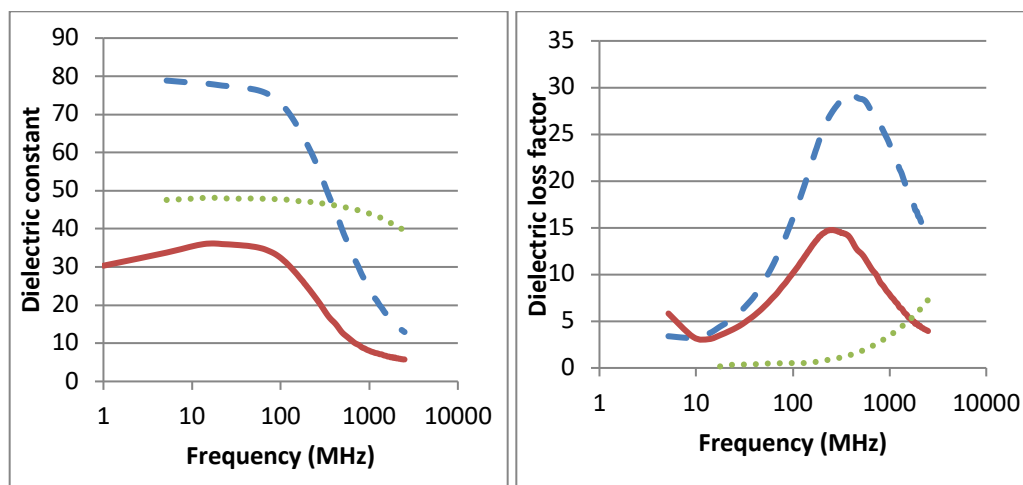


Figure 1. Dielectric properties of 70% glycerol (Blue dash), 95% ethanol (Red solid) at -20 °C and distilled water (Green dot) at 0 °C under frequency 1-2500 MHz

The temperature distributions of tempered cuboid- and step-shape beef samples with and without surrounding medium are shown in Figure 2. Serious burning, at the edges and corners, was found on both samples when no surrounding medium was applied, especially in step-shape sample. In the step-shape sample, the corner was heated to 46.8 °C when the thin section reached -4 °C. After immersing food samples into crushed ice, the edge burn was reduced but the corner was still over heated and reached 16.6 °C. Both ethanol and glycerol solution showed excellent improvement in tempering uniformity by successfully reducing edge heating.

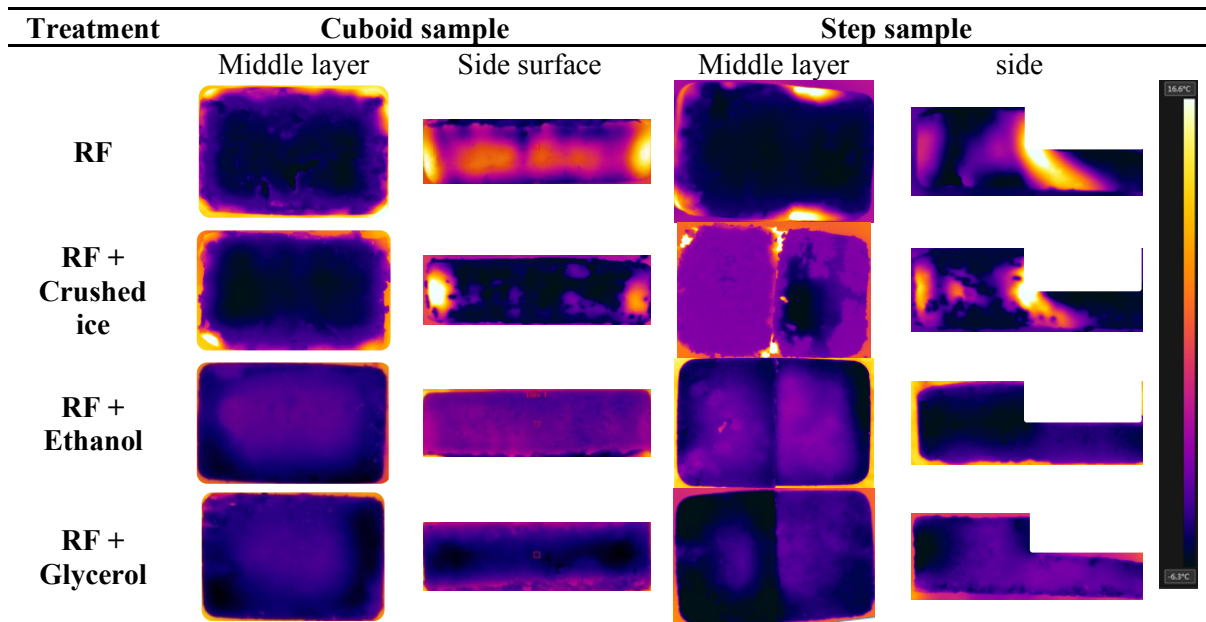


Figure 2. Temperature distribution of frozen beef with two shapes

## DISCUSSION

Ethanol and glycerol solution were both applicable in reducing edge heating during RF tempering of frozen meat product. In future industrial application, glycerol might be a better choice since it is without potential fire hazard. The solvent immersion strategy with RF heating is practical and cost effective for the food industry.

## CONCLUSION

Shapes influenced the heating behaviors significantly. There needs to be more attention when designing a versatile industrial RF thawing line of frozen meat and fishery products with various shapes. In this study, three surrounding medium were selected based on their dielectric properties and suitability of being applied in the food industry. Crushed ice could partially eliminate the edge heating due to its porous nature and melting point at 0 °C. Ethanol and glycerol solutions both proved to be effective and had the potential to be extended to industrial application.

## REFERENCES

- [1] Y. Llave, S. Liu, M Fukuoka, et al. Computer simulation of radiofrequency defrosting of frozen foods. *J. Food Eng.*, 152(C) pp.32-42, 2015
- [2] Sanders, H. R. Dielectric thawing of meat and meat products. *J of Food Tech*, 1, 183–192. 1966
- [3] Jason, A. C., & Sanders, H. R. Dielectric thawing of fish. *Food Tech*, 16(6), 101–112. 1962
- [4] Jiao, Y., Shi, H. J., Tang, J. M., Li, F., & Wang, S. J. Improvement of radio frequency (RF) heating uniformity on low moisture foods with Polyetherimide (PEI) blocks. *Food Res. Intl*, 74, 106-114. 2015

# Continuous In-Flow Microwave Preservation of Particulate Foods at High Temperatures

**B. Raaholt<sup>1</sup>, L. Hamberg, S. Isaksson<sup>1</sup>**

<sup>1</sup>RISE Research Institutes of Sweden, Agrifood and Bioscience, Frans Perssons väg 6, SE-412 76 Göteborg, Sweden

**Keywords:** microwave, minimal processing, quality, texture, mouthfeel, piece integrity

## INTRODUCTION

A pilot-scale process for continuous in-flow microwave processing of particulate foods, designed and implemented at RISE Agrifood and Bioscience, was evaluated for heat treatment of a particulate model food at high temperature conditions at 2450 MHz. The evaluation shows advantages in terms of e.g. better maintained pieces, texture, and mouthfeel.

Rapidness in heating of the product was evaluated after tubular microwave heating for different time-temperature conditions. These correspond to the required microbiological inactivation for a model product intended for storage at ambient conditions. Rapidness as well as flexibility of the microwave HTST process were also considered advantageous, vs. conventionally heated processing.

## METHODOLOGY

The tubular microwave system combines two microwave modes (Wäppling Raaholt, 2016) and is here evaluated as an alternative to high-temperature short-time (HTST) processing for a particulate model product studied here. The effects on product quality of the microwave heated soup, containing pieces of carrots, were investigated in terms of quality parameters (texture, piece integrity and colour). Micro-structural analysis contributed to get an understanding of the effects of heating at a microscopic scale.

## RESULTS AND DISCUSSION

The process is considerably more rapid than a conventional HTST process. Furthermore, it shows a large process flexibility. The described microwave HTST process results in a flexible process by means of a large number of different combinations of target temperature and time in the same equipment.

Microstructural analysis shows that the traditionally heated carrot pieces (cooked in lab scale) have larger ruptures in the cell wall structure than carrot pieces that are microwave heat treatment. The reason behind this could be related to the fact that microwave heating offers a more rapid coming-up time to the target temperature due to volumetric heating. Since microwave heating occurs volumetrically throughout the carrot piece, less time will thus be needed for heat transfer to level-out temperatures after microwave HTST processing. For traditionally cooked carrots on the other hand, heat transfer is the sole phenomenon behind the process of heating-up to target temperature. This results in a larger thermal strain to traditionally heated carrot pieces. Thus, the results show that microwave HTST processing offers more rapid heat treat of the model particulate product.

## CONCLUSIONS

Tubular in-flow microwave heating, in terms of microwave HTST processing of high-concentrated large particulate products offers rapid and flexible processing as well as advantages in terms of product quality. Among the advantages in product quality are: better maintained piece integrity with regard to shape of the carrot pieces and potentially improved perceived texture. Texture measurements also correspond well to perceived mouthfeel, which showed a promising potential for the quality of the microwave treated carrots.

It was also indicated that the relative size of the carrot pieces is slightly reduced with increasing temperature without changing the shape significantly. This might correspond to slight 'shrinkage' in size of the carrot pieces during heat processing. However, the shape was maintained (95% confidence level). The results from the texture analysis illustrate that it is possible to control the texture of the pieces of carrots by selecting the heating conditions accordingly within the studied interval, to achieve carrot pieces that range in texture from 'al dente' (traditionally cooked for 1–2 min) to very soft pieces of carrot (traditionally cooked for 5 min).

## REFERENCES

- [1] Wäppling Raaholt B, Isaksson S, Hamberg L. 2016. Continuous tubular microwave heating of homogeneous foods: evaluation of heating uniformity in pilot-scale at constant total microwave power. *J Microwave Power*. 50(1):43–65.

# Analysis of food heating in a multi-source solid state microwave oven

Christopher Hopper<sup>1,\*</sup>, Gaia Mannara<sup>2</sup>, Michele Sclocchi<sup>1</sup>, Giorgio Grimaldi<sup>1</sup>  
and Francesco Marra<sup>2</sup>

<sup>1</sup>IBEX, ITW Food Equipment Group, Glenview, IL, USA

<sup>2</sup>University of Salerno, Department of Industrial Engineering, Italy

\*Corresponding author: christopher@ibex.one

**Keywords:** solid state microwave, rapid cooking oven, food quality.

## INTRODUCTION

The potential of high power solid-state (SoSt) sources has been investigated for several years now. To date, there are limited experimental studies of multi-source solid-state rapid cooking oven performance, based on combination of heating means such as microwave (MW) and convective heating. Still, magnetron based MW ovens lack in providing uniform heating and tailored power cooking/heating cycles. This compromises the food structure and affects the quality of the product perceived by the consumer. This paper presents experimental results obtained using the IBEX ONE (ITW, Glenview, IL, USA), solid-state microwave/convection oven. Analysis has been performed comparing simulations with measurements for regularly-shaped loads with known physical properties. The range of heating uniformity and efficiency available through frequency and phase modulation is also characterized. Furthermore, a quality framework protocol has been used to compare cooking/heating performance with respect to magnetron-based rapid cook ovens.

## SOLID-STATE MICROWAVE GENERATION AND INTELLIGENT COOKING

Solid-state RF/MW generation relies on solid semiconductors as opposed to electron tube technology. These devices typically operate at tens of volts as opposed to magnetrons which operate at several kilovolts. The basic components of the system are the RF/MW generator, the power amplifier, and the delivery components. In the synthesizer circuit, a small signal at the required phase and frequency is generated and stabilized before being passed to the amplifier. The RF power transistors and architectures provide a full range of power control, phase shifting, and frequency adjustment allowing microwaves to use complex combinations. Currently, the IBEX ONE architecture allows access to several parameters in real-time. This feedback can change during the cooking process and

is necessary for a closed-loop system. In this context we define intelligence to mean the ability to obtain relevant feedback from the system and respond in a way which appropriately respects the desired outcome of the customer.

### **SIMULATION VS EXPERIMENT**

“What-if” scenarios were explored by means of process simulations conducted by means of COMSOL and MATLAB software. The effect of different configurations, such as phase between generators, is something which can be simulated and the results can be used to identify where hot/cold spots are expected to occur and how manipulating the phase and frequency can be used to improve uniformity. Comparison of thermal maps provided by simulation with the ones experimentally determined were used to validate the model. Figure 1 shows two examples of simulations vs. experimental results for given combinations of frequency and phase.

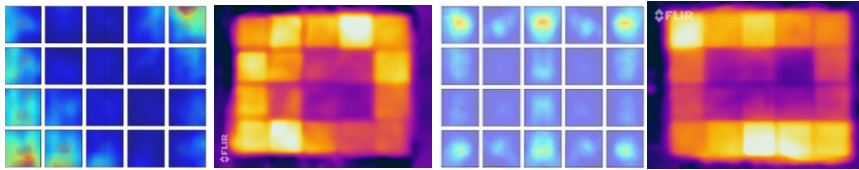


**Figure 1** From left to right: Simulation of one phase configuration at 2410 MHz, thermal image of the same, simulation of another phase configuration at 2450 MHz, and associated thermal image.

While the simulations and experimental data do not match exactly (as expected), they do provide a fair indication of where constructive and destructive interference is expected to occur. This information allows for sophisticated cooking algorithms to be developed and tested.

### **MATERIALS AND METHODS**

Texture profile analysis (TPA), together with color analysis, was applied to samples processed in different ovens in order to compare the SoSt system with traditional MW systems to get information about the performance of these with respect to the product. TPA is a compression test widely used to quantify several structural parameters of a food product [1]. The apparatus used for this work was an Instron Universal Testing Machine (5944, Instron). Color analysis, based on the CIElab scale, has been performed by acquiring pictures of the sample after the process and analyzing them using image processing toolbox of MATLAB.

### **RESULTS**

The results are presented in the form of a comparison between structural parameters. Figures 2-3 show results obtained from TPA analysis on chicken breasts [2], and breakfast sandwiches cooked with different recipes, optimized in a previous phase: the toughness [J] represents the energy that the sample absorbs

before it breaks, and the BSI [N/mm] represents the highest value of the force reached during the test, normalized to the thickness of the sample.

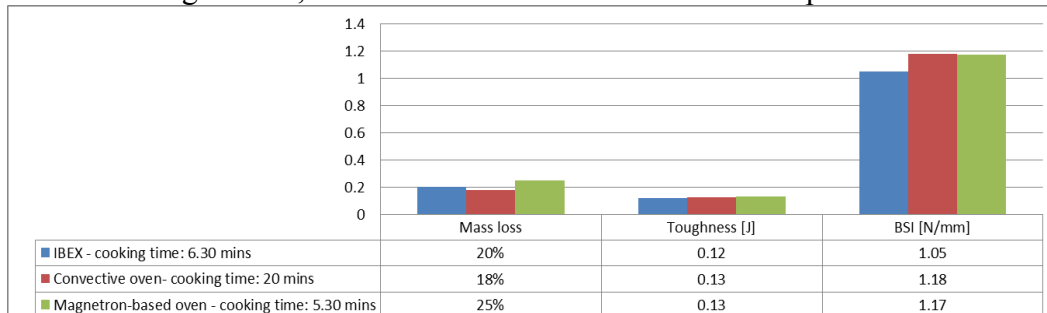


Figure 2 TPA results for chicken breasts

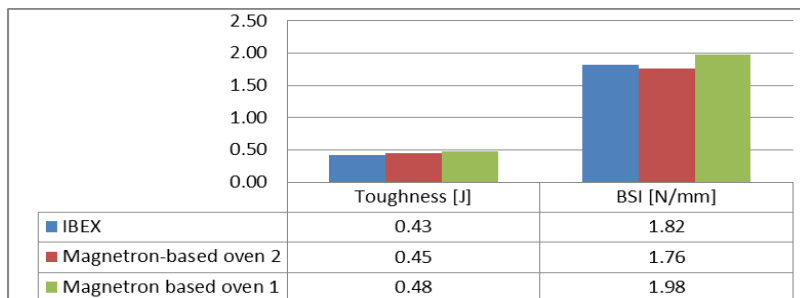


Figure 3 TPA results for breakfast sandwiches

**DISCUSSION**

The results show that there is no noticeable difference in the final texture, but we can observe differences in the amount of water lost, for chicken breast, when processed in the magnetron-based oven, which is perhaps too aggressive for this kind of product, and a reduction of 60% of the cooking time with respect to the traditional convective oven.

**CONCLUSION**

The ability to manipulate phase, frequency, and amplitude can result in improved heating uniformity, as suggested by simulations and demonstrated with experimental results. Structural properties of food products prepared with the IBEX ONE oven are similar, and in some cases better, than those obtained by means of magnetron-based ovens, or traditional convective cavities.

**REFERENCES**

[1] H. H. Friedman, J.E. Whitney, and A.S. Szczesniak. The Texturometer - A New Instrument For Objective Texture Measurement, Journal of Food Science, Volume 28, pp 390-396, 1963.  
 [2] L.J. Bratzler - Measuring the tenderness of meat by means of a mechanical shear, Master of Science Thesis, Kansas State College, USA, 1932.

# Virtual Tools for the Simulation of RF Assisted Thawing of Food Products

Tesfaye F. Bedane and Francesco Marra

Department of Industrial Engineering, University of Salerno, Fisciano (SA), Italy

**Keywords:** heating uniformity, RF heating, thawing, virtualization

## INTRODUCTION

The use of virtual tools based on mathematical modeling helps reduce the cost of expensive prototypes and shortens the time-to-market of new systems. After being massively applied to industrial sectors such as automotive, aerospace and IT, virtual tools are being appreciated in food industry R&D, especially in the design of processes and systems characterized by multiphysics interactions, such as in microwave (MW) and radio-frequency (RF) assisted heating. Particularly, this work was devoted to show how virtual tools could be used to optimize the temperature distribution during food thawing assisted by RF heating. RF heating has been applied successfully to different food processes such as, drying, disinfestation and post-baking [2], but in food thawing, it carries with it a major challenge related to temperature uniformity and possibility to develop hot spots above temperature limits imposed by National Food Agencies' regulations [1]. In fact, improving the heating uniformity is essential to ensure the quality and safety of the product according to the regulatory requirements. The overall goal of this work was to develop and validate virtual tool for the simulation of RF assisted thawing of foods, and then to show how such tool can be used to design systems/processes with improved temperature uniformity.

## MATERIALS AND METHODS

A multiphysics model that coupled the heat transfer equation with power generation term and Gauss law derived from quasi-static approximation of Maxwell's equations was used to predict the temperature distribution in the food product [3]. All thermophysical and dielectric properties used in the simulation were temperature dependent and apparent specific heat method was used to approximate the specific heat change during phase transition [1], [3]. Minced lean beef meat blocks of size  $20 \times 20 \times 10 \text{ cm}^3$  ( $T_0 = 16.31 \text{ }^\circ\text{C}$ ) and  $19 \times 12.5 \times 5.5 \text{ cm}^3$  ( $T_0 = -20 \text{ }^\circ\text{C}$ ) were thawed in 50-ohm and free running oscillator RF systems, respectively. Computer models considering both the 50-ohm (27.12 MHz, max power 0.6 kW) as shown in Figure (1a) and the free running oscillator RF systems (27.12 MHz, max power 6 kW) shown in Figure (1b), were developed to simulate the thawing time and temperature distribution. For the 50-ohm RF system, the effect of power cycling (continuous and non-continuous) at the same treatment time was investigated. The effect of food product movement on the conveyor belt with/without

movement of the top electrode considering the time/space boundary conditions on thawing time and final temperature profile of the food product were investigated for the case of FRO system. Moving mesh framework was used to simulate the movement of food product on conveyor belt and top electrode.

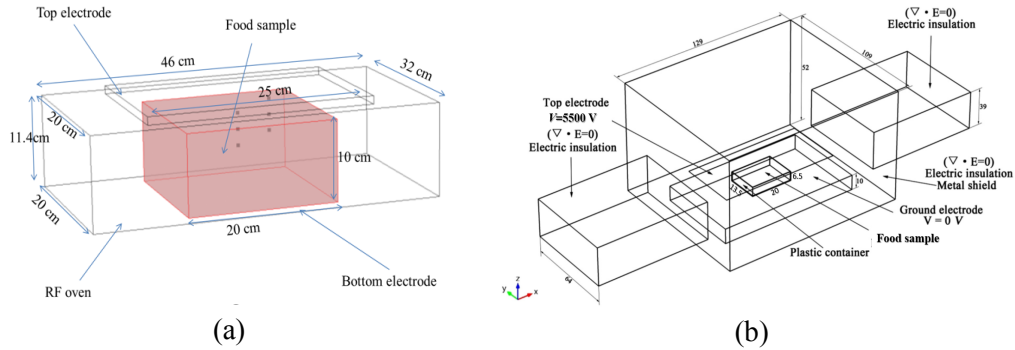
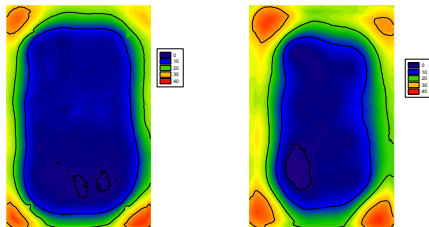


Figure 1. Schemes of RF heating systems: 50-ohm system (a) and free-running oscillator system (b); all dimensions in cm.

a) Experimental (Max T/min T)  
 Top (37.7/-0.5 °C) Middle (37.6/-1.9 °C)



b) Simulated (validation)  
 Top (42.2/2.6 °C) Middle (35.5/-0.2 °C)

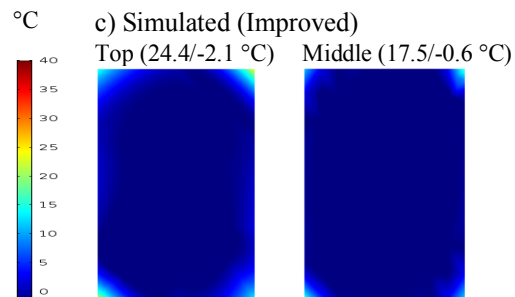
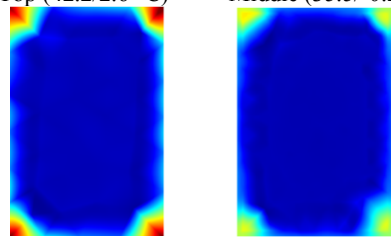


Figure 2. Comparison (Max T/min T) of experimental (a) and simulated temperature (°C) distribution of lean beef meat thawed using free running oscillator RF system, 6 kW, 10 cm electrode gap and 21 min (b) and sample thawed using upward moving top electrode and moving conveyor belt (c).

**RESULTS**

In Figure 2, the comparison of experimental and simulated surface temperatures (max T/min T) on top and middle of lean beef block thawed on a moving conveyor belt speed of 2.93 m/h using a free running oscillator RF system at 6 kW and thawing time of 21

min is shown. Figure 2c represents temperature profile on the top and middle surface during thawing on improved configuration, i.e. moving food product on conveyor belt and upward moving of top electrode (5 cm away during entire treatment time).

## DISCUSSION

The model developed using 50-ohm RF heating system used to locate the points with hotspots within the food product and demonstrated the possibility to mitigate non-uniformity of temperature distribution using a power cycling method with an optimum on/off times during the process. Non-continuous thawing using 500 W RF power for 25 min followed by 10 min stop time and later 10 min RF heating at the same power resulted in improved uniformity of temperature distribution with respect to continuous one.

The computer model developed to simulate RF thawing using free-running oscillator system was validated (Figure 2) and simulation results indicated that combination of moving food product with upward moving of top electrode (Figure 2c) during thawing process reduced the overheating observed on the corners and surfaces of the food under the same thawing time. Volume average end-point temperature of  $0.61 \pm 1.97$  °C was achieved during moving food product on conveyor belt (2.93 m/h) in combination with upward movement of top electrode (5 cm away during treatment time) whilst for the case of only moving food product on conveyor belt, it was  $2.03 \pm 6.87$  °C. The power density distribution in the food product changed as the food product moves in the cavity and as the dielectric loss factor of the food product increase due to increase in temperature as thawing progress [4]. Moving food product between electrodes in combination with gradually upward moving top electrode resulted in better uniform thawing of the food product and undesirable overheating on the corners of the food product were minimized.

## CONCLUSION

The virtual tool developed has demonstrated a good trustability and further used to investigate strategies to improve uniformity of temperature distribution. The model can also be used to understand and improve the industrial continuous thawing systems to achieve optimum thawing time with temperature distribution within the regulations set by authorities and quality of the food product is maintained.

## REFERENCES

- [1] T.F. Bedane, L. Chen, F. Marra, and S. Wang, Experimental study of radio frequency (RF) thawing of foods with movement on conveyor belt. *Journal of Food Engineering*. 201: 17-25, 2017.
- [2] Z. Huang, F. Marra, J. Subbiah, and S. Wang, Computer simulation for improving radio frequency (RF) heating uniformity of food products: A review., *Crit. Rev. Food Sci. Nutr.*, 1–25, 2016.
- [3] R. Uyar, T.F. Bedane, F. Erdogdu, T.K. Palazoglu, K.W. Farag, and F. Marra, Radio-frequency thawing of food products – A computational study, *J. of Food Engineering*, 146, 163–171, 2015.
- [4] J. Chen, S.K. Lau, L. Chen, S. Wang, and J. Subbiah, Modelling radio frequency heating of food moving on a conveyor belt, *Food and Bioprocess Processing*, 102: 307-329. 2017.

# Microwave Drying of Fabrics

Jiwen Deng, Wenjie Fu, Xiaoyun Li and Baoqing Zeng

School of Physical Electronics, University of Electronic Science and Technology of China, Chengdu 610054, China

**Keywords:** Microwave drying; fabrics; tensile strength; loss tangent.

## INTRODUCTION

Microwave drying is a special application for microwave heating [1]. Because of microwave direct heating of water and the lack of thermal conduction from the outside to the inside, microwave drying has the advantages of high efficiency compared with traditional heat drying and has a number of potential applications. Currently, microwave drying is used in pharmaceutical and food processing [2, 3]. To expand the application fields of microwave drying, we have attempted to use microwaves for drying clothes.

In this study, the effects of the microwave drying of several types of fabrics under various powers and processing times are investigated. The results are useful for expanding the application of microwave drying, developing the related microwave drying products, and solving the problem of the low efficiency of traditional drying.

## METHODOLOGY

To investigate the effects of the microwave drying of fabrics and explore the relationship between microwave characteristics and the drying effect, several types of fabrics have been dried using microwaves, and the variations in the fabric characteristics have been investigated.

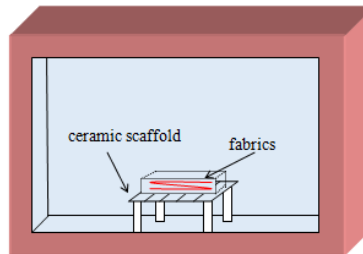


Figure 1. Configuration of microwave drying experiment.

Figure 1 shows the experimental configuration for the microwave drying of fabrics. A 2.45-GHz microwave oven was used as the drying cavity. In the experiments, the fabric samples were folded and placed on a drying rack located in the center of the microwave oven. To avoid the microwave breakdown phenomenon, the drying rack was made of ceramic, not metal. Each of these fabric samples was cut into a square. Before drying, the samples were wet with water and then dried using a microwave oven. During the drying process, the fabric samples were weighed every 30 s to investigate the microwave drying process. The environmental temperature during the experiments was around 10°C. In the

experiments, two initial conditions were considered in the experiments. The first condition was that the fabric samples had similar sizes and wet-to-dry weight ratios (wet-to-dry weight ratio = (water weight + fabric weight)/fabric weight). The second condition was that the fabric samples had similar fabric and water weights.

Moreover, the tensile strength variation of the fabrics after microwave drying was a key element for making microwave drying practical. In this study, we used fabrics with similar initial sample size and wet-to-dry weight ratio; further, the samples dried by using three different methods were compared. The first method was natural air-drying. The second method was normal microwave drying. The third method was excessive microwave drying in which the fabric samples were dried using microwaves, which consumed five times as much time as normal microwave drying. All of the treated fabrics were cut into 5 cm × 20 cm pieces, and the threshold tensile strength was measured with a digital tension meter.

**RESULTS**

The experimental results of microwave drying effects are presented in Figs. 2-3, and the experimental results of tensile strength variation are displayed in Figs 4.

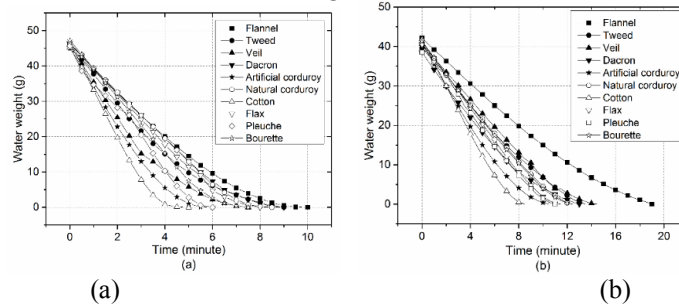


Figure 2. Water weight variation of experimental fabrics during microwave treatment: (a) 700-W microwave power; (b) 300-W microwave power.

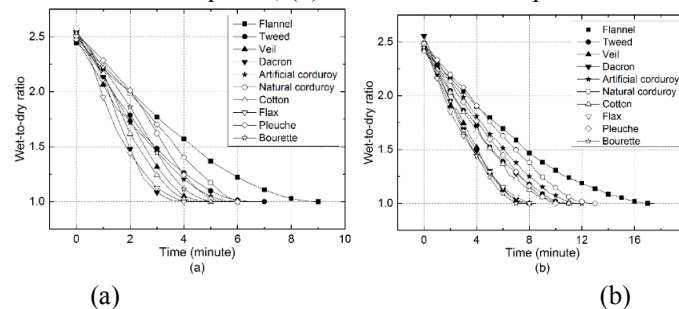


Figure 3. Wet-to-dry weight ratio variation of experimental fabrics during microwave treatment: (a) 700-W microwave power; (b) 300-W microwave power.

The results showed that the drying speed of the 700-W-power microwaves was faster than that of the 300-W-power microwaves. Under the same initial condition, drying by the 700-W microwaves consumed less time than drying by the 300-W microwaves. The results showed that different fabrics exhibited different trends for the similar initial

condition and the same microwave drying process. The effect of microwave drying depended on the material of the samples.

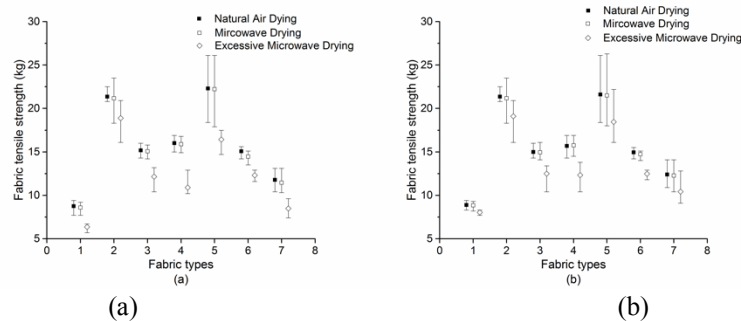


Figure 4. Tensile strength of (1) cotton, (2) denim, (3) natural corduroy, (4) artificial corduroy, (5) tweed, (6) flannel, and (7) veil with microwave treatment: (a) 700-W microwave power; (b) 300-W microwave power.

Figure 4 shows that the tensile strengths of all of the tested fabrics that were dried using natural air-drying and microwave drying in the cases of both 700-W power and 300-W power were similar. The tensile strengths of all of the tested fabrics dried using excessive microwaves were weaker than those of the fabrics dried using microwaves in the cases of both 700-W power and 300-W power. The tensile strengths of fabrics dried using excessive microwaves in the case of 700-W power were weaker than those of the fabrics dried using excessive microwaves in the case of 300-W power. The results showed that normal microwave drying affected the tensile strengths of the fabrics slightly and that excessive microwave drying reduced the tensile strengths of the fabrics obviously. At large power values, the tensile strengths of the fabrics dried using excessive microwaves were weak.

## DISCUSSION AND CONCLUSION

The microwave drying experiment demonstrated that microwaves could be used to dry fabrics. The results revealed that different fabrics took different amounts of time to dry under similar initial conditions during the same microwave drying process. The results also indicated that normal microwave drying was similar to natural air-drying and would not destroy the fabrics. However, excessive microwave drying would destroy the fabrics. The higher the microwave power was the more serious was the fabric damage.

## REFERENCES

- [1] T. Santos, M. A. Valente, J. Monteiro, J. Sousa and L. C. Costa, Electromagnetic and thermal history during microwave heating. *Appl. Therm. Eng.*, vol. 31, no 16, pp. 3255-3261, 2011.
- [2] R. H. Walters, B. Bhatnagar, S. Tchessalov, K.-I. Izutsu, K. Tsumoto and S. Ohtake, Next Generation Drying Technologies for Pharmaceutical Applications. *J. Pharmaceutical Sci.*, vol. 103, no 9, pp. 2673-2695, 2014.
- [3] B. Rejasse, S. Lamare, M. D. Legoy and T. Besson, Influence of microwave irradiation on enzymatic properties: applications in enzyme chemistry. *J. Enzyme. Inhib. Med. Chem.*, vol. 22, no 5, pp. 518-526, 2007.

# MW Processing of Bakery Products to Prevent Checking & Breakage; State of the Art (BRICE Project)

**Patricia LE-BAIL**<sup>a,b</sup>, **Jean Yves MONTEAU**<sup>b,c</sup> & **Alain LE-BAIL**<sup>b,c</sup>

a INRA BIA, 44300 Nantes, France

b SFR IBSM 4202, INRA-CNRS

c ONIRIS, CNRS UMR 6144 GEPEA BP 82225, 44322 Nantes, France

**Keywords:** Checking, breakage, rusks, biscuits, crackers, microwave, radiofrequency, food.

## INTRODUCTION

The water content dry bakery products such as rusk, crackers, biscuits and similar products is in the range of 3 to 5% (dry mater basis). At the end of processing, will be toasting for rusk, or a combined baking-drying process in the case of biscuits and crackers; however, a water gradient is still present within these products. It has been seen that the appearance of cracks (checking) that may result in breakage of the product, is linked to tiny moisture gradients within the product (often lower than 1%). Thus, any thermal or other process that will provide mobility to water, in order to minimize the said moisture gradient, will contribute to the control of checking and breakage of dry cereal products. This presentation discusses the state of the art of this problem, including modelling of the stress that develops during equilibration after processing (storage). MW and RF appear from the literature as relevant means to control checking, cracks and breakage.

## DRY BAKERY PRODUCTS AND GLASS TRANSITION

Dry bakery products like biscuits, rusks, crackers... are baked on continuous baking lines in the industry. The quality and crispness of these products is closely linked to the low water content after processing. The target for all these products is usually in the range of 3 to 4.5/5% maximum with an optimal around 3.5/4%. At this level of water content, water is adsorbed water with a strong bond to the matrix. The isosteric heat of desorption, the energy needed to desorb water bound to a dry matrix, is several folds higher than the heat of vaporisation of water (around 2450 kJ/kg at atm. pressure) as shown in Figure 1 below. The glass transition temperature corresponds to a temperature below which the biopolymers of the products (here starch and proteins biopolymers) that are in a quasi-melted state during processing, with temperatures ranging between 120 and 150°C, will undergo a very high increase in viscosity during the temperature drop following processing. Figure 2 below, provides values of glass transition for starch and gluten proteins, the major constituents of dry baked products. Starch, which has a higher molar mass than proteins, appears to be the major contributor to the glass transition and to the associated mechanical properties of dry baked products. Starch is also the major ingredient by mass and, is therefore, a major player in the crispness of dry baked products. From this Figure, it is clear that increasing the temperature increases the mass diffusivity.

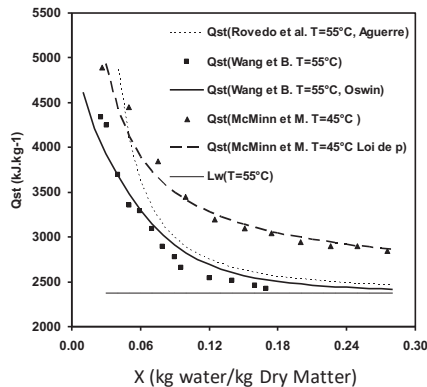


Figure 1: Isosteric heat of desorption “Qst” in function of water content “X” for potato. (Zuniga, 2005)

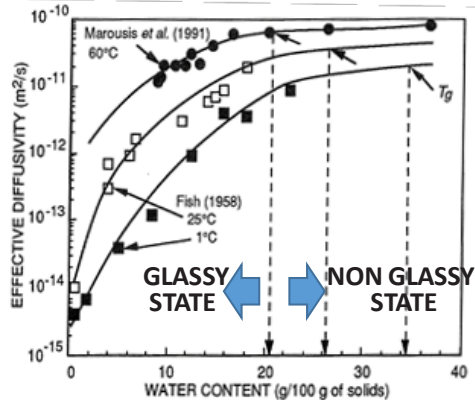


Figure 2: Mass diffusivity of water in gelatinized wheat starch in function of water content and temperature (Roos, 2015)

**WATER EQUILIBRATION IN DRY BAKERY PRODUCTS DURING STORAGE**

The tiny moisture gradient between the center and the outer zones of the baked product induces moisture diffusion (thickness ranging from ca. 3 mm (crackers) to ca. 1 cm (rusk)). The mass diffusivity of water is severely depressed when the matrix is in glassy state as illustrated in the Figure 2. The evaluation of the characteristic time of diffusion  $t_D$  can be determined by equation (1) below from reference [2], with L = distance over which diffusion is considered (m), and D mass diffusivity (m<sup>2</sup>/s).

$$t_D = \frac{4 L^2}{\pi^2 D} \text{ in secondes} \tag{1}$$

Computations using this equation has been done with L=1 mm indicating that increasing the temperature of the product above the glass transition will result in a very significant decrease of the time needed for water diffusion from 7 days to 0.1 days with D = 10<sup>-13</sup> to 10<sup>-10</sup> m<sup>2</sup>/s.

**MICROWAVES TO CONTROL CHECKING AND BREAKAGE.**

Ahmad et al. (2001) proposed the use of MW (2450 MHz) to control checking of biscuits and dry cereal products. Around 1.7 J/g was applied to biscuits (30x 40 x 4 mm). As main results, the breaking strength and the moisture profile of conventional and MW processed biscuits are shown in the figures below. These authors found that based on a large sampling, checking was reduced from an average of 61% to 5% among MW processed biscuits with minimal processing time of 15 seconds.

**CFD MODELING OF STRESS DURING RUSK STORAGE**

CFD modelling of moisture equilibration in rusk during storage has been performed with COMSOL software. This hydro-mechanical model has been designed to determine the stress and strains during storage, to predict checking. Results show that the highest strain occurs around bubbles in the crumb. Therefore, the distribution of the cells in the crumb is likely to interfere with the checking phenomena. Further investigations are envisaged to study the optimal processing conditions, using MW or RF, to allow strain relaxation during storage of dry baked products as function of their geometry, cellular distribution and moisture distribution. A dilatometry bench has been designed to determine coefficient of water expansion and thermal expansion. The Poisson

coefficient is also an important parameter that will be determined with microscopic images of product exposed to strain.

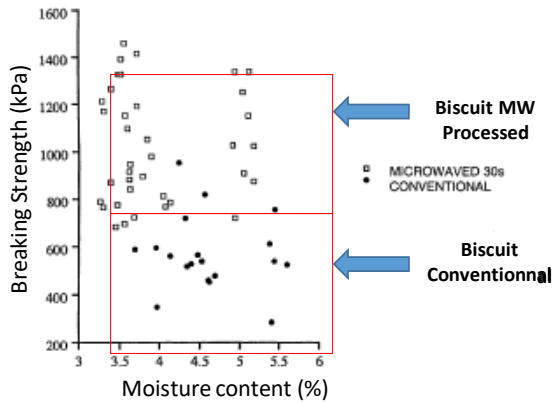


Figure 3: Breaking strength of biscuits in function of the moisture content (Ahmad et al., 2001)

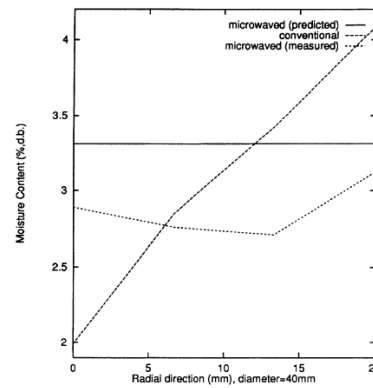


Figure 4: Moisture profile vs radial direction for MW & conventional biscuits (Ahmad et al. 2001)

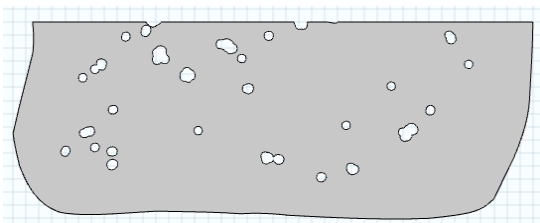


Figure 5: Scheme of the rusk modelled (8 cm long x 3 cm half width). Cells are inserted in the matrix to mimic the presence of bubbles.

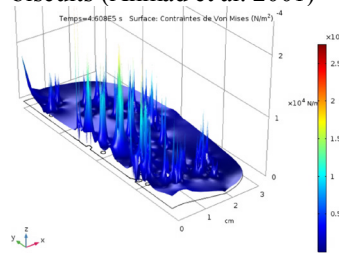


Figure 6: Stress field during modelling demonstrating that the highest stresses are obtained around the gas cells.

**CONCLUSION**

MW and also RF processing, applied to dry cereal products, can be an efficient means to equilibrate water after baking of dry products, in order to control checking and breakage during storage. Energy related to a temperature rise above the glass transition is needed; also isosteric heat of desorption can be considered to optimize energy demand for process.

**ACKNOWLEDGEMENTS:** Regional Council of “Pays de la Loire” funds this project

**REFERENCES**

[1] R. Zuniga, PhD Univ. Nantes N° ED 0367-182, “études numérique et expérimentale des transferts couplés masse-chaleur : modélisation, simulation et optimisation d’un traitement thermique dynamique de surface d’un produit alimentaire”  
 [2] Y. Roos, S. Drusch, Phase Transitions in Foods, 2<sup>nd</sup> Edition, Ed. Academic Press, ISBN: 9780124080867, 2015.  
 [3] S.S. Ahmad, M.T. Morgan, M.R. Okos, Effect of microwave on the drying, checking and mechanical strength of baked biscuits, J. of food engineering, vol 50, pp 63-75, 2001.

# Evaluating Control of *Ascochyta lentis* in Lentil Seeds by Means of Microwave Processing

Saeedeh Taheri, Graham Brodie

The University of Melbourne, Australia

**Keywords:** Microwave, disinfection, *Ascochyta lentis*, lentil, uniformity

## INTRODUCTION

The increasing world population needs much more food than ever before. One way of responding to the growing demand for food, is to reduce loss of agricultural products. An important contributor to food waste is spoilage and crop disease due to fungal infestation. *Ascochyta* blight is a seed borne disease which can be partially controlled by thermal treatments [1, 2]. It is hypothesized that the difficulty of controlling *Ascochyta spp.* in legumes could be because of the special position of these fungi in the seed. In most seeds with this infection, fungi are located beneath the seed coat and 40% of seeds also have infected embryos [3]. By considering this assumption, microwave heating may be a good choice to be part of an integrated pest management procedure as it can heat volumetrically, quickly penetrating the seed coat and heating through to the embryo of the seed.

## METHODOLOGY

A domestic microwave oven, SANYO with working volume of  $33 \times 23 \times 33.5 \text{ cm}^3$  and 10 power levels (10%, 20%..., 100%), was used for the experiment. A calibrated water load test [4] revealed that the microwave oven produced an average power of 486 W at full power. For each treatment, around 50 g of red lentils, adjusted to moisture contents of 9.4, 13.3, 16.5, 22.3% (wb), were put in a glass petri dish with inner and outer diameters of 13.8 and 14.2 mm. The plate was placed in the centre of the turntable before selecting the power level and exposure time. To assess the temperature distribution as well as the mixing temperature of the samples, thermal photos were taken, using a FLIR C2 thermal camera, immediately after treatment. To evaluate the effect of cooling temperature on the germination, one batch of seeds was cooled at 24 °C and the other at 10 °C. Following cooling to room temperature, the plates were weighed to measure moisture loss. Power levels and exposure times were 30%, 40%, 50% and 30 secs and 60 secs. All treatments were done three times. To evaluate the heat uniformity, thermal photos were processed with ThermaCAM Researcher Pro 2.10. Temperature uniformity index was calculated by dividing the standard deviation by the difference of mean and initial temperature. Germination test was done on 20 seeds per treatment in 9 -cm plates on Watman paper no. 1, by placing 10 seeds per plate. After 2 and 5 days at 23 °C, germinated seeds were counted. Seeds were considered as germinated on day 2 when their roots appeared. On day 5, just the normal germinated seeds were considered in calculations.

To see the effect of microwave processing on *Ascochyta lentis*, 50g of seeds with moisture content of 22% were inoculated with a fungal spore solution at a concentration of  $10^6$  cfu/ml, and leaving them at room temperature overnight to let the spores germinate. After this time, seeds were treated in microwave oven. After each treatment seeds were subcultured on PDA. Statistical analysis was done by analysis of variance at 95% confidence level and mean analysis was done by Tukey's test and a general linear model was used to compare groups of data. Data are the mean of three or four replicates.

## RESULTS AND DISCUSSION

Moisture content, power and exposure time significantly ( $\alpha < 0.05$ ) affected the heat uniformity and surface temperature. According to Figure 1, temperature uniformity index (TUI) generally decreased by increasing power levels and exposure time. A low TUI is an indicator of good temperature uniformity. TUI at high power (50% power level) did not change significantly with moisture content (MC), while at 30% and 40%, the TUI decreased after 13.3% MC and was the lowest at 22.36%. Improvement in heat uniformity at higher moisture contents could be due to more evaporation from the surface of the seeds, which is also the reason for constant average and maximum temperature after 13.3% MC. Figure 2 shows the effect of power level and exposure time at different moisture contents on red lentils' germination. At 50% power level and an exposure time of 60 secs, lentil seeds' germination was significantly lower at 22.36% MC than 13.3%, despite almost the same final temperature and uniformity. This might stem from the faster heating at higher moisture contents and different time-temperature history of the seeds. According to **Error! Reference source not found.**, cooling temperature did not have a significant effect on the germination and viability of lentils. This could be due to the small size of red lentil, which make the cooling process fast. It can also be concluded that fall in germination is due to the microwave power absorption and is not just a thermal effect. Table 2 shows the effect of microwave processing on the control of *Ascochyta lentis*, artificially inoculated on the seeds. At 30% power level after 60 secs, 87.5% of lentil seeds were free of fungi, in comparison with 0% of the control samples. At this process parameters, lentils' maximum and average temperature were 74 and 52 °C respectively with surface TUI of 0.31.

Table 1 effect of cooling temperature on the germination of the seeds (data are mean $\pm$ SE and n=3)-for each group, means with no shared letter are significantly different

Moisture content %	power level %	time (seconds)	Germination 2d %		Germination 5d %	
			10°C	24°C	10°C	24°C
16.5	30%	60	83.3 $\pm$ 3.3 <sup>a</sup>	73.3 $\pm$ 6.7 <sup>a</sup>	80 $\pm$ 5 <sup>g</sup>	80 $\pm$ 10 <sup>g</sup>
	40%	60	56 $\pm$ 7.4 <sup>ab</sup>	55 $\pm$ 0 <sup>ab</sup>	63.9 $\pm$ 10.7 <sup>g</sup>	56.7 $\pm$ 4.4 <sup>gh</sup>
	50%	60	31.7 $\pm$ 10.1 <sup>bc</sup>	23.3 $\pm$ 1.7 <sup>c</sup>	23.3 $\pm$ 6.7 <sup>h</sup>	23.3 $\pm$ 1.7 <sup>h</sup>
20	30%	60	71 $\pm$ 6.6 <sup>de</sup>	85 $\pm$ 5 <sup>d</sup>	76.1 $\pm$ 5.6 <sup>i</sup>	85 $\pm$ 5 <sup>i</sup>
	40%	60	30 $\pm$ 10 <sup>f</sup>	46.7 $\pm$ 8.3 <sup>ef</sup>	38.3 $\pm$ 7.3 <sup>ij</sup>	51.7 $\pm$ 8.3 <sup>jk</sup>
	50%	60	22.3 $\pm$ 2.7 <sup>f</sup>	12.5 $\pm$ 2.5 <sup>f</sup>	16.7 $\pm$ 6 <sup>k</sup>	12.5 $\pm$ 2.5 <sup>k</sup>

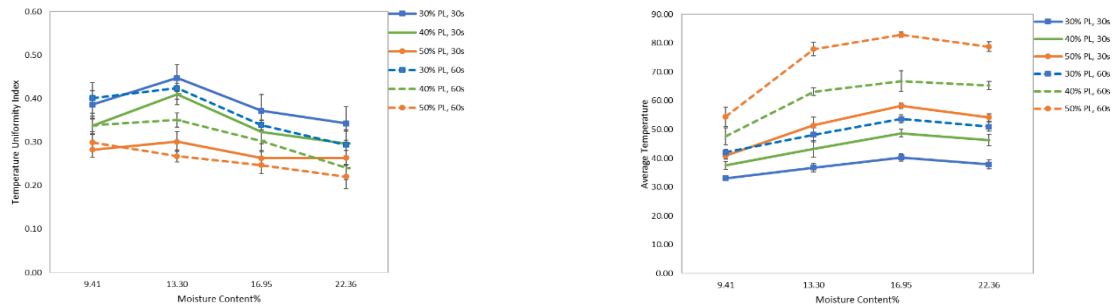


Figure 1 temperature uniformity index (left) and average surface temperature(right) of different moisture contents of lentils treated at different power levels and exposure time (data are mean±SD and n=4); PL=power level; s=seconds

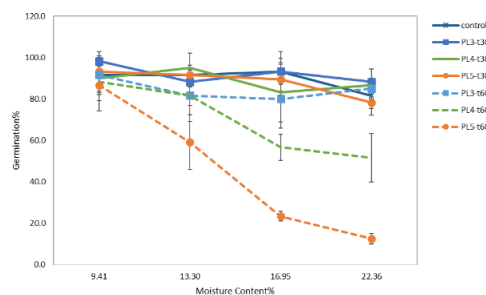


Figure 2 germination of different moisture contents of lentils treated at different powers and exposure time, cooled at 24°C (data are mean±SD and n=3); PL=power level; s=seconds

Table 2 microwave treatment of inoculated seeds with *Ascochyta lentis* (ongoing experiment), data are mean±SD with n=4

power level %	time (seconds)	final disease control%
control	0	0 ± 0
30%	60	87.5 ± 4.3
40%	30	27.5 ± 8.3
50%	60	100 ± 0

**CONCLUSION**

Microwave processing could be considered as a potential non-chemical method to control seed borne *Ascochyta lentis*. However, for a more realistic estimation of disease control, it is recommended to treat naturally infected seeds in the future as well as evaluate the fungi control in dry seeds.

**REFERENCES**

1. Kaiser, W. and R. Hannan, *Seed-treatment fungicides for control of seedborne Ascochyta lentis on lentil*. Plant disease, 1987. **71**(1): p. 58-62.
2. Ahmed, S. and S.P.S. Beniwal, *ASCOCHYTA BLIGHT OF LENTIL AND ITS CONTROL IN ETHIOPIA*. Tropical pest management, 1991. **37**(4): p. 368-373.
3. Mancini, V. and G. Romanazzi, *Seed treatments to control seedborne fungal pathogens of vegetable crops*. Pest management science, 2014. **70**(6): p. 860-868.
4. Brodie, G., et al., *Microwave soil heating for controlling ryegrass seed germination*. Transactions of the ASABE, 2009. **52**(1): p. 295-302.

# Coupled Simulation of Electromagnetic and Thermal Fields for Multi-Source Microwave Oven

Jiayuan Zhong, Baoqing Zeng, Jianlong Liu

University of Electronic Science and Technology of China, Chengdu, China

**Keywords:** Multi feed microwave oven; coupling simulation; finite element; heating uniformity

## INTRODUCTION

For industrial application, the multi-source excitation has been widely used to generate enough output power, but because the position of the feed port may be relatively close, the coupling phenomenon may occur between magnetrons that will affect the output power, efficiency, and reliability of magnetron. Using the coupled simulation for high frequency electromagnetic and temperature fields, the efficiency optimization and homogeneity improvement of a four-tube microwave oven have been designed. HFSS is widely used in high frequency electromagnetic simulation [1]-[2], and we also employ HFSS to conduct electromagnetic simulation of microwave oven models. The simulation results are accurate enough to design a microwave oven. The feasibility of HFSS+ANSYS simulation has been verified in Sabbagh's report [3].

## METHODOLOGY

Based on the ANSYS Workbench platform HFSS+Transient Thermal module, the coupled simulation of high frequency electromagnetic and thermal temperature fields was realized, and the temperature value of an object after microwave heating was obtained.

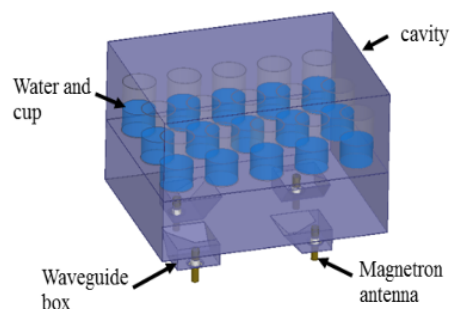


Figure 1. Model of the microwave oven

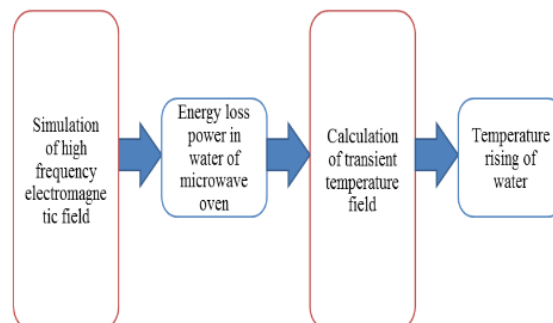


Figure 2. Simulation process

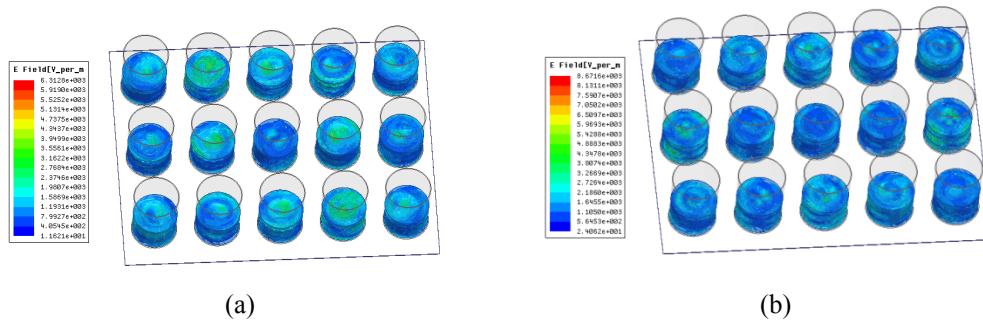


Figure 3. Electric field distribution map a (original) and b(optimized)

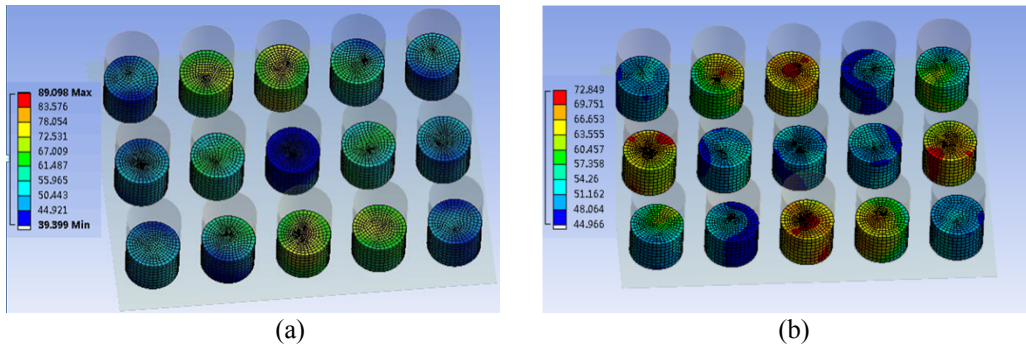


Figure 4. Temperature distribution map a(original) and b(optimized)

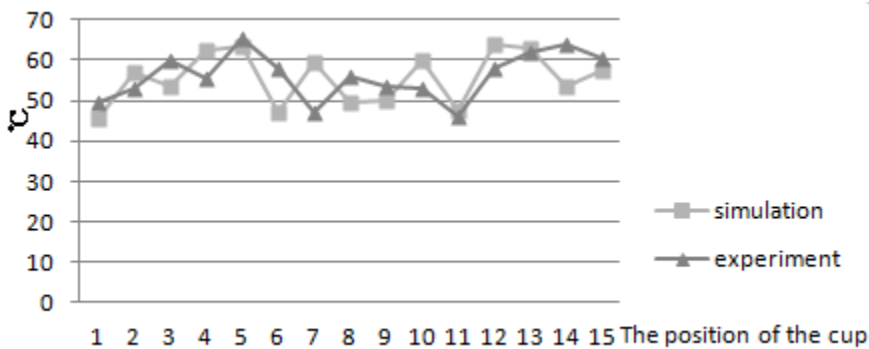


Figure 5. Comparison diagram of experimental and simulation results.

To understand the influence of the relative position of magnetron on the heating efficiency and uniformity, we placed 15 × 100 ml water in plastic cups with diameter 60 mm in a 428 × 333 × 241 mm cavity and adjusted the relative position of four magnetrons; the microwave power can reach 4,000 W.

## RESULTS

The simulation results show that the positions of the magnetron feeds have a great influence on the heating. When the positions of four magnetron feeds are optimized, the average temperature is increased and the uniformity of heating is improved, and the overall efficiency of the microwave oven is also increased.

Figure 5 shows the simulated results and the experimental data; it appears that the error of most points is within 5°C, and the error of only three points is higher than 5°C, but it less than 10°C, which proves that the simulation could be used in design of the microwave oven.

## DISCUSSION

Using the ANSYS Workbench platform HFSS+Transient Thermal module, the electric field distribution and the temperature distribution in microwave oven can be simulated. It can be more intuitive compared with the experimental results. However, this method still has shortcomings. The temperature parameters obtained by Transient Thermal module do not feed back to HFSS, so there is a certain deviation.

COMSOL is also a powerful multiphysics simulation software and widely used in electromagnetic thermal coupling simulation [4]. ANSYS is easier to operate, and it can directly import data into the HFSS simulation model. So we chose the HFSS+ANSYS combination to conduct electromagnetic-thermal coupled simulation, and verified the correctness of its simulation results. In the future, we will also use COMSOL to simulate the electromagnetic-thermal coupling in order to study the influence of the two different methods on the simulation results.

## CONCLUSION

The direct comparison between simulation results and experimental results is achieved. It can be used in the development and design of a microwave oven, which is beneficial to shorten the R&D cycle and reduce its cost.

## REFERENCES

- [1] X. W. Tang, X. Wang, B.Q. Zeng, A study on simulation of A45L turntable microwave oven's cooking performance, *Vacuum Electronics*, 2013.
- [2] H. Ju, Q. Zhao, X. Sun, M. Yang, Microwave oven design using HFSS simulation software, *Materials Review*, 2007-S2.
- [3] M. El Sabbagh, Electromagnetic-thermal analysis study based on HFSS-ANSYS link, *Electrical Engineering and Computer Science Technical Reports*, 46, 2011, [https://surface.syr.edu/eecs\\_techreports/46](https://surface.syr.edu/eecs_techreports/46)
- [4] X.L. Hu, X.Q. Yang, and G.Z. Jia, Effective optimization of temperature uniformity and power efficiency in two-ports microwave ovens, *J. of Microwave Power and Electromag. Energy*, vol. 48, no 4, pp. 261-268, 2014.

# Design of a L-Band High Power Hermetic Window for Industrial Microwave Heating

Liang Tang, Haibing Ding, Weisong Li, Dengfeng Lu, Ke Tang, Ren Xiao,  
Nanyang Liu

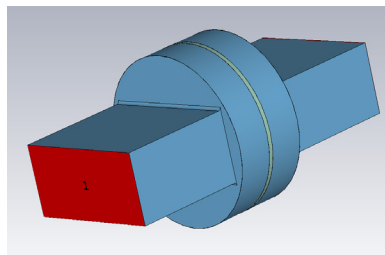
Key Laboratory of High Power Microwave Sources and Technologies, Institute of Electronics, Chinese Academy of Sciences, Beijing, China

**Keywords:** hermetic windows, industrial heating, vacuum sealing, ceramic window, L-band

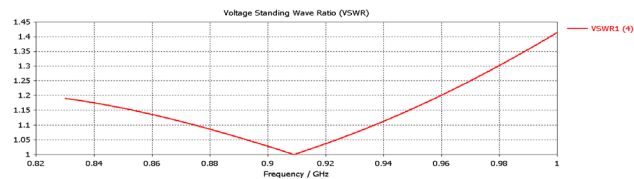
## INTRODUCTION

In industrial microwave heating or drying systems, airtight sealing windows are needed to prevent moisture, humidity, contaminants, even oxygen and any outside atmosphere from entering the heating chamber, while allowing the microwaves pass through. This paper introduces a new kind of WR975 waveguide hermetic window, satisfying low vacuum requirement, with advantages of a simple structure, low cost and no need of welding. Two kinds of materials, ceramic and teflon are considered to be used as the isolating medium. The vector network analyzer test results of the hermetic window are given at the end of the paper, and the results are that the VSWR is less than 1.2 and the insert loss is less than 0.2 dB, at the central frequency of 915 MHz within 100 MHz bandwidth.

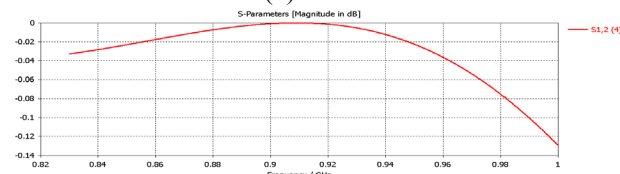
## SIMULATION



(a) 3D simulation model



(b) VSWR

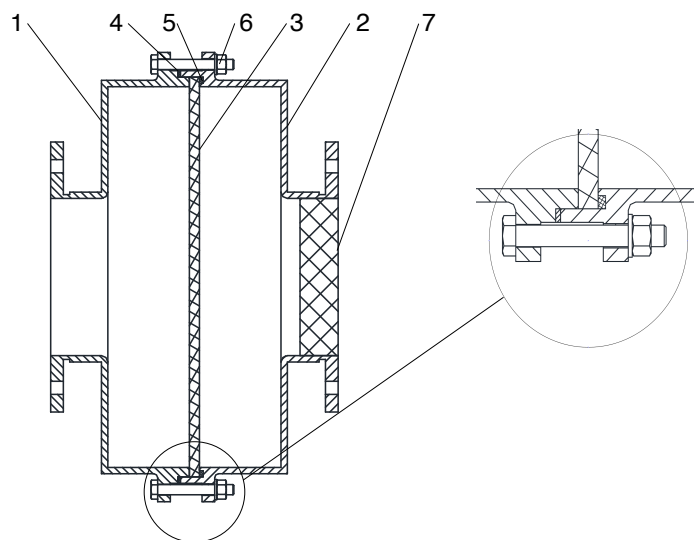


(c) S21

Figure 1. (a) 3D simulation model, (b) and (c) Al<sub>2</sub>O<sub>3</sub> ceramic optimization results of S-Parameters

Fig. 1 (a) shows a 3-dimensional model of the hermetic window. A round dielectric sheet is inserted into the middle of the round waveguide, which is paralleling with the waveguide flanges. Fig. 1 (b) and (c) show the optimization results, the VSWR and the scattering parameter S<sub>21</sub>, when the material of dielectric sheet was chosen to be Al<sub>2</sub>O<sub>3</sub> ceramic. The diameter and thickness of the Al<sub>2</sub>O<sub>3</sub> ceramic are 300 mm and 7.9 mm respectively after optimization. It is essential that there is no resonant mode within the operating bandwidth.

### STRUCTURE



1. left half body, 2. right half body, 3. ceramic, 4. gasket, 5. vacuum sealing o-ring, 6. connecting bolts, 7. waterproof screen

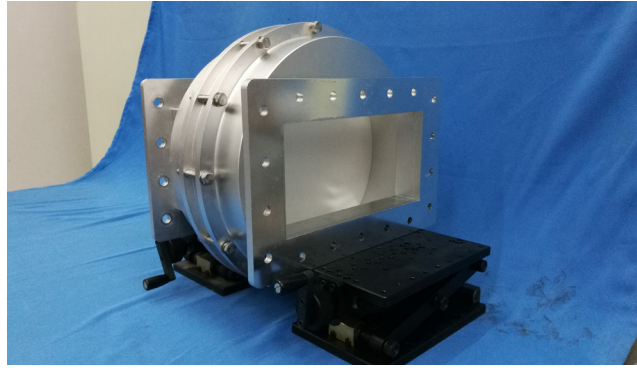
Figure 2. Section view of hermetic window

Fig. 2 shows the section view of the hermetic window. The structure is simple and easy to assemble. The left and right half parts are composed of a flange, a segment of WR975 waveguide and a tapering waveguide which turns into a non-standard circular waveguide. The two parts are easily connected by bolts. A copper gasket is inserted between the two parts for good electrical contact, preventing leakage of microwave. A sealing o-ring hermetically seals the ceramic with the right half waveguide. It must be noted that it is vacuum sealed on one side with the o-ring and not on the other side. A water proof screen protects the ceramic from moisture and dust. Contaminants or water drops condensed from moisture will be heated by microwave and cause secondary electron emission on the surface of ceramic, causing thermal stress breaking the ceramic.

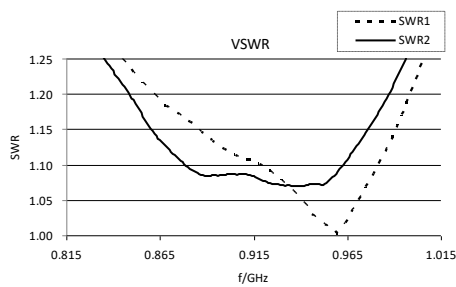
### RESULT

Fig. 3 (a) is the photo of the hermetic window design. Fig. 3 (b) and (c) gives the scattering parameters of the designed hermetic window tested using Agilent 8720D

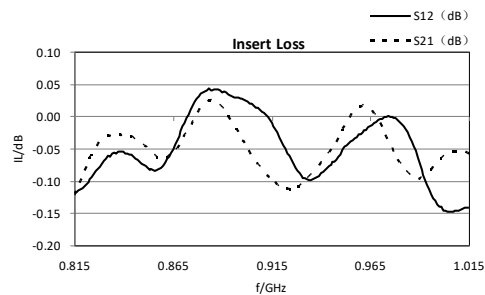
vector network analyzer. S11 or VSWR is worse than the simulation results, but the VSWR is less than 1.2 from 865 MHz to 965 MHz. The bandwidth is more than 100 MHz. Insert loss is less than 0.2 dB within the operating bandwidth.



(a) WR975 hermetic window



(b) VSWR



(c) Insert Loss

Figure 3. The hermetic window designed and S-Parameters

## CONCLUSION

The hermetic window designed was used in experiments for more than 100 hours. It works steadily and robustly under the experiment condition that the average transfer power of the microwave is 20 kW and VSWR of the load is more than 3.

## REFERENCES

- [1] W.X. Wang, *Microwave Engineering Technology*, National Defence Industry Press, 2009
- [2] Yaogen Ding, *Design, Manufacture and Application of High Power Klystron*, National Defense Industry Press, Beijing, 2010.
- [3] H.C. Kim, J.P. Verboncoeur, Y.Y. Lau, Invited Paper - Modeling RF Window Breakdown: from Vacuum Multipactor to RF Plasma. *IEEE Transactions on Dielectrics and Electrical Insulation*, 14(4). 774 - 782. 10.1109/TDEI.2007.4286505.

# Implementation of 100kW L-band Window-type Water Load

Zhiqiang Zhang, Liang Tang, Haibing Ding

Key Laboratory of High Power Microwave Sources and Technologies,  
Institute of Electronics, Chinese Academy of Sciences, Beijing, China

**Keywords:** water load, L-band, continuous wave, magnetron

## INTRODUCTION

In the development and deployment of high power microwave systems, water loads are widely used for absorbing the microwave energy into a high loss fluid medium. In recent years, several kinds of window-type microwave water loads from S-band to Ka-band have been developed by Institute of Electronics, Chinese Academy of Sciences (IECAS). Nowadays a new kind of L-band window-type water load for continuous wave magnetron with microwave power tolerance of 100 kW is developed. Al<sub>2</sub>O<sub>3</sub> 95% ceramic is used as the microwave window between the waveguide and water chamber. Test results show that the VSWR of the water load developed is less than 1.2 at the central frequency of 915 MHz and within the bandwidth of 50 MHz.

## IMPLEMENTATION

Table 1. parameters of the L-band water load

Parameter	Unit	value
Central Frequency	MHz	915
Bandwidth	MHz	50MHz
VSWR	-	<1.2
Operation mode	-	Continuous Wave
Power	kW	100
Water flow	L/min	100

The parameters of the water load developed is shown in table 1. The water load developed is window-type. This kind of water loads has the advantages of small in size, light in weight, simple in structure and wide in bandwidth. The water load is mainly composed of three main parts, waveguide, water chamber and the dielectric sheet between them. The photo of the water load is shown in Fig. 1.

The waveguides used at L-band are WR975 with CPRF flanges. The waveguides are made of aluminum for light weight. The water chamber is cylindrical, and the material is stainless steel for higher mechanical strength. Comparing with square or

rectangular water chamber, cylindrical is sturdier in structure and easier to deal with the sealing issues, because of the round matching edges.



Figure 1. 100 kW window-type water load

In the reference article <sup>[2]</sup>, three types of materials, ceramic, mica, Teflon are considered to be used as microwave window of water load. The permittivity of these three materials is 8.9, 7.0 and 2.2 respectively. According to simulation result, the VSWR when ceramic is used can be optimized as small as 1.08 at the central frequency of 915 MHz and with the bandwidth of 50 MHz, because the permittivity of water used as cooling medium is about 88 at normal temperature. The ceramic has sufficient mechanical strength to bear the pressure of cooling medium. The ceramic is an ideal material and chosen to be used as the microwave window.

There are three seals in the water load. The ceramic is not paralleling with the wider inner surface of the waveguide. The angle between them is approximately 22.5 degrees. Microwave reflected from the ceramic will be reflected back again on the inner surface of the waveguide. The energy of the microwave attenuates after reflections, and finally absorbed by water. As a result there is a standing wave field between ceramic window and waveguide inner surface. An annealed copper gasket is used to improved contact between the waveguide and the ceramic, preventing the leakage of microwaves. If the annealed copper gasket is deleted, the microwaves will transfer along the gap between the ceramic and the metal matching surface, and discharge sparks will occur on the groove between the chamber cover and the half part with the waveguide.

A Viton o-ring hermetically seals water between the chamber cover and the ceramic. A Teflon o-ring is used to hermetically seal the waveguide and the water chamber cover, so the waveguide can be pressurized.

## RESULTS

In order to dissipate microwave power, the flow of water needs to reach 100 L/min. Through water pressure test, the ceramic used can bear the water pressure of 6 kg/cm<sup>2</sup>.

Fig. 2. show the testing method and the results of the water load designed. The VSWR is less than 1.1 within the bandwidth of 20 MHz and less than 1.2 within 50 MHz. The relative bandwidth is more than 5%.



(a) water load under testing



(b) VSWR

Figure 2. The water load under test and results

## CONCLUSION

The water load designed has larger power tolerance than dry loads, has smaller volume than absorbing type water loads, and has basically the same volume of the fixed frequency water loads. Meanwhile it has wider bandwidth. It provides a convenient and reliable way in design of high average power microwave vacuum electronic devices including magnetrons and klystrons and debugging of microwave system in L-band.

## REFERENCES

- [1] W.X. Wang, *Microwave Engineering Technology*, National Defence Industry Press, 2009, pp.69-71.
- [2] D.P. Gao, R. Zhang, H.B. Ding, Ke Tang, Design of 100kW Water Load for P-band Continuous Wave Magnetron, *Conference: 2015 IEEE International Vacuum Electronics Conference(IVEC2015)*, 10.1109/7224006.
- [3] H.B. Ding, D.P. Gao, L. Tang, Ke Tang, Design of S-band 50kW Window-type Water Load, *J. Vacuum Electronics*, 2016(04), pp. 26-28.